Cellular stress induces RIS dependent sleep and ALA dependent sedation via EGF receptor signaling in *Caenorhabditis elegans*

Dissertation

for the award of the degree
"Doctor rerum naturalium"
(Dr. rer. nat.)
of the Georg-August-Universität Göttingen

within the doctoral program Systems Neuroscience
of the Göttingen Graduate Center for Molecular Biosciences, Neurosciences and Biophysics (GGNB)

submitted by
Jan Konietzka
from Frankfurt am Main, Germany

Göttingen, 2019

Thesis Committee Members

Dr. Henrik Bringmann (1st Reviewer)	Max Planck Research Group "Sleep and Waking", MPI for Biophysical Chemistry, Göttingen
Prof. Dr. Ralf Heinrich (2nd Reviewer)	Department of Cellular Neurobiology Georg-August-Universität Göttingen
Dr. Oliver Valerius	Research Group "Mass Spectrometry - Yeast group" Georg-August-Universität Göttingen

Examination Board Members

Prof. Dr. Reinhard Schuh	Max Planck Research Group "Molecular Organogenesis" MPI for Biophysical Chemistry, Göttingen
Prof. Dr. Andreas Stumpner	Department of Cellular Neurobiology Georg-August-Universität Göttingen
PD Dr. Gerd Vorbrüggen	Research Group "Molecular Cell Dynamics" Georg-August-Universität Göttingen

Date of oral examination: July 5, 2019

Affidavit

I herewith declare that this thesis was produced entirely by myself and that I have only used sources and materials cited. The thesis has not been submitted to any other examination board for any other academic award.

Göttingen, April 30, 2019
Jan Konietzka

Summary

Why do we sleep? This question is still unsolved, although sleep is such a fundamental behavioral state in all organism with a nervous system. Several physiological mechanisms, like memory consolidation, metabolic waste clearance, or immune system boosting, depend on sleep but none was sufficient to answer yet, why our consciousness has to shut off every night.

The nematode and model organism *Caenorhabditis elegans* has a minimalistic nervous system of exactly 302 neurons. Still, it provides three different types of sleep, which are linked to either-or one of two sleep neurons. The sleep-active neuron RIS controls developmentally-regulated lethargus sleep and environment-stimulated L1 arrest sleep. Stress-induced sleep (SIS) depends on the interneuron ALA. The clear structure of the nervous system, next to the straightforward genetic accessibility of *C. elegans*, made it an easy choice to use the worms for exploring sleep on a molecular level.

To investigate what defines RIS and ALA on the molecular level, I obtained different transcriptomes for both neurons. I got one transcriptome, which was based on RNA sequencing of fluorescence-activated cell sorted (FACS) RIS neurons. Additionally, Cao et al. (2018) used single-cell combinatorial indexing RNA sequencing to publish a data set of 42’035 single cell transcriptomes, spanning all *C. elegans* L2 cells. From this data set, clusters representing RIS and ALA could be identified and used for the generation of transcriptomes for both cells, respectively.

The transcriptomes provided me with genes enriched in RIS, which were potentially important in sleep control in this neuron. I used mutated alleles of these genes for a behavioral sleep screen. A nonsense-allele of the invertebrate-type lysozyme *ilys-4* and a gain-of-function allele of the epidermal growth factor receptor (EGFR) *let-23* caused worms to sleep more in L1 arrest. Both were known to express in ALA, but I was able to confirm their additional expression in RIS via fluorescent reporters. I also showed the *let-23(gf)* phenotype mainly depends on RIS.

SIS was known to be mediated via LET-23 in ALA. I used genetic ablations of ALA and RIS, and a RIS-specific knock-out of *let-23* to demonstrate that SIS is also highly

dependent on LET-23 signaling in RIS. Calcium imaging revealed that ALA activates broadly over the time span of SIS, while RIS activity correlates with individual sleep bouts of SIS. This is likely mediated via EGF signaling in ALA and RIS, as overexpression of EGF activated both neurons and caused movement quiescence of the worms. Next, I used optogenetic manipulation to show that ALA is able to activate RIS. This may function to some extent via the ALA neuropeptides encoded by *flp-24*, as shown in an overexpression experiment. I could confirm that worms survival after cellular stress is affected by ALA-induced sedation, but discovered survival does not depend on the RIS-induced sleep bouts.

In this thesis, I showed that SIS depends on EGF receptor signaling in RIS, besides the known pathway in ALA. RIS seems to be the major controller of sleep in the worm, as I now discovered that it is involved in all types of sleep in *C. elegans*. Furthermore, I demonstrated that stress-induced EGF receptor signaling acts parallel in ALA and RIS, which inherit different mechanistic properties and thus provide a discrete response. ALA sedates the worm, while RIS activity causes sleep bouts. This dual system allows the worm to fine-tune the behavioral response to cellular stress. Sedation and sleep representing distinct but interacting pathways in *C. elegans* might be a general principle, which also holds true in other organisms.

Table of Contents

1. Introduction 1

1.1. Basics of sleep 1

1.2. Complex sleep – REM & NREM 1

1.3. Functions of sleep 2

1.4. Neuronal control of sleep 3

1.5. Molecular control of sleep 3

1.6. Model organism *Caenorhabditis elegans* and its nervous system 4

1.7. Optogenetics in Caenorhabditis elegans 5

1.8. Lethargus sleep and L1 arrest sleep in *Caenorhabditis elegans* 6

1.9. Stress-induced sleep in *Caenorhabditis elegans* 8

1.10. Conservation of sleep in *Caenorhabditis elegans* 9

2. Thesis Aims 11

2.1. Aim 1 – Discover what defines RIS as a sleep-active neuron 11

2.2. Aim 2 – Identify the role of the EGF pathway in RIS and oppose it to ALA 12

3. Materials and Methods 13

3.1. Worm maintenance and strain genereation 13

3.1.1. Worm maintenance and strains used in this study 13
3.1.2. Molecular biology and transgenic strain generation 14
3.1.3. Transformation by DNA microinjection 14
3.1.4. Transformation by microparticle bombardment 15
3.1.5. CRISPR-based gene editing 16
3.1.6. Strain generation by genetic crossing 17

3.2. Generation of the transcriptomes 17

3.2.1. Transcriptome extraction from single-cell RNA sequencing data 17
3.2.2. Bulk sequencing of FACS-isolated cells 18
3.2.3. Transcriptome generation of bulk sequenced FACS-isolated cells 18
3.2.4. Single cell sequencing 19
3.2.5. Differential expression analysis of RIS versus all cells 19
3.2.6. Differential expression analysis of RIS versus all neurons 20
3.2.7. Differential expression analysis of ALA and 20
comparison with RIS 20

3.3. Microscopy imaging and behavioral analysis 21

3.3.1. Long-term imaging using hydrogel microchambers 21
3.3.2. Microscopy setups for imaging 22
3.3.3. Calcium imaging and optogenetics 22
3.3.4. Reporter gene expression in RIS 23
3.3.5. Mutant sleep screen during L1 arrest 24
3.3.6. Induction of cellular stress by heat shock 24
3.3.7. Induction of protein overexpression through temperature increase and *hsp-16.41p* 26
3.3.8. Lifespan assay 26

3.4. Quantification and statistical analysis 27

3.4.1. Sleep detection using frame subtraction 28
3.4.2. Statistical tests 29

4. Results 31

4.1. Single RIS neuron Transcriptome 31

4.2. RIS transcriptome-based L1 arrest screen 37

4.3. The EGFR acts in ALA and RIS to induce sleep after cellular stress 40
4.4. Cellular stress and EGF signaling depolarize ALA and RIS 45
4.5. ALA rather than RIS support survival after stress 49
5. Discussion 51
5.1. The starting point of this thesis 51
5.2. Genes enriched in the sleep-active neuron RIS 51
5.3. L1 arrest sleep screen 53
5.4. RIS vs. ALA transcriptome 56
5.5. EGF receptor signaling in RIS and ALA 57
5.6. ALA is a sedating and sleep-promoting neuron 57
5.7. EGFR activates RIS to induce sleep bouts following cellular stress 58
5.8. Sedation is protective after cellular stress rather than sleep bouts 59
6. References 61
7. Abbreviations 68
8. List of figures 69
9. List of tables 70
10. Appendix 71
10.1. Supplementary tables 71
11. Acknowledgements 102

1. Introduction

1.1. Basics of sleep

Why do we sleep? This question is not as easy to answer as the questions, why we have to eat, drink or breath. Although sleep is as much a physiological basic need as the other three, the lack of sleep causes within days severe physiological and cognitive problems in the organism and can ultimately lead to the death of it (Rechtschaffen & Bergmann, 2002). Many physiological functions have been discovered happening during and being dependent on sleep, but none was sufficient yet to explain its existence.

Sleep is defined as a reversible but homeostatic regulated behavioral state of quiescence with an increased arousal threshold (Campbell & Tobler, 1984; Siegel, 2008). It can be distinguished from a coma by its quick reversibility to wakefulness if a strong enough stimulus is applied. The increased arousal though can be lethal to the individual, e.g. a sleeping skink which becomes eaten by a predator snake (Shine, 1984). This means sleep is on a physiological level so essential that it could not be obliterated by evolution so far (Siegel, 2008). For its pivotal function also speaks the homeostatic regulation. It is possible to avoid sleeping for some time, but an increasing and homeostatic sleep drive forces the organism to sleep at one point.

Although its intrinsic function has not been discovered yet, many physiological processes happening during sleep have been identified. These might be secondary functions of sleep which were incorporated into the already existing state of behavioral quiescence during evolution. This seems plausible as different types of sleep can be found across the whole Animalia kingdom. A more complex type of sleep, for example, appears in mammals and birds. Sleep in those classes can be separated into two distinct and alternating phases, which are rapid eye movement sleep (REM) and non-rapid eye movement sleep (NREM) (Allada & Siegel, 2008; Campbell & Tobler, 1984).

1.2. Complex sleep – REM & NREM

REM and NREM sleep can be easily identified by electroencephalogram (EEG) and electromyogram (EMG), which measure cortical activity and muscle tone, respectively.

The REM sleep features rapid movement of the eye, although skeletal muscles are paralyzed in a state called atonia. With EEG theta waves of 4 to 8 Hz and slow alpha waves can be found. Besides that, the brain shows activity similar to wake (Steriade, Timofeev, & Grenier, 2001). Also blood pressure, pulse and body temperature resemble the wake state (Parmeggiani, 2003). In contrast NREM sleep features a decrease in body temperature and a slowdown of the heart rate (Parmeggiani, 2003). Brain metabolism is decreased, and electrophysiological activity is more synchronous (Maquet, 2000; Steriade et al., 2001). EEG measurements show higher voltage but slower waves in NREM sleep compared to the wake state. NREM sleep can be divided into three different substages according to their dominant EEG waves. The three stages are N1 "sleep onset", N2 "light sleep" and N3 "deep sleep" (Iber, Ancoli-Israel, Chesson, & Quan, 2007).

1.3. Functions of sleep

With this broad range of diverse sleep phases, it is no surprise that sleep serves several function in the organism. First of all, the proposed function of saving energy might be an adaptive link rather than a function of sleep as stated in the review from Krueger *et al.* (2016). Discovered functions of sleep rather range from memory consolidation to the clearance of harmful metabolites in the brain like β-amyloid (Diekelmann & Born, 2010; Xie et al., 2013). Also in certain circumstances sleep can counteract aging (Wu, Masurat, Preis, & Bringmann, 2018). Further, a link to the immune system was revealed by presenting that a lack of sleep, for example, lead to increased tumor growth or has negative effects on graft rejections in mouse experiments (Hakim et al., 2014; Ruiz et al., 2017). Converse the immune response can also alter normal sleep pattern (Ruiz et al., 2017).

The recent hypothesis for the function of sleep focus on the modulation of brain connectivity and plasticity, like the idea that sleep tunes the brain for criticality (Krueger et al., 2016; Pearlmutter & Houghton, 2009). These hypotheses are of particular interest as not only complex organism like mammals and birds but also evolutionary old organism like jellyfish have a sleep-like state (Nath et al., 2017). If sleep is already present in a simple nervous system like cnidarians have, its original function might be linked to the nervous system itself.

1.4. Neuronal control of sleep

To understand the function of sleep the neuronal and molecular control of it has to be revealed. Sleep is promoted by sleep-active neuronal networks and nuclei, which also inhibit wake-active brain regions (Bringmann, 2018). During the wake state it is completely reversed, and the wake-active brain regions promote the wake state and inhibit parallel the sleep-active brain loci. This bidirectional interaction enables a fast switching from one brain state to the other in the format of a so-called "flip-flop" switch (Saper, Chou, & Scammell, 2001; Saper, Scammell, & Lu, 2005). Switching happens in the range of a few seconds (Takahashi, Kayama, Lin, & Sakai, 2010; Wright, Badia, & Wauquier, 1995). Interestingly such a "flip-flop" switch seems to be also present for REM and NREM sleep as they are mutually exclusive and inhibit each other (Lu, Sherman, Devor, & Saper, 2006).

In the human the wake-active neuronal network consists of cholinergic neurons in the pedunculopontine and laterodorsal tegmental nuclei, noradrenergic neurons in the locus coeruleus, serotoninergic neurons in the dorsal and median raphe nuclei, dopaminergic neurons next to the dorsal raphe nucleus and also histaminergic neurons in the tuberomammillary nucleus (Saper, Fuller, Pedersen, Lu, & Scammell, 2010).

The counterparts are γ-aminobutyric acid (GABA)ergic and peptidergic sleep-active neurons located to a large extent in the preoptic area (POA) of the hypothalamus. Other brain regions containing sleep-active neurons in the human are the basal forebrain, lateral hypothalamus, cortex, and the medulla of the brain stem (Bringmann, 2018).

1.5. Molecular control of sleep

Therefore, it is known which brain regions are at least responsible for sleep and also to a large extent which signaling molecules they use to induce sleep. This leads to the question of how sleep is regulated. It is known that sleep is controlled by different mechanisms, although they might overlap on the molecular level (Franken & Dijk, 2009).

On the one hand, is circadian control, which mediates the timing of sleep in circadian rhythm dependent animals. While diurnal animals sleep during the night, it is vice versa in nocturnal animals. The top-level control is a master oscillator and pacemaker in the suprachiasmatic nucleus (Moore & Eichler, 1972; Ralph, Foster, Davis, & Menaker, 1990). On a genetic level the transcription factor CLOCK (Circadian Locomotor Output Cycles Kaput) is mediating the circadian rhythm. The protein CLOCK controls the expression of the gene *period*, which is a well-conserved and is needed for resetting of the circadian clock to light cues (Albrecht, Zheng, Larkin, Sun, & Lee, 2001).

On the other hand, homeostatic and allostatic processes ensure that the organism sleeps enough by regulating sleep length and depth (Bringmann, 2018). Responsible neurons are located in the human brain for example in the median preoptic nucleus and the ventrolateral preoptic area. They are sleep-active and their activity increases in case of sleep deprivation (Alam, Kumar, McGinty, Alam, & Szymusiak, 2014).

The upstream pathway of homeostatic sleep regulation is not known so far, but increased neuronal activity causes an increase in sleep drive (Krueger et al., 2016; Vyazovskiy, Borbély, & Tobler, 2000). This lead to the hypothesis of sleep-promoting molecules, so-called somnogens, which accumulate during the wake state. Sleep drive would correlate to the amount of present somnogens. A highly likely candidate for a homeostatic sleep-regulating somnogen is adenosine (Porkka-Heiskanen & Kalinchuk, 2011). Other somnogens in turn, like cytokines, seem to induce allostatic sleep-regulating pathways. Particular the cytokines tumour-necrosis factor and interleukin-1β can increase sleep (Bryant, Trinder, & Curtis, 2004). This is an additional hint for the link of sleep and the immune system.

1.6. Model organism *Caenorhabditis elegans* and its nervous system

Sleep is a very complex but on a molecular level still scarcely understood process. To unravel its mysteries, on the one hand, simple but on the other hand, sufficient enough complex model organism is needed, which is present in the form of *Caenorhabditis elegans*.

C. elegans is a nematode and a commonly used model organism in neurobiology. It was the first organism with a fully sequenced genome, and 36% of its ~20'000 protein-coding genes have human homologs (The C. elegans Sequencing Consortium, 1998). For a significant portion of the *C. elegans* genes, mutated alleles exist which offers an easy option for experiments with genetic knock-outs. The biggest part of these alleles was created by the million mutation project (Thompson et al., 2013). One of the most fascinating features of those worms is its eutely. It has an invariant cell lineage which has been completely mapped (Sulston & Horvitz, 1977).

Under normal conditions most of the worms found are self-fertile hermaphrodites, while just around 0.2% are males (Corsi, 2015). Self-fertile hermaphrodites are particular helpful in research as a single worm, e.g. carrying a new transgenic trait, can be used to start a new colony and homozygous hermaphrodites will produce genetically identical offspring(Altun & Hall, 2009). Still, males exist and can be used for crossing purposes.

Each adult hermaphrodite hermaphrodite consists of precisely 959 somatic cells, from which 302 are neurons (Herman, 2006). These build an invariant nervous system and were sorted into 118 classes. So far 6'400 synapses and 900 gap junctions are known (White, Southgate, Thomson, & Brenner, 1986). Other than hermaphrodites' males have 1031 cells including 383 neurons (Herman, 2006).

C. elegans neurons do not have classical action potentials with an influx of sodium ions (Lockery, Goodman, & Faumont, 2009). They rather feature graded regenerative potentials, which are mediated by voltage-gated Ca^{2+} channels. The Ca^{2+} ions function as intracellular signaling molecules, like mediating the release of neurotransmitter via synaptic vesicle fusion (Chapman, 2008).

1.7. Optogenetics in Caenorhabditis elegans

This offers the option to directly measure neuronal activity, by measuring Ca^{2+} levels via the fluorescent calcium indicator GCaMP (Tian et al., 2009). Its fluorescence increases in the presence of Ca^{2+}, for example when a graded regenerative potential is present in the neuron.

On the other way round, neurons can be artificially activated via light-gated ion channels. One example is the red-shifted variant of channelrhodopsin (ReaChr), which opens in the presence of green light in the range of λ ~590–630 nm wavelength for Ca^{2+} ions (Lin, Knutsen, Muller, Kleinfeld, & Tsien, 2013). This can trigger downstream processes like any regular intrinsic Ca^{2+} appearance. As *C. elegans* is susceptible to transgenic manipulation, both optogenetic tools can be genetically expressed in single target neurons given a specific genetic promoter is known.

1.8. Lethargus sleep and L1 arrest sleep in *Caenorhabditis elegans*

Most important, the worms feature phases of reversible but homeostatic regulated behavioral quiescence with an increased arousal threshold, which were therefore identified as sleep. In fact, the worms feature several different types of sleep.

One prominent form of sleep in *C. elegans* is lethargus sleep. If the worms are grown on 20°C they develop from a hatching egg to adulthood in roughly 48 hours. During this period the worms pass through four larval stages (L1 to L4), each separated by a molt and each molt preceded by a 60-90 minutes phase of lethargus sleep (Figure 2) (Altun & Hall, 2009; Raizen et al., 2008). The timing of those molts are controlled by the protein LIM-42, while *lim-42* is a homologue to the earlier mentioned *period* and thus hints to a conserved mechanism of sleep timing control (Jeon, 1999; Monsalve, Van Buskirk, & Frand, 2011; Raizen et al., 2008).

A newly discovered form of sleep in *C. elegans* is called L1 arrest sleep. It appears after the L1 larvae does not find any food past hatching (Wu et al., 2018). After approximately 24 hours it starts to sleep in short bouts of around 5 minutes every hour. Frequency and length of these L1 arrest bouts increase with a further lack of food.

Both sleep types, lethargus and L1 arrest, were shown to be mediated via the single interneuron RIS (Turek, Lewandrowski, & Bringmann, 2013; Wu et al., 2018). It is a GABAergic and peptidergic neuron, which is located on the dexter side in the ventral ganglion and projects a process to the nerve ring (Figure 1) (White et al., 1986). GCaMP measurements in RIS showed activity peaks upon the beginning of quiescence.

Furthermore, the exclusively release of RIS neuropeptides but not the release of GABA alone was sufficient to induce quiescence in the worm (Turek et al., 2013). More precise, the in RIS mainly present neuropeptide FLP-11 is needed for sleep induction (Turek, Besseling, Spies, König, & Bringmann, 2016). FLP-11 expression is regulated via the AP2 transcription factor APTF-1, which itself is controlled via the GABAergic neuron defining transcription factor LIM-6 (Turek et al., 2016). Nonsense mutations in *aptf-1* prevent movement quiescence in both sleep types, although feeding quiescence during lethargus sleep is not affected (Turek et al., 2013; Wu et al., 2018).

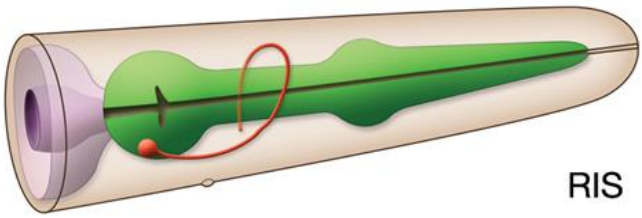

Figure 1 – Interneuron RIS

Schematic representation of a *C. elegans* head (anterior-right, dorsal-up). Including the interneuron RIS (red) projecting its process around the pharynx (green). The pharynx is connected to the intestine (rose, cut). This figure was adopted from WormAtlas.

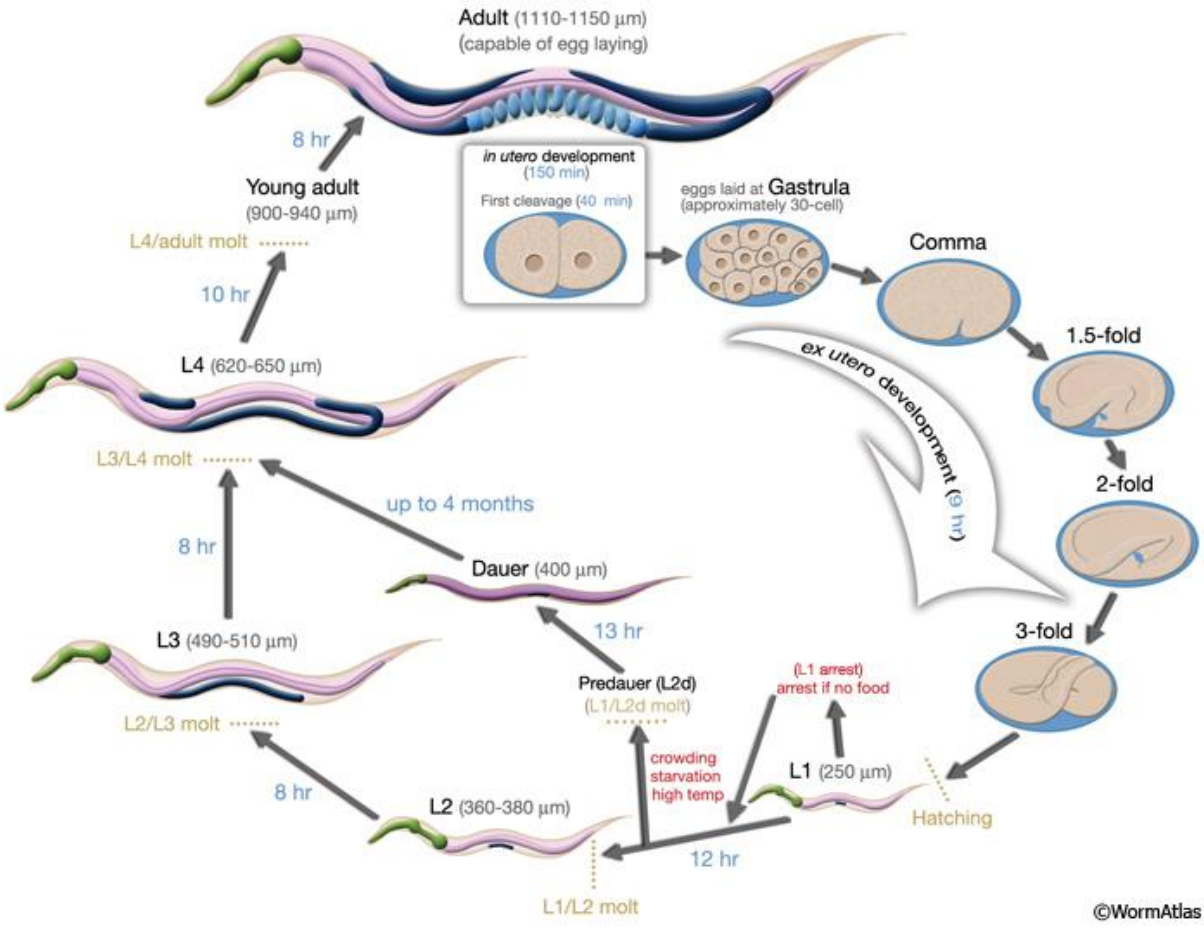

Figure 2 – *C. elegans* life cycles

Life cycle of *C. elegans* from egg to egg-laying adult. In general, after hatching from the egg the worms goes through four larval stages (L1 – L4) until reaching adulthood. Each larval stage is ended by a phase of lethargus sleep and then molting. Larvae which do not find any food after hatching stop in a L1 arrest phase but continue developing regular after access to food supply. L1 larvae in a challenging environment can access an alternative developmental route and become resilient dauer larvae. Duration of each life stage is stated in blue, while the size is indicated in grey brackets. This figure was adopted from Altun and Hall (2009).

1.9. Stress-induced sleep in *Caenorhabditis elegans*

Stress-induced sleep (SIS) is a third and well-described type of sleep in *C. elegans*. Worms show a reversible feeding and locomotion quiescence subsequent to the exposure of various noxious stimuli (Hill, Mansfield, Lopez, Raizen, & Van Buskirk, 2014). This includes hyperosmotic, alcohol, cold, tissue damage as well as heat stress. The worms show quiescence during the stimuli but also in a time window of approximately 60 min after. So far it has been reported that the quiescence after the stimuli is dependent on the interneuron ALA (Hill et al., 2014). It is located in the dorsal ganglion of the head and projects to the dorsal cord and, while passing the nerve ring, to the posterior end of the worm (Figure 3) (White et al., 1986). Like RIS, it is a peptidergic neuron and its

discovered neuropeptides are FLP-13, NLP-8, FLP-7, and FLP-24 (Nath, Chow, Wang, Schwarz, & Sternberg, 2016; Nelson et al., 2014). Nonsense mutation alleles of the homeobox genes *ceh-14* and *ceh-17* cause the development of a nonfunctional ALA neuron, which is useful for ALA ablation experiments (C. Van Buskirk & Sternberg, 2010).

ALA also expresses a epidermal growth factor receptor (EGFR) as well as its downstream pathway via PLCγ (Cheryl Van Buskirk & Sternberg, 2007). The *C. elegans* homolog names for EGF, its receptor and PLCγ are respectively LIN-3, LET-23, and PLC-3. Besides various other functions LIN-3 has in the worm, it was shown that LIN-3 release upon a noxious stimulus causes some SIS via ALA neuropeptide release (Nath et al., 2016; Cheryl Van Buskirk & Sternberg, 2007). The release of FLP-7 neuropeptides does not have an obvious quiescence effect, while FLP-13, NLP-8, and FLP-24 can inhibit locomotion and an avoidance response (Nath et al., 2016). FLP-13 neuropeptide release also causes feeding quiescence (Nelson et al., 2014).

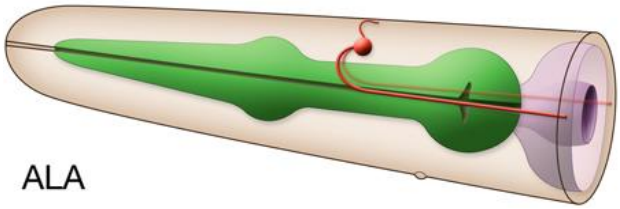

Figure 3 – Interneuron ALA

Schematic representation of a *C. elegans* head (anterior-left, dorsal-up). Including the interneuron ALA (red) projecting its process to the posterior end of the worm. The pharynx (green) is connected to the intestine (rose, cut). This figure was adopted from WormAtlas.

1.10. Conservation of sleep in *Caenorhabditis elegans*

It is very intriguing that not only sleep itself seems to exist across all animal phyla, but also the mechanisms controlling it seems to be conserved across the species. *C. elegans* features the GABAergic/peptidergic sleep-active neuron RIS, while humans have GABAergic/peptidergic sleep-active neurons in the POA, and fruit flies (*Drosophila melanogaster*) have them in four different main brain regions (Bringmann, 2018). The same is true for the link of EGF-signaling and sleep, which was not only found in

C. elegans but also in fruit flies and rabbits, for example (Foltenyi, Greenspan, & Newport, 2007; Kushikata, Fang, Chen, Wang, & Krueger, 1998). If sleep is so conserved, it is from great advantage to use the easily accessible model organism *Caenorhabditis elegans* with its simple nervous system of just 302 neurons to unravel on the one hand the function of sleep and on the other hand the molecular mechanisms behind it.

2. Thesis Aims

One of the biggest unsolved mysteries in neuroscience are the molecular pathways of sleep control. To explore sleep on a molecular level in the mammalian model organism mouse or even in humans would be unnecessarily complicated, because of the complexity of the brain and its inaccessibility on a cellular level without damaging the organism. *C. elegans* in contrast is a widely used model organism for various scientific disciplines. The easy maintenance, genetic accessibility, transparency and invariant nervous system of precisely 302 neurons makes it also valuable for neuroscientific research. That is why I used *C. elegans* to unravel the molecular pathways of sleep control.

At the start of my thesis, the sleep-active neuron RIS and its conserved mechanism of sleep control via neuropeptides and GABA was known. The mainly in RIS present neuropeptide FLP-11 and its genetically control via transcription factor APTF-1 had been discovered. RIS is highly involved in sleep control, but the upstream mechanism of this control or other specialties of this neuron were utterly unknown. This lead to my first thesis aim:

2.1. Aim 1 – Discover what defines RIS as a sleep-active neuron

I obtained three different transcriptomes of RIS. They were produced by two different methods, fluorescence-activated cell sorting with following RNA sequencing (FACS/RNA-seq) and single-cell combinatorial indexing RNA sequencing (sci-RNA-seq). I checked the most enriched genes in those transcriptomes, if either *C. elegans* strains with severe mutations or fluorescent reporter expression for these genes existed. 102 genes were covered by strains with severe mutation alleles, and for 20 genes existed fluorescent reporter lines. I used the fluorescent reporters to confirm their expression in RIS and as a method of validation of the transcriptomes. Further, I screened all strains carrying a severe mutation allele for an L1 arrest sleep phenotype.

Interestingly, I found the EGF receptor signaling pathway expressed and enriched in RIS, which was known before, for its expression in ALA and mediating SIS via neuropeptide release in from this neuron. This occurrence led to my second thesis aim:

2.2. Aim 2 – Identify the role of the EGF pathway in RIS and oppose it to ALA

I used several behavioral, genetic and optogenetic approaches to identify the role of the EGF pathway in RIS and ALA. Via genetically ablation of RIS and ALA, and conditional knock-outs of the EGF receptor *let-23* in RIS combined with a heat shock, I analyzed SIS in young adult larvae. I checked with the help of the calcium ion sensor GCaMP the neuronal activity of ALA and RIS in case of a heat shock or EGF/LIN-3 overexpression. Also, that RIS can be activated by optogenetic stimulation of ALA and by overexpression of the ALA neuropeptide gene *flp-24*. I could show ALA is a sedating neuron, while RIS directly induces sleep bouts. Finally, I confirmed worm survival after cellular stress depends on sedation of ALA, but is not affected by sleep bouts induced by RIS.

3. Materials and Methods

All methods described in this thesis are part of the manuscript we are currently writing. The manuscript is entitled “Epidermal Growth Factor signaling promotes sleep-active neuron depolarization to increase sleep following cellular stress”. It is based on a collaborative project. Sections not written by myself are pointed out directly in advance.

3.1. Worm maintenance and strain genereation

3.1.1. Worm maintenance and strains used in this study

C. elegans was cultured on Nematode Growth Medium (NGM) agarose plates seeded with *E. coli* OP50 and incubated at 20˚C (Brenner, 1974; Stiernagle, 2006). A list of all *C. elegans* strains can be found in **Table 2**.

3.1.2. Molecular biology and transgenic strain generation

All constructs were cloned using the MultiSite Gateway system (Invitrogen, Carlsbad, CA) with pCG150 (Addgene plasmid #17247), which contains *unc-119(+)*, as the destination vector for LR reactions (Merritt & Seydoux, 2010). For verification, all constructs were Sanger sequenced. Genes encoding GCaMP3.35 and ReaChR were used that were codon-optimized for expression in *C. elegans* (Redemann et al., 2011). The following plasmids were generated and used in this study:

Table 1 – Constructs created and used for transgenic strain generation

construct name	construct structure
K351	*flp-24p::SL1-GCaMP3.35-SL2::SL2-mKate2::unc-54 3'UTR, unc-119(+)*
K358	*flp-24p::ReaChr::mKate2-unc-54 3'UTR, unc-119(+)*

3.1.3. Transformation by DNA microinjection

DNA microinjection was used for the generation of transgenic *C. elegans* strains (Evans, 2006). A young adult hermaphrodite was transferred using a ~0.5 µL drop of Halocarbon oil 700 (Sigma) into a ~2 µL drop of the same oil on an agar pad. To generate the agar pad before the start of the injections, a drop of 3% agarose in water was placed onto a glass slide, flattened with a glass slide, and dried for one hour on a 95°C heating block before. The worm was gently positioned with an eyelash to fix it on the agarose surface. Next, the glass slide with the fixed worm was placed onto a microinjection microscope setup, which consisted of an inverted microscope (Nikon, Eclipse Ti-S), a micromanipulator (Eppendorf, Patchman) and an electrical microinjector (Eppendorf, FemtoJet). A microinjection needle (Eppendorf, Femtotips 2), pre-filled with DNA, was mounted on the microinjector. The needle was filled with DNA solution containing TE buffer, the target construct DNA, a co-injection marker DNA and was filled up with pCG150 DNA (Addgene plasmid #17247 (Merritt & Seydoux, 2010)) to a final concentration of 100 ng/µL. As co-injection marker coel::RFP (*unc-122p::RFP*) was used, which expresses a red fluorophore in the coelomocytes (Addgene plasmid #8938 (Miyabayashi, Palfreyman, Sluder, Slack, & Sengupta, 1999)).

The construct was injected at the following concentrations:
goeEx727: K358 10 ng/µL, coel::RFP 10 ng/µL, pCG150 80 ng/µl

The needle was inserted carefully into one arm of the gonad with the help of a micromanipulator, and DNA solution was injected with an injection pressure of 29.0 psi for an injection time of 0.4 seconds. Constant pressure was at 2.00 psi. The needle was retracted from the gonad and the worm was recovered with a 2 µL drop of M9. The worm was retracted from the liquid using a platinum wire pick and a drop of bacteria and transferred to a fresh NGM plate. After growing the worm at 20°C for 48 hours, F1 larvae were inspected with a fluorescence microscope for the expression of the co-injection marker and positive transformants were selected.

3.1.4. Transformation by microparticle bombardment

A second method used for the creation of transgenes was gold microparticle bombardment. *unc-119(ed3)* were used for bombardment and transformants were selected based on phenotypic rescue conferred by the *unc-119(+)* present in the plasmid that was used for transformation (Praitis, Casey, Collar, & Austin, 2000; Wilm, Demel, Koop, Schnabel, & Schnabel, 1999). Gold microparticles (chemPUR) sized 0.3-3 µm were coated with the DNA using spermidine (Sigma-Aldrich, 50 mM) and polyvinylpyrrolidone (Sigma-Aldrich, P-5288, Mol. 360, 0.1 mg/ml in 96% EtOH). Synchronized young adult worms were transferred onto NGM plates, which contained a 1 cm diameter bacterial lawn in their center and were cooled down by placing them on ice prior to transferring the worms. 20 µL of gold particle suspension was loaded onto the filter of a particle gun (Caenotec, Braunschweig). Helium (purity 5.0) was used at 8 bar to accelerate the particles into a vacuum chamber (-0.4 bar) onto the worms. Each construct was transformed eight times. Worms were recovered by cutting each NGM plate into six pieces after transformation and placing each piece onto a 12 cm NGM plate. Transformants were selected after two weeks incubation of the plates at 25°C. To select motile transformants, a 1 x 1 cm piece of an NGM plate seeded with OP50 was placed onto the plate and transformants were removed 0.5 - 1 h later from the bacterial lawn.

3.1.5. CRISPR-based gene editing

CRISPR-based gene edited *let-23(zh131)* allele was kindly provided by Silvan Spiri and Prof. Dr. Alex Hajnal. They added a *frt::gfp::3xFlag* sequence in the 3' region of the *let-23* locus, and they added a second *frt* site 2 kb upstream of *frt::gfp* and 5`to the protein kinase domain in the *let-23* locus (Figure 4).

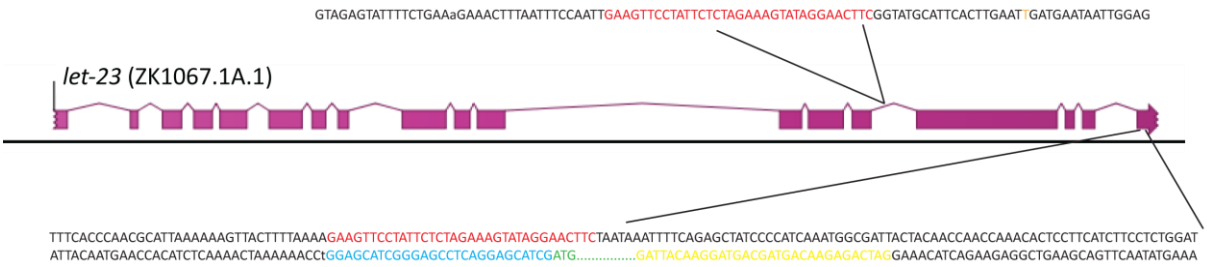

Figure 4 – CRISPR/Cas9-based editing of the let-23 locus

A schematic representation of the generation of the conditional *let-23* allele *zh131*. Sections shows *let-23(ZK1067.1A.1)* on Chromosom II, Color coded sequences refer to insertions in *zh131*: Black: genomic sequence; Red: FRT sites; Orange: mutation of PAM for sgRNA3_let-23BtyrK; Blue: linker sequence; Orange: mutation of PAM; Green: GFP; Yellow: Flag Tag.
This figure was kindly provided by the research group of Prof. Dr. Alex Hajnal.

The *ilys-4(syb700)* deletion allele was generated by SunyBiotech using CRISPR/Cas9 and deletes 1270 nucleotides (the entire coding region) of the *ilys-4* gene between the following flanking sequences:

gttcttgtgcgaatatctgaaattttattgtcattcagattcagattttcagatgtcta
cactggaaacgaatatcatgatcttacagcagacattctcattatcagatttgaaagaa
cataaattgcactgaaaaacatattaaaaattttgctccttccctatccaaaatatata
taataaataaattagaaatttcatattttaaaattacagtcacagatgaagccgccgtg
aatgaaaaaactcccaaa-
tgaacatttttaatacttcagtcgcatatttatattgggaagagcattttctgtgcca
cattgctctctaataaataattattttactatacggagattttcgagctactgaactaa
attgaa

3.1.6. Strain generation by genetic crossing

Transgenes were backcrossed two times against N2. For following genotypes during strain crossing, the animals were genotyped using either Duplex PCR genotyping of single worms (mostly to detect deletions) (Ahringer, 2006), tetra-primer ARMS-PCR (to detect single nucleotide changes)(Ye, 2001), or sanger sequencing (to detect single nucleotide changes). Primers used for genotyping are listed in **Table 3**.

3.2. Generation of the transcriptomes

3.2.1. Transcriptome extraction from single-cell RNA sequencing data

Data generated via ‘Bulk sequencing of FACS-isolated cells’ was kindly provided by Prof. Dr. David M Miller III and based on the method described in Spencer et al. (2014). Generating and processing the transcriptomes “FACS/RNA-seq RIS vs. all”, “sci-RNA-seq RIS vs. all”, “sci-RNA-seq RIS vs. neurons”, and “sci-RNA-seq ALA vs. neurons” was done by Dr. Andreas Leha from the “Medical Biometry and Statistical Bioinformatics” core facility at the UMG, Göttingen. Dr. Leha also kindly provided the following methods parts “Transcriptome generation of bulk sequenced FACS-isolated cells”, “Single cell sequencing”, “Differential expression analysis of RIS versus all neurons”, “Differential expression analysis of RIS versus all cells”, and “Differential expression analysis of ALA and comparison with RIS” for it.

3.2.2. Bulk sequencing of FACS-isolated cells

RIS was specifically labelled using *mKate2* expression from the *flp-11* promotor (Turek et al., 2016) and isolated from a population of synchronized L2 larvae via FACS. It is followed up by RNA sequencing of the sorted cells. This method has been used to generate several validated neural transcriptomes in *C. elegans* (Lim et al., 2016; Spencer et al., 2014).

3.2.3. Transcriptome generation of bulk sequenced FACS-isolated cells

To analyze data for bulk sequencing, Quality Control of the input reads was done using fastQC (version v0.11.2; Andrews, Simon, 2014, "FastQC A Quality Control tool for High Throughput Sequence Data" https://github.com/s-andrews/FastQC). Star (version 2.4.0) was used to align reads to the reference assembly WBcel235 of *Caenorhabditis elegans* (Dobin et al., 2013). Gene annotation was used from release 94. Multiqc (version 1.5) was used to facilitate quality control on the input data as well as the alignment statistics (Ewels, Magnusson, Lundin, & Käller, 2016). Gene level counts were generated using RSEM (version 1.2.19) to deal with multimapping reads (Li & Dewey, 2011). All downstream analyses have been performed in R (version 3.4.0; Core Team, 2018, R: A Language and Environment for Statistical Computing. Vienna, Austria: R Foundation for Statistical Computing. https://www.R-project.org/). Read counts were normalized using tximport (version 1.8.0) (Soneson, Love, & Robinson, 2015). Counts per million (CPM) values were generated for first unbiased analyses. Correlation based clustering and a principal component analysis (PCA) analysis were conducted to assess sample structure and identify potentially problematic samples. Differential expression analysis was done using edgeR (version 3.24.3) fitting a negative binomial generalized log-linear model to the read counts for each gene (Robinson, McCarthy, & Smyth, 2010). P values are results from a likelihood ratio test and have been adjusted for multiple testing using Benjamini-Hochberg. The significance level was set to alpha = 5% for all statistical tests.

Three biological replicates of isolated RIS and three biological replicates of control cells (all cells) were collected and bulk sequenced. One RIS sample was excluded from the analysis as it did not cluster with the other replicates. 4'504 genes were down regulated in RIS according to this analysis of which 3'183 were statistically significant. 3'197 genes

were up regulated of which 1’188 were statistically significant. Among the four most strongly enriched genes was *flp-11*, with an enrichment of 890-fold. Differential genes are listed in **Table 4**.

3.2.4. Single cell sequencing

For single-cell sequencing, the data set from Cao et al. (2017) was used in this analysis. To identify the transcriptome cluster corresponding to RIS within the neuronal sci-RNA-seq clusters we used our previous observations that only RIS strongly and specifically expresses *flp-11* neuropeptides (Turek et al., 2016). Gene counts and t-SNE based cell clusters were used as provided by the authors. Using the expression of the marker gene *flp-11*, one cluster was identified as the RIS cells. Cells with less than 70 UMI counts were discarded from the analysis. Only genes with at least one count in at least 5 cells were considered in the subsequent analysis. Differential expression analysis was done using edgeR (version 3.24.3)(Robinson et al., 2010), fitting a negative binomial generalized log-linear model to the read counts for each gene. P values are results from a likelihood ratio test and were adjusted for multiple testing using Benjamini-Hochberg. Differential expression analysis was performed twice, once comparing RIS genes to all other remaining genes and once comparing RIS genes to all other cells. The significance level was set to alpha = 10% for all statistical tests. All analyses have been performed in R (version 3.4.0; R Core Team 2018). The single cell count data by Cao et al. (2017) contains counts for 20’271 genes in 42’035 cells derived from L2 larvae. Cluster 13 was identified as the RIS cell cluster, containing 44 RIS cells.

3.2.5. Differential expression analysis of RIS versus all cells

Here the analysis was conducted on all 42’035 cells from the single-cell data set (Cao et al., 2017). Post filtering, there were 9’497 genes available in 39’634 cells (of which 44 were RIS cells) for differential expression analysis. The results were compared to the results obtain from Bulk-RNAseq data. 7’719 genes were down regulated in RIS according to this analysis of which 138 were statistically significant. 1’410 genes were up regulated of which 243 were statistically significant. The most strongly enriched gene was *flp-11*, with an enrichment of 588-fold. Differential genes listed in **Table 5**.

Comparing the differentially and significantly expressed genes from the single-cell sequencing data set with the differentially and significantly genes from the bulk sequencing data set there were 228 genes present in both data sets. Comparing all differentially expressed genes from the single-cell sequencing data set with the differentially and significantly genes from the bulk sequencing data set there were 691 genes present in both data sets.

3.2.6. Differential expression analysis of RIS versus all neurons

Here the analysis was conducted on the 7'603 neuronal cells only. Post filtering, there were 9'497 genes available in 7'448 cells (of which 44 were RIS cells) for differential expression analysis. 8'100 genes were down regulated in RIS according to this analysis of which 6 were statistically significant. 1'331 genes were up regulated of which 60 were statistically significant. The most strongly enriched gene was *flp-11*, with an enrichment of 157-fold. Differential genes listed in **Table 6**.

Comparing the differentially and significantly expressed genes from the single-cell sequencing data set with the differentially and significantly genes from the bulk sequencing data set there were 58 genes present in both data sets. Comparing all differentially expressed genes from the single-cell sequencing data set with the differentially and significantly genes from the bulk sequencing data set there were 479 genes present in both data sets.

3.2.7. Differential expression analysis of ALA and comparison with RIS

Genes expressed in ALA were also extracted from the data set from Cao et al. (2017) as above. To identify the transcriptomes corresponding to ALA we used the previous observations that ALA expresses *nlp-24*, *flp-13*, and *flp-7* neuropeptides (Nath et al., 2016; Nelson et al., 2014). Cells with less than 70 UMI counts were discarded from the analysis. Only genes with at least one count in at least 5 cells were considered in the subsequent analysis. Here the analysis was conducted on the 7'603 neuronal cells only.

Post filtering, there were 9’497 genes available in 7’448 cells for differential expression analysis. 22 cells, which formed part of cluster 11, were identified as ALA (Cao et al., 2017). Differential expression analysis was done using edgeR [version 3.24.3; @edgeR] fitting a negative binomial generalized log-linear model to the read counts for each gene (Robinson et al., 2010). P values are results from a likelihood ratio test and have been adjusted for multiple testing using Benjamini-Hochberg. The significance level was set to alpha = 10% for all statistical tests. Differential expression analysis was performed comparing ALA cells to the remaining pan-neuronal cells. 8’286 genes were down regulated in RIS according to this analysis of which 0 were statistically significant. 1’189 genes were up regulated of which 22 were statistically significant. Among the top enriched genes were *nlp-24*, *let-23*, *flp-7*, and *nlp-8*, which have previously been demonstrated to be expressed in ALA, indicating that the ALA transcriptome was correctly identified (Nath et al., 2016; Cheryl Van Buskirk & Sternberg, 2007). Differential genes listed in **Table 7**.

Pairwise correlations of logFC from tests vs pan-neuronal background were computed. Columns and rows were ordered following hierarchical clustering. All neuronal clusters with less than 100 cells were compared to the remaining pan-neuronal background. Based on the resulting logFC, pairwise correlations and hierarchical clustering were calculated.

3.3. Microscopy imaging and behavioral analysis

3.3.1. Long-term imaging using hydrogel microchambers

Imaging of behavior and calcium activity was performed using Agarose Microchamber Imaging (AMI) as described (Bringmann, 2011; Turek, Besseling, & Bringmann, 2015). Shortly, a polydimethylsiloxane (PDMS) mold was used to create microcompartments from melted 3% high-melting agarose (Fisher Scientific GmbH) dissolved in S-Basal (Stiernagle, 2006). The following chamber sizes were used: 190 µm x 190 µm x 15 µm (X length x Y length x Z depth) for L1, 370 µm x 370 µm x 45 µm for adults. The microchambers were filled with either eggs (for L1 arrest experiments) or young adults (for heat shock experiments), sealed with a cover slip, and attached with double-side adhesive tape (Sellotape) into an opening milled into a 3.5 cm plastic Petri dish. An additional 2 mL volume of 3 % high melting agarose was filled to form a ring around the

agar block containing the micro compartments, serving as a moisture reservoir. The space between the agarose pad and the agarose ring of the Petri dish was filled with melted 3% low melting agarose dissolved in S-Basal. The sample equilibrated for at least 2 h before the start of imaging. For imaging, a home-made heating lid was used that kept the temperature at 25°C to avoid condensation.

3.3.2. Microscopy setups for imaging

Imaging was performed on either a TiE or Ti2 inverted microscope (Nikon) with an automated XY stage (Prior, Nikon). The following objectives were used: 40x 0.45 NA dry, or 60x 1.4 NA oil for reporter co-expression experiments, 10x NA 0.45 dry with DIC filter for L1 arrest experiments and 20x NA 0.75 dry with an additional 0.7 lens placed in the c-mount of the camera for all experiments with young adult worms. Adults were imaged using the 10x objective. L1s were imaged with the 20x objective. This constellation allowed fitting 1 and 30 chambers simultaneously onto the camera chip for adults and L1, respectively. Microscopes were equipped with red-light (Semrock BrightLine HC 785/62, 45 mm diameter) dia illumination for differential interference contrast (DIC), which was used for behavioral imaging. Standard filter sets were used for GFP/GCaMP (ET-EGFP, Chroma) and mKate2 (TexasRed, Chroma) fluorescence imaging and optogentic stimulation. Images were acquired using either am electron multiplying charge-coupled device (EMCCD) camera (iXon DU-897D-C00-#BV, 512 x 512 pixels, Andor) or back-illuminated sCMOS camera (Prime 95B, 1’174 x 1’174 pixels, Photometrics) for fluorescence imaging. For experiments requiring only DIC imaging, an sCMOS camera (Neo, 2’560 x 2’160 pixels, Andor) was used. For fluorescence illumination and optogenetics an LED system was used (CoolLED). The LED system provided light with the wavelength of 488 nm for GFP excitation and 565 nm for mKate2 excitation and was triggered via the transistor-transistor logic (TTL) “fire out” signal of the camera. The software used to control the microscope and image acquisition was either iQ2/iQ3 (Andor) or NIS elements (Nikon).

3.3.3. Calcium imaging and optogenetics

For 490nm illumination for GCaMP imaging, light intensity was 0.16 mW/mm^2 using a 20x objective. EM gain was set to 200 and exposure time was 20 ms. For 565 nm illumination (mKate2 imaging), light intensity for was 0.06 mW/mm^2 using a 20x objective. Light intensities were quantified using a light voltmeter (PM100A, Thorlabs). Samples were fixed on the microscope for long-term imaging experiments using a home-made aluminum sample holder for 3.5 cm plastic dishes. For ReaChR experiments, worms were fed with all-trans Retinal (Sigma, ATR). 20 µL of a 0.2 mM ATR solution was added to a seeded NGM plate and L3/L4 worms were placed on it. The plate was stored dark at 20°C in an incubator and were used for optogenetic experiments the following day. For control experiments worms grown without ATR were used.

For optogenetic experiments worms were placed into microchambers and imaged at a frame rate of 0.3 frame/s. The optogenetic experiment consisted of three parts. First, RIS GCaMP baseline activity was recorded for 5 min, followed by a 5 min optogenetic activation period (1.09 mW/mm^2) while we continued to record GCaMP fluorescence. After the end of the activation period an additional 5 min of GCaMP fluorescence was recorded. Green light illumination for optogenetic activation was shuttered so that it only occurred in between the acquisitions. Each worm was probed optogenetically for 3 to 4 times with a break of at least 2 hours in between each trial. All trials for each worm were averaged to obtain one N. Individual worms that did not express ReaChR in the ALA neuron were identified post hoc and were censored.

3.3.4. Reporter gene expression in RIS

Genes enriched in the RIS transcriptome were tested with existing reporter strains reported in the literature to be expressed in RIS. Reporter strains expressing GFP were crossed with an mKate2-expressing reporter strain for RIS. *mKate2* expression was driven via the *flp-11* promoter. Cross progeny animals were immobilized in a 5 µL drop of levamisole on a 200 µL high-melting agarose pad on a glass slide and covered with a cover slip. Co-expression of both fluorescent gene reporters was either tested with a spinning disc system (488 nm, 565 nm lasers, Andor Revolution, Yokogawa CSU-X1, Nikon TiE) or on a standard widefield fluorescence microscope setup (Nikon TiE, LEDs 488 nm, 565 nm). On both setups either 40x, 60x or 100x oil objectives were used. A

z-stack was taken through the worm's head and the maximum projection was calculated. The gamma values for each color channel were adjusted for display.

3.3.5. Mutant sleep screen during L1 arrest

L1 arrest screening was done with AMI. Usually five strains plus a wild type (N2) control were filmed in one experiment. For this experiment, 12 pretzel stage eggs per strain were taken from a growing population and transferred into microchambers (190 µm x 190 µm x 15 µm). Each egg was transferred using an eyelash into an individual chamber while care was taken to not transfer any food. The eggs of each strain were arranged in adjacent microchambers so that they formed a characteristic pattern and thus were unambiguously identifiable. After the agarose microchambers were sealed, they were placed into an incubator at 20°C in the absence of light for 48 hours, during which the worms hatched and arrested at the L1 larval stage. Then the arrested worms were imaged using DIC for 12 h with a frame rate of 0.2 frames/s and exposure time of 20 ms using a 10x objective combined with an additional 1.5x lens (total magnification was 150 x). Sleep bouts were extracted for individual worms using frame subtraction and mutants with either significantly decreased or increased sleep fraction were retested. If the mutant strain had not yet been outcrossed against N2 after mutagenesis, it was outcrossed two times before retesting. If the phenotype persisted, it was outcrossed for an additional two times (to a total of 4 x) and tested again. Only mutations that produced a significant sleep phenotype after 4 x outcrossing were scored as screen hits.

3.3.6. Induction of cellular stress by heat shock

All heat shock experiments were performed in young adult worms before the first egg was laid. AMI was used with chambers of the size 370 µm x 370 µm x 45 µm. 8 to 10 young adult worms were transferred into a 5 µL drop of sterile distilled water placed on the agarose pad containing the microchambers with as little food as possible. While the liquid soaked into the agarose, individual worms were distributed into individual agarose microchambers with an eyelash. The microchambers were sealed with a cover slip and attached with double-faced adhesive tape to an opening of a metal plate that was part of a home-made temperature control device. The temperature control device contained the

sample in a 10 x 10 mm opening of a metal plate (490 x 200 mm) and contact between the metal plate and the microchambers was created by filling the space with additional liquid agarose. The temperature of the metal plate and sample was measured by a Pt1000 temperature sensor that was placed in close proximity of the sample. Temperature was controlled by a Peltier element and its controller (Peltier-Controller TC0806, CoolTronic). The Peltier element transported energy from or to a metal grid acting as a heat sink, which itself was equilibrated with the surrounding air temperature using a small fan (Figure 5).

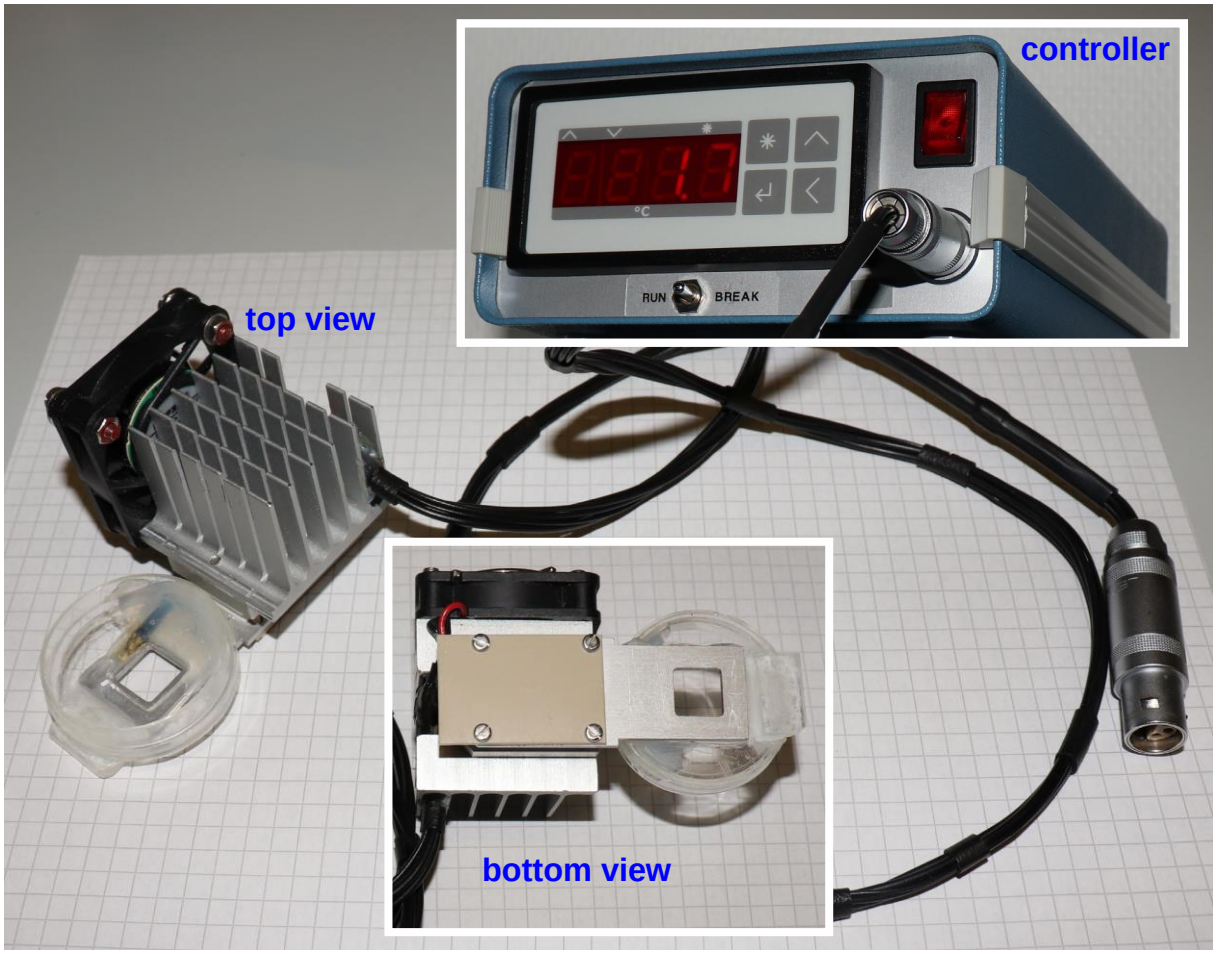

Figure 5 – Heat control device

An agarose microchamber on a glass slide can be placed in the hole of the metal plate (bottom view, right side), which is attached to a Peltier element. Heat is transported by the Peltier element from the metal plate to a metal grid, which is equilibrated with the surrounding air temperature using a small fan (top view). A small petri dish is also glued to the metal plate to allow the filling with agarose, serving as a moisture reservoir and creating contact between the metal plate and the microchambers.

For the heat shock experiments, the device with the agarose pad and worms was stored in a dark 20°C incubator to equilibrate for 90 minutes. The device was then placed into a standard glass slide holder on an imaging microscope, connected to the Peltier controller and the temperature was set to 22°C. The plastic dish containing the microchambers was closed by a heated lid, whose temperature was set to 25°C to avoid drying out of the sample and condensation on the lid. Each worm was imaged for 3 hours with a sampling rate of 0.05 frame/s. In the first 60 minutes, baseline activity was imaged. Then the heating lid temperature was turned to 37.5°C and after 3 min the Peltier-Controlled metal plate was set to 37,0°C for a duration of 20 min to deliver the heat shock. To end the heat shock, the Peltier-Controller was set to 22°C and the lid was set to 25,0°C again. After the end of the heat shock, imaging was continued for an additional 2 h.

3.3.7. Induction of protein overexpression through temperature increase and *hsp-16.41p*

For overexpression of *lin-3* and *flp-24*, the *hsp-16.41* promoter and a temperature increase was used (Nath et al., 2016; Cheryl Van Buskirk & Sternberg, 2007). The handling procedure of delivering this temperature increase for inducing gene expression was the same as the procedure of delivering a heat shock. The only differences were the length and the magnitude of the temperature stimulus. The length was slightly increased from 20 to 30 min but the temperature was increased to only 30.0°C and the heating lid to only 30.5°C, both for 30 min. Worms were filmed for another 6 hours after the temperature increase, with 22°C and the lid set to 25.0°C. Control experiments without the heat shock-inducible transgene showed that this milder temperature increase was insufficient to trigger measurable stress-induced sleep.

3.3.8. Lifespan assay

Lifespan measurement were performed after heat shock similar to previously described. Briefly, a synchronized population of young adult worms was subjected to a heath shock and survival was followed (Hill et al., 2014; Kaeberlein et al., 2006). Worm populations were synchronized by isolating embryos and hatching them in the absence of food (Lewis & Fleming, 1995). For each strain, two 6 cm plates full with gravid hermaphrodites were

taken. Worms were harvested by washing them off with 2 mL M9, and transfer into a 1.5 mL Eppendorf tube. Worm were pelleted by centrifugation at 4.8 * 10^3 rcf, the supernatant was removed and 500 µL of freshly prepared bleach solution was added to the pellet. To prepare the bleach solution, a stock solution of 1:1 1M NaOH solution and hypochlorite solution was diluted 1:2 with distilled water. Tubes with worms and bleach solution were mixed for 90 seconds by gentle manual agitation. Eggs were pelleted by centrifugation and the pellet was washed with 1 mL M9. Pelleting and bleaching was repeated and followed by three washing steps with 1 mL of M9 each.

The isolated eggs were resuspended in 1 mL M9 and transferred to a clean 1.5 mL Eppendorf tube. The tube was placed on a spinning shaker overnight. On the next day eggs had hatched and larvae were arrested at the L1 stage. 200 µL of each strain was pipetted on an NGM plate containing bacterial food. Worms were allowed to develop until the young adult stage in a dark 20°C incubator. For the heat shock a water bath (GFL, 1083) was heated to 40°C, and the correct temperature was verified by the internal and an additional external thermometer of the water bath (Greisinger electronic, GMH3710). The temperature was monitored during the whole heat shock process. For each strain 50 young adult worms were transferred onto 5 NGM plates, to obtain exactly 10 worms per seeded plate. These plates were sealed with parafilm and simultaneously placed into the water bath. The plates were placed into the water so that the half that contained the agar with the worms was down and submerged in the water. After 20 min, all plates were removed simultaneously from the bath and placed on ice for exactly 2 minutes. Water on the outside of the plates was removed with paper towels and the plates were stored in a dark incubator at 20°C. Every 24 h worm survival was counted by an experimenter that was blind to the genotype of the worms. Each worm that was not spontaneously moving was stimulated with a short pulse (10-20 s) of blue LED light delivered by a stereomicroscope (Leica, M165 FC). If the worm reacted to this light stimulus it was scored as “alive”. If no reaction was observed it was counted as “dead” and removed from the plate. Worms which could not be found on the plate, e.g. crawling up the plate wall and dry out, were counted as “censored”.

3.4. Quantification and statistical analysis

3.4.1. Sleep detection using frame subtraction

All imaging data was saved as single .tif files and were further analyzed using home-made MATLAB (MathWorks) routines. Sleep bouts were defined by immobility, which was detected using a frame subtraction algorithm as described (Nagy, Raizen, & Biron, 2014). For the analysis, the image was cropped to only contain one microchamber containing one individual worm. For each frame, intensity values of each pixel were subtracted from the consecutive frame and the average of the absolute values for each frame was computed. The mean intensity was smoothed over 40 frames. The smooth function used was a robust version of a linear regression, which used weighted linear least squares and a 2nd degree polynomial model, by assigning lower weight to outliers in the regression (`smooth(y,method,'rloess')`). Intensities of the smoothed data were then normalized with 1 presenting the highest intensity value, and 0 the lowest intensity value. A sleep bout during L1 arrest was defined as a smoothed normalized value that was lower than 40% of the maximum intensity for at least 120 seconds. The sleep bouts extracted from the data set for each worm were used to calculate the mean sleep bout length, sleep bout frequency, and fraction of time spent in sleep bouts. Individual traces in which no sleep bouts were visible by manual inspection were scored as not containing any sleep bouts. The fraction of time spent in quiescence was used as a main criterion to score phenotypes in the genetic screen. Data for different individuals was averaged and statistically compared with wild type N2 data obtained from an internal control (worms analyzed on the same agarose chip). In adult worms, sleep was defined by the same criteria as in L1 arrested larvae. To statistically compare after the heat shock, sleep data was binned by averaging data corresponding to time intervals of each 30 min following the heat shock.

Neuronal activity of the worms was measured with the green fluorescent calcium sensor GCaMP3 expressed either from the RIS-specific *flp-11* or from the ALA-specific *flp-24* promoter (Tian et al., 2009; Turek et al., 2016; Wu et al., 2018). RIS was extracted based on fluorescence intensity using a home-made MATLAB routine. For RIS extraction, the pixels of each frame were binned 4:1 and the highest intensity pixel was identified that defined the center of the RIS neuron. The x-y position of this highest pixel was used to center a region of interest containing RIS and to crop this region from the original frame. The size of the region of interest was chosen to contain RIS and a limited amount of background (13 x 13 pixels for overexpression experiments and 21x21 pixels for

optogenetic experiments). To identify RIS within the region of interest, its mean intensity was calculated and pixels that had a higher intensity than 25% of the mean of all pixels were counted as “signal”. Pixels below 25% mean signal intensity were counted as “background”. To calculate RIS intensity, the mean of all “background” intensities was subtracted from the mean of all “signal” intensities. Accurate tracking by the software algorithm was manually controlled at four time points (first frame, the frame after 1/3 of the movie, the frame after 2/3 of the movie, and the last frame in the movie). Image series in which RIS could not be identified automatically were censored. ALA position was identified by manually selecting the center for cropping a region of interest. For this procedure, a semi-automatic MATLAB routine was used that performed the same downstream data analysis as the automatically tracking routine.

Neural intensities measured before applying the heat shock were used as baseline and data was normalized as difference over baseline (ΔF/F). To determine sleep bouts in calcium imaging data sets, movement of the animal was detected based on the position of the center of the tracked head neuron. To extract sleep bouts, first the speeds were normalized, similar as described before but without any smoothing. Sleep was defined as time periods of less than 1.5% of the normalized movement speed.

3.4.2. Statistical tests

Statistical tests used were Wilcoxon rank tests for paired samples and Cox proportional hazards regression to test survival rates (both calculated in MATLAB). P values for differential expressed genes in the transcriptomes are results from a likelihood ratio test and have been adjusted for multiple testing using the Benjamini-Hochberg Procedure with a false discovery rate of 5% for FACS/RNA-seq data or 10% for sci-RNA-seq data, respectively (calculated in R). The specific tests used are described in the figure captions and the results section. The graphs show mean ± SEM unless noted. Compact boxplots were used for the visualization of L1 arrest screen data, with the box representing the 25%-75% range, the black dot representing the median and empty circle representing outliers. All other boxplot show individual data points, the box represents the 25%-75% range, and the thin gray line is the median. Whiskers for both types of boxplots corresponds to approximately +/–2.7σ, which is 99.3 percent coverage if the data are

normally distributed. Both types of boxplots were plotted via the (`boxplot`) function of MATLAB. For each experiment at least two biological replicates were performed and the number of biological replicates is stated in the figure legend.

4. Results

All results described in this thesis are part of the manuscript we are currently writing. The manuscript is entitled “Epidermal Growth Factor signaling promotes sleep-active neuron depolarization to increase sleep following cellular stress”. It is based on a collaborative project and the results presented in the section “Single RIS neuron Transcriptome” were produced by the collaboration partners as stated here: Generation of the FACS/RNA-seq raw data was done by research group of Professor David M. Miller, III, Ph.D., Vanderbilt University, Nashville, Tennessee, USA. The data used for the generation of all sci-RNA-seq transcriptome was published by Cao et al. (2017). My colleague Max Fritz identified the clusters representing RIS and ALA neurons in the sci-RNA-seq data initially. Generation of the “FACS/RNA-seq RIS vs. all” transcriptome, and RIS sci-RNA-data transcriptomes “RIS vs all”, “RIS vs neuron”, and “ALA vs neuron” from the present raw data was done by Dr. Andreas Leha from the Core Facility, Medical Biometry and Statistical Bioinformatics, „Universitätsmedizin Göttingen" (UMG), Germany.

The conditional allele *let-23(zh131[FRT::let-23::FRT::GFP::LoxP::FLAG::let-23]) II.*, used in the section “The EGFR acts in ALA and RIS to induce sleep after cellular stress”, was created and kindly provided by the research group of Prof. Dr. Alex Hajnal, University of Zurich, Switzerland.

4.1. Single RIS neuron Transcriptome

To identify the molecular pathways important in the sleep-active neuron RIS, I obtained three different RIS transcriptomes. One transcriptome was produced in a collaboration with the research group of Professor David M. Miller, III, Ph.D. via RNA-seq of fluorescence-activated cell sorted (FACS) RIS cells (Spencer et al., 2014). The other two transcriptome were extracted from the single cell transcriptome (SCT) dataset of Cao et al. (2017).

This Cao et al. dataset was produced by using sci-RNA-seq. They were able to create 42’035 SCTs spanning all L2 cells of *C. elegans*, which were sorted into according clusters. My colleague Max Fritz identified Cluster 13 as RIS, because of the highly enriched presence of the gene *flp-11* and *aptf-1* compared to all other neuronal clusters

(Figure 6A and Figure 6B). *Aptf-1* is mainly and *flp-11* almost exclusively expressed in RIS (Turek et al., 2016, 2013). Cluster 13 had an logFC of 7.3 for *flp-11* compared to all neuronal clusters. In total, 60 genes were significantly upregulated, while 6 genes were significant less expressed in the 44 cluster 13 cells.

Gene expression of cluster 13 was also compared to gene expression in all L2 cells from the sci-RNA-seq data set and revealed a significantly enriched expression of *aptf-1*, *C10C6.7*, *unc-25* and *unc-47*. These genes were reported before to be expressed in RIS (Jin, Jorgensen, Hartwieg, & Horvitz, 1999; McIntire, Reimer, Schuske, Edwards, & Jorgensen, 1997; Turek et al., 2016, 2013). It was an additional confirmation for cluster 13 consisting of RIS cells. In general this sci-RNA-seq RIS vs. all transcriptome had 381 significant differentially expressed genes, with 243 genes enriched and 138 de-enriched. So, two RIS sci-RNA-seq transcriptomes were obtained by either comparing cluster 13 to all L2 cells or to all neurons.

The transcriptome obtained by Prof. Miller group used FACS to collect a pool of RIS cells, which were used in the next step for RNA-seq (Spencer et al., 2014). They used a *C. elegans* strain HBR1261, which expresses the red fluorophore mKate2 under the *flp-11* promoter specifically in RIS. After dissociating L2 larvae, they were able to separate red glowing RIS neurons from all other non-fluorescent cells. Expression levels of genes in these RIS L2 cells were statistically compared to the gene expression of a dataset consisting of all *C. elegans* L2 cells. In the RIS dataset 1’188 genes were enriched and 3’183 genes were de-enriched.

An overlap list of the three transcriptomes, FACS/RNA-seq RIS vs all, sci-RNA-seq RIS vs all, sci-RNA-seq RIS vs neurons, contained 51 genes which were significantly enriched in all of them (**Table 8**). These genes are likely true-positive hits and might play a crucial role in RIS-dependent sleep regulation.

For validation of the combined RIS transcriptome, I checked the expression of 14 genes in RIS, for which fluorescent reporter strains were available. These strains were crossed with the RIS expressing mKate2 strain and checked under the microscope for colocalization. Six genes had already been reported before to express in RIS and were not checked again: *unc-47* (McIntire et al., 1997), *lim-6* (Hobert, Tessmar, & Ruvkun, 1999),

unc-25 (Jin et al., 1999), *aptf-1* (Turek et al., 2013), *C10C6.7* and *flp-11* (Turek et al., 2016). The gene *srd-32* was recently reported to express in RIS but checked for confirmation (Vidal et al., 2018). Seven genes, *nlp-11*, *ser-7*, *zig-2*, *sbt-1*, *ilys-4, plc-3* and *let-23* I newly confirmed to express in RIS (Figure 6C and Figure 7). It is worth pointing out that three reporter, *let-23*, *plc-3* and *ilys-4* also expressed in the interneuron ALA (Gravato-Nobre, Vaz, Filipe, Chalmers, & Hodgkin, 2016; C. Van Buskirk & Sternberg, 2010; Cheryl Van Buskirk & Sternberg, 2007). *srd-32* was recently reported to express in RIS, which I confirmed here (Vidal et al., 2018). The three genes *nlp-11*, *ser-7*, and *zig-2* just showed faint expression in RIS. Not all checked reporter strains colocalized in RIS as six strains did not show any visible expression there (Figure 8). These genes were *nlp-13*, *nlp-37*, *nlp-8*, *flp-1*, *ins-27*, and *ins-24*.

A summary of the reporter check can be found in Figure 6D. Nine genes appeared in all three transcriptomes. The missing expression of six genes in RIS could be caused by either being false positive hits of the transcriptome or false negative reporter strains. The transcriptome derived from FACS/RNA-seq had all previously known and the newly discovered reporter. As it had a high number of enriched genes, more broadly expressed genes are presumably also in the list. The single-cell transcriptomes seemed to contain genes, which expressed in RIS much more specific.

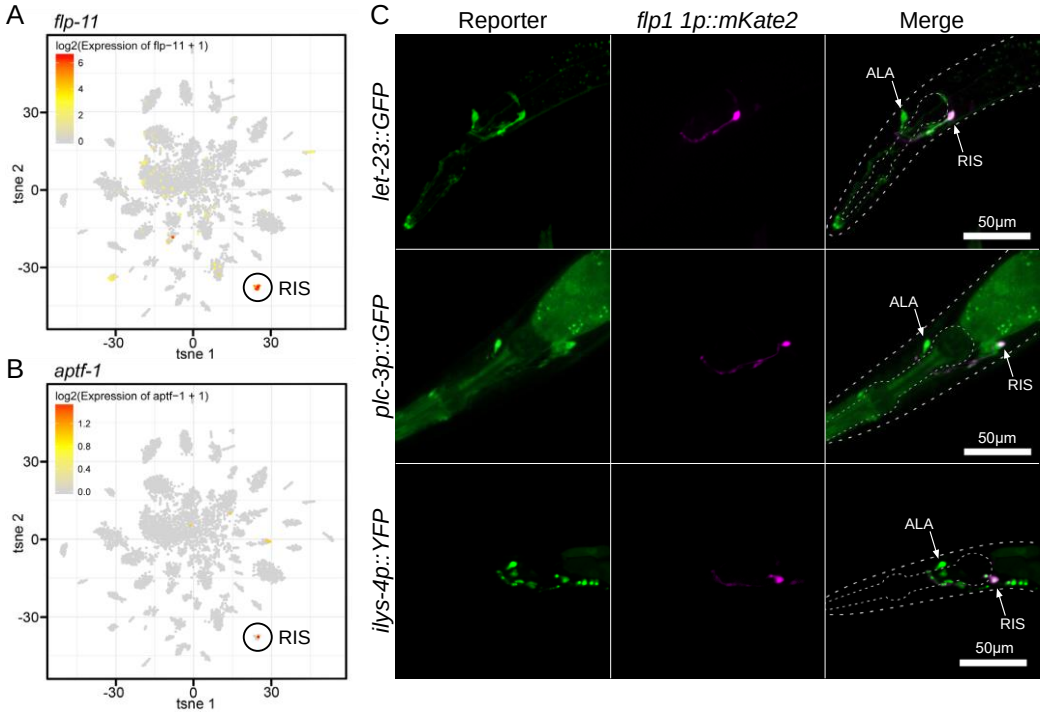

D

Gene	Reporter	FACS/RNA-seq [RIS vs all]	sci-RNA-seq [RIS vs all]	sci-RNA-seq [RIS vs neurons]
flp-11	Turek et al. (2016)	**9,8**	**9,2**	**7,3**
C10C6.7	Turek et al. (2016)	**9,8**	**2,4**	**1,1**
aptf-1	Turek et al. (2013)	**8,6**	**1,3**	**0,5**
lim-6	Hobert et al. (1999)	**7,2**	0,5	0,1
unc-25	Jin et al. (1999)	**6,2**	2,2	0,3
unc-47	McIntire et al (1997)	**6,3**	**1,7**	0,5
srd-32	Vidal et al. (2018) + Fig.7	**6,6**	0,5	0,1
let-23	Fig.6C	**4,3**	2,2	**1,5**
plc-3	Fig.6C	**3,4**	**1,9**	**1,0**
ilys-4	Fig.6C	**7,0**	**3,4**	1,6
sbt-1	Fig.7	**5,7**	**4,1**	**1,8**
nlp-11	Fig.7	**7,5**	**4,8**	**2,7**
ser-7	Fig.7	**4,7**	**2,1**	0,8
zig-2	Fig.7	0,4	**1,9**	0,6
nlp-8	Fig.8	**7,3**	**5,1**	**3,0**
nlp-13	Fig.8	**7,5**	**4,2**	**2,2**
nlp-37	Fig.8	0,4	**2,0**	0,7
flp-1	Fig.8	0,7	**4,0**	1,7
ins-24	Fig.8	**2,2**	**1,8**	0,7
ins-27	Fig.8	**3,3**	**1,6**	**0,6**

Figure 6 – Sleep-active RIS neuron transcriptome computed from single-cell data

(A-B) Identification of RIS from sci-RNA-seq data. tsne-plots of all neuronal cells were color coded for log2 expression values of (A) *flp-11* or (B) *aptf-1*.
(C-D) Validation of RIS enriched genes using fluorescent transgene reporters. (C) Example micrographs for *let-23::GFP*, *plc-3p::GFP*, *ilys-4p::GFP*, and their co-localization with *flp-11p::mKate2*. Dashed lines display the outlines of the head and pharynx (anterior is left, dorsal is up). ALA and RIS are indicated with white arrows. Scale bar is 50µm. (D) Table summarizing genes tested for fluorescence-reporter expression in RIS via colocalization of *flp-11p::mKate2* and comparison of RIS transcriptomes obtained by either bulk sequencing of FACS-isolated cells or sci-RNA-seq. Enrichment is displayed as log2FC and color coded with darker green color indicating more enrichment in RIS. Significantly enriched genes are displayed as bold and underlined. For statistical comparison a likelihood ratio test was used, adjusted for multiple testing using Benjamini-Hochberg (α = 5% for FACS/RNA-seq, α = 10% for sci-RNA-seq).

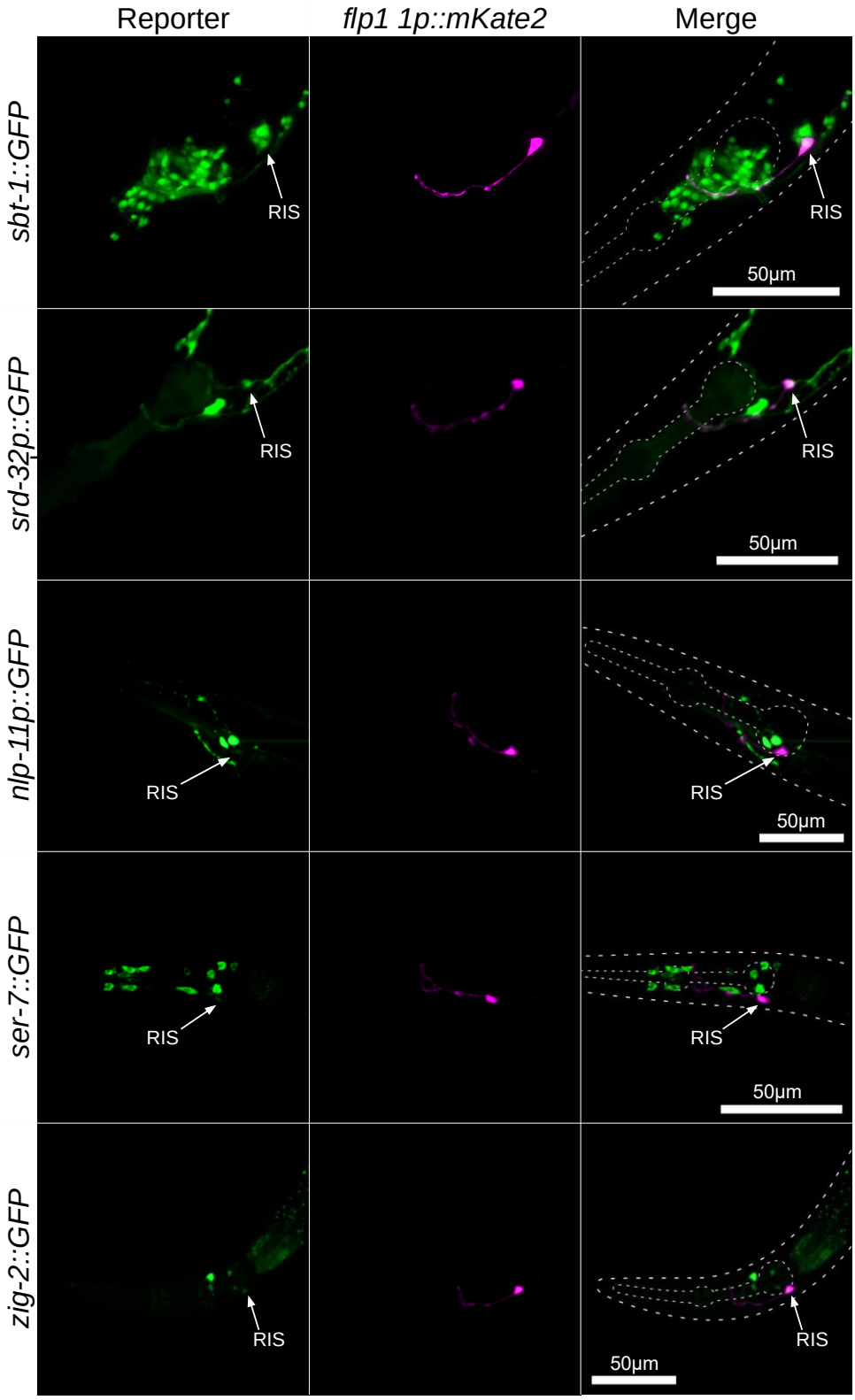

Figure 7 – RIS enriched genes for which fluorescence transgene reporters are expressed in RIS

Validation of RIS enriched genes using fluorescent transgene reporters. Example micrographs for *srd-32p::GFP*, *sbt-1::GFP*, *nlp-11p::GFP, ser-7::GFP, zig-2::GFP*, and their co-localization with *flp-11p::mKate2*. Dashed lines display the outlines of the head and pharynx (anterior is left, dorsal is up). RIS is indicated with a white arrow. Scale bar is 50µm.

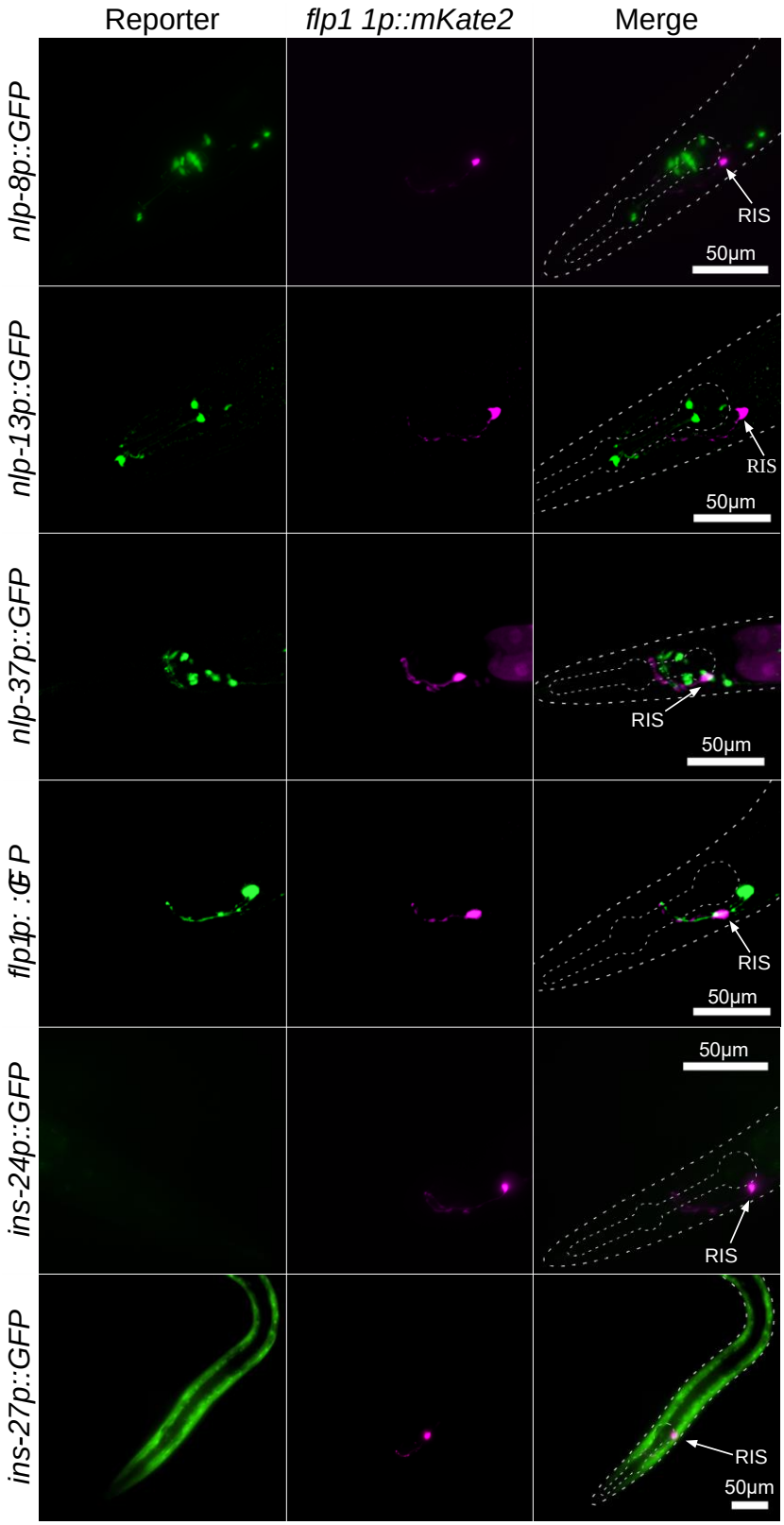

Figure 8 – RIS enriched genes for which fluorescent transgene reporters do not show RIS expression

Validation of RIS enriched genes using fluorescent transgene reporters. Example micrographs for *nlp-8p::GFP*, *nlp-13p::GFP*, *nlp-37p::GFP*, *flp-1p::GFP*, *ins-24p::GFP*, *ins-27p::GFP*, and their co-localization with *flp-11p::mKate2*. Dashed lines display the outlines of the head and pharynx (anterior is left, dorsal is up). RIS is indicated with white arrows. Scale bar is 50µm.

4.2. RIS transcriptome-based L1 arrest screen

To identify genes which play a role in the molecular control of RIS and sleep, I did a behavioral screen based on the newly obtained RIS transcriptomes. I was particular interested what really specifies RIS on a molecular level, so I focused on the sci-RNA-seq transcriptome for the screen. I checked the top hits in the transcriptomes for the availability of severe genetic mutations. These were found via the online *C. elegans* gene and protein function search tool GExplore V1.4 (Hutter & Suh, 2016). Missense mutations were excluded, while nonsense mutations, altered splicing sites, deletions, insertions, readthroughs, and complex changes were included in the screen. Approximately two-thirds of genes were covered with severe genetic mutations. 104 alleles were screened, with 43 alleles coming from the Million Mutation Project (MMP), 16 alleles from the "National Bioresource Project for the Experimental Animal Nematode *C. elegans*" from Japan and 45 alleles from other sources (Mitani, 2009; Thompson et al., 2013).

I used L1 arrest sleep for the behavioral screen, because it was not developmentally regulated like lethargus sleep. It was shown that L1 arrest is a robust sleep state (Wu et al., 2018). The L1 larvae were starved for 48 hours after hatching and then recorded with AMI for 12 hours. Worms showed short quiescence bouts without movement. Length and frequency of these bouts were quantified via image subtraction as well as the total quiescence fraction for the whole 12 hours (Nagy et al., 2014). Each strain carrying a mutation was statistically compared to N2 wild type worms. Strains which showed a significant difference were backcrossed against N2 wild type strain and their L1 arrest sleep was measured again. 16 alleles were excluded from the screen as the worms showed severe developmental problems. They often died in the egg or as an early L1 larvae, but if they still survived 48 hours without food, they were small and deformed so L1 arrest sleep could not be properly quantified. The excluded alleles were *sma-1(e30)*, *T21D12.12(gk191670)*, *glb-23(gk205062)*, *F54H5.5(gk335875)*, *glb-32(gk360316)*, *lmd-4(gk389517)*, *B0416.3(gk481746)*, *lgc-4(gk509234)*, *F57B10.4(gk712994)*, *frpr-16(gk722062)*, *Y116A8B.4(gk869095)*, *Y57G11C.36(gk961271)*, *nhr-194(gk784872)*, *ida-1(ok409)*, *nlp-8(ok1799)*, and *C39B10.1(ok2789)*.

Eight alleles showed movement quiescence, which deviated more than 50% from the wild type mean and was significant (Figure 9A). Four alleles had less quiescence:

aptf-1(gk794), *flp-11(tm2706)*, *goa-1(sa734)*, and *frpr-3(gk240031)*. The other alleles showed more quiescence, e.g. *nhr-128(gk960157)*. *ilys-4* had two alleles, *syb700* and *gk402093*, which produced a similar increased fraction of L1 arrest sleep.

Another interesting hit was a gain-of-function allele (*sa62*) of *let-23*. This lead to a two times increased movement quiescence fraction in L1 arrest. As *let-23* is the sole *C. elegans* homolog of the EGF receptor it was interesting to find out, that the two downstream pathways via PLCγ/PLC-3 on the one side, and Grb2/SEM-5, Ras/LET-60, and Raf/LIN-45 on the other side were also enriched in the RIS transcriptome (Figure 9B). The IP3 receptor ITR-1, which is the downstream target of the PLCγ/PLC-3, was de-enriched in Cluster 13. This was to be expected as it is broadly expressed in *C. elegans* (Moghal & Sternberg, 2003). All canonical EGF signaling genes were expressed in RIS.

The presence of the EGF receptor signaling pathway in RIS suggests that not only ALA, but also RIS is involved in the EGF response to cellular stress (Cheryl Van Buskirk & Sternberg, 2007). To check for more similarities an ALA vs. neurons sci-RNA-seq transcriptome was obtained similar to the RIS vs. neurons sci-RNA-seq transcriptome. A 22 cell-spanning sub-cluster of neuronal cluster 11 was identified to represent ALA because of the expression of *flp-24*, *flp-13*, and *flp-7* (Nath et al., 2016; Nelson et al., 2014). ALA also expressed all canonical components of the EGF intracellular signaling pathway as previously reported (Figure 9C, Cheryl Van Buskirk and Sternberg 2007; Nath et al. 2016). Pairwise correlations of differential expression for all discernable neuronal transcriptomes and hierarchical clustering revealed a relatively low degree of similarity in gene expression for RIS and ALA (Figure 9D). Thus, ALA and RIS both express EGFR signaling components but otherwise their overall molecular contents are different suggesting that both neurons are activated by EGF but are functionally divergent.

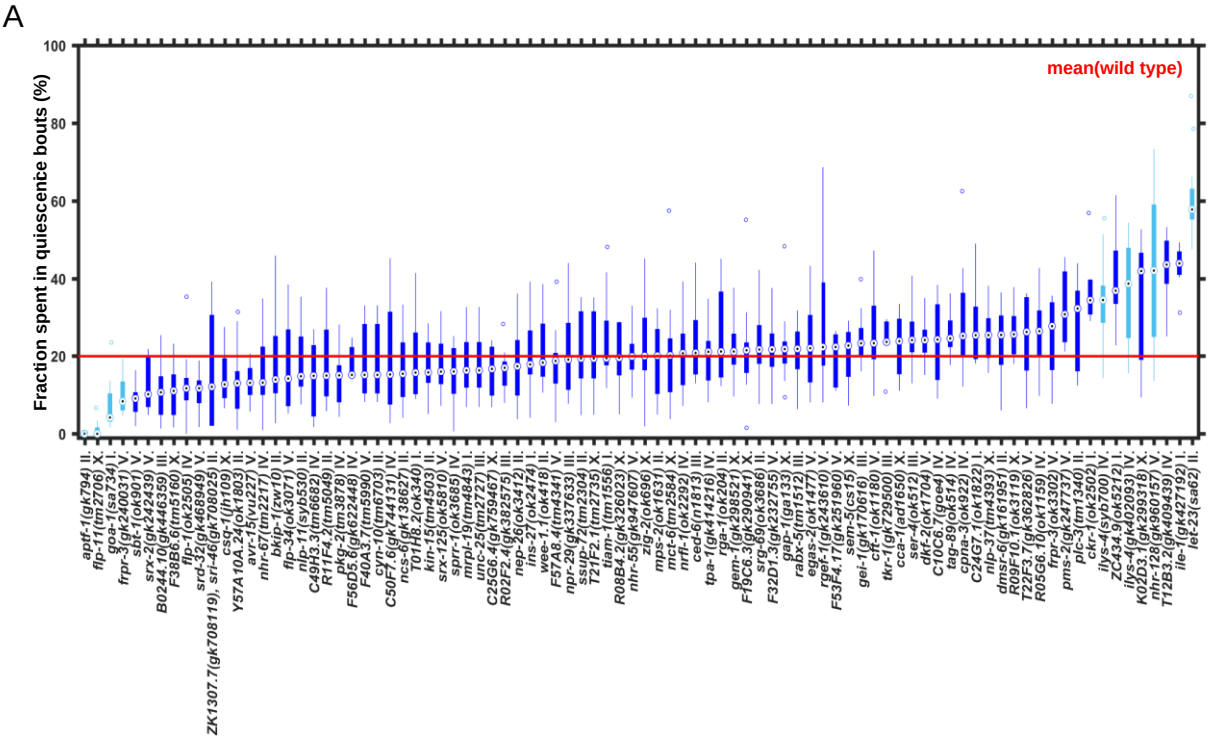
A
mean(wild type)
Fraction spent in quiescence bouts (%)
100
80
60
40
20
0

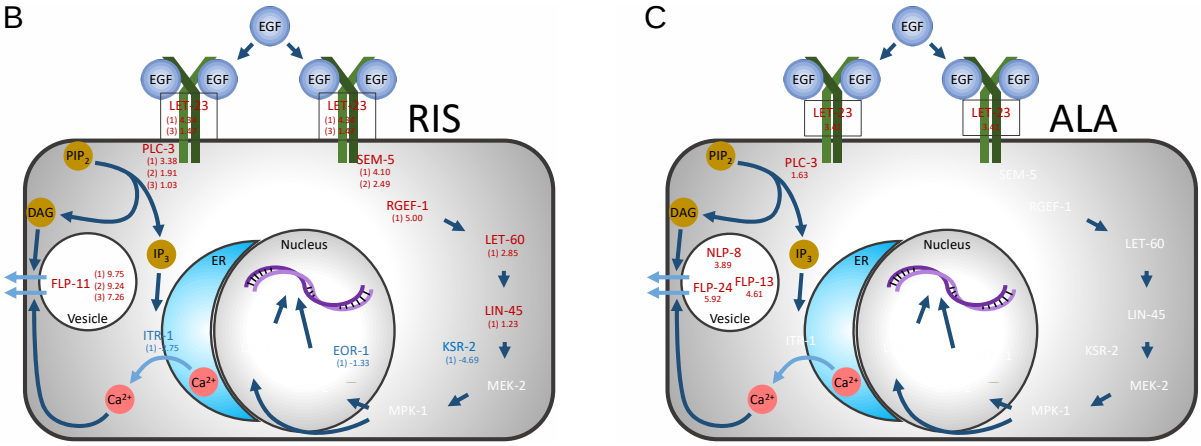
B
RIS
EGF
LET-23
PIP2
PLC-3
SEM-5
RGEF-1
DAG
IP3
ER
Nucleus
LET-60
FLP-11
Vesicle
LIN-45
ITR-1
EOR-1
KSR-2
Ca2+
MEK-2
MPK-1

C
ALA
EGF
LET-23
PIP2
PLC-3
DAG
IP3
ER
Nucleus
NLP-8
FLP-24
FLP-13
Vesicle
LET-60
LIN-45
KSR-2
Ca2+
MEK-2
MPK-1

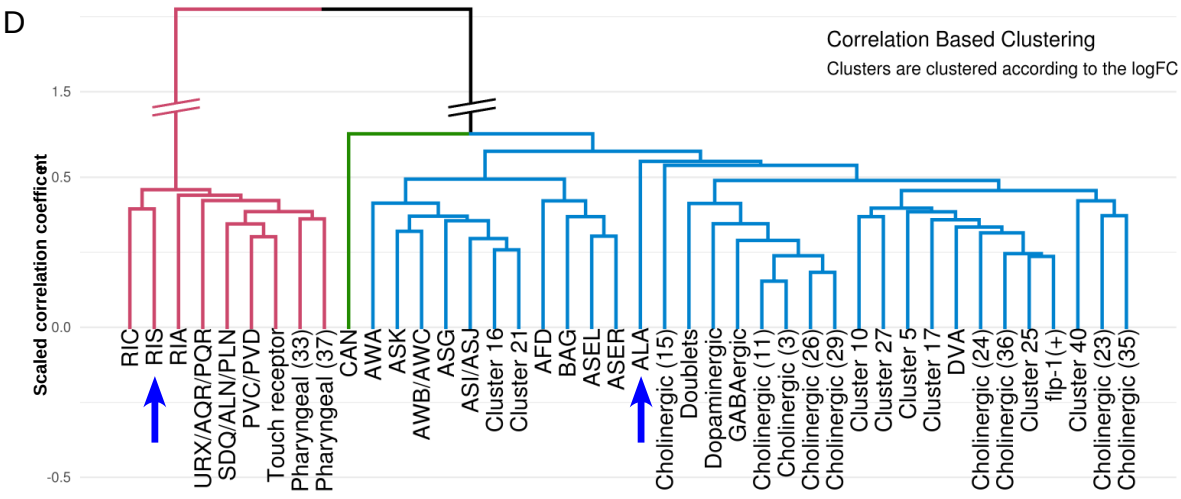
D
Correlation Based Clustering
Clusters are clustered according to the logFC
Scaled correlation coefficent
1.5
0.5
0.0
-0.5
RIC
RIS
RIA
URX/AQR/PQR
SDQ/ALN/PLN
PVC/PVD
Touch receptor
Pharyngeal (33)
Pharyngeal (37)
CAN
AWA
ASK
AWB/AWC
ASG
ASI/ASJ
Cluster 16
Cluster 21
AFD
BAG
ASEL
ASER
ALA
Cholinergic (15)
Doublets
Dopaminergic
GABAergic
Cholinergic (11)
Cholinergic (3)
Cholinergic (26)
Cholinergic (29)
Cluster 10
Cluster 27
Cluster 5
Cluster 17
DVA
Cholinergic (24)
Cholinergic (36)
Cluster 25
flp-1 (+)
Cluster 40
Cholinergic (23)
Cholinergic (35)

Figure 9 – The EGFR signaling machinery is expressed in both ALA and RIS neurons

(A) L1 arrest sleep screen for mutants of genes that are enriched in RIS. Every allele screened is represented by a blue boxplot (alleles are on the x-axis, fraction (%) spent in movement quiescence on the y-axis), wild type mean is displayed as a red line. Alleles that deviated more than 50% of the wild type mean and were significantly different to the respective control data are indicate in turquoise, $p < 0.05$, Wilcoxon signed-rank test. The strongest increase of sleep is seen in a gain-of-function mutation of *let-23*.
(B-C) Both ALA and RIS express EGF pathway components. Shown are enrichments of canonical EGFR signaling components in RIS (B) and ALA (C). Proteins (green) or neuropeptides (light blue), which were found to be significantly differentially expressed in at least one of the transcriptomes are indicated (enriched is red, de-enriched is blue, no significant change is white). (B) Gene expression changes are displayed as log2FC ((1) indicates RIS vs. all, FACS/RNA-seq; (2) indicates RIS vs. all, sci-RNA-seq; (3) indicates RIS vs. neuron, sci-RNA-seq). (C) Gene expression changes are displayed as log2FC (ALA vs. neuron, sci-RNA-seq). PIP2: phosphatidylinositol 4,5-bisphosphate, IP3: inositol trisphosphate, DAG: diacylglycerol, ER: endoplasmic reticulum. Likelihood ratio test, adjusted for multiple testing using Benjamini-Hochberg, $\alpha = 5\%$ for FACS/RNA-seq, $\alpha = 10\%$ for sci-RNA-seq.
(D) Despite an overlap of expression of EGFR signaling components, RIS and ALA are divergent in overall gene expression. Correlation-based clustering of all neuronal clusters identified from single-cell sequencing. Scaled correlation coefficient with 0 meaning perfect positive correlation and 2 meaning perfect negative correlation. Blue arrows indicate the clusters corresponding to RIS and ALA.

4.3. The EGFR acts in ALA and RIS to induce sleep after cellular stress

As the *let-23(gf)* allele produced a much-increased sleep in L1 arrest and I discovered it is expressed in both known sleep neurons, ALA and RIS, the question how much each neuron is contributing to the phenotype came up. To test their roles, I genetically ablated each neuron in the *let-23(gf)* mutation background and measured the L1 arrest quiescence fraction. RIS ablation was achieved by the *flp-11* promoter-driven expression of the apoptosis inducer *egl-1* (Wu et al., 2018). ALA was functionally ablated by a mutation in the *C. elegans* homeobox gene *ceh-17*. The allele *ceh-17(np1)* disturbs the expression of a group of genes in ALA, including *let-23* and *plc-3*, while additionally interfering with its process outgrowth (C. Van Buskirk & Sternberg, 2010). RIS ablation completely eliminated L1 arrest sleep in the *let-23(gf)* mutant. ALA ablation on the other hand caused a decrease of L1 arrest quiescence duration, although still being increased compared to wildtype levels (Figure 10A). This result showed that both sleep neurons are responsible for the increased sleep in the *let-23(gf)* mutant. ALA caused some mild increase in the EGFR-triggered quiescence duration but RIS was needed to induce those sleep bouts in the first place while also increasing their summed duration.

This result and the newly discovered occurrence of the EGFR signaling pathway in RIS led to the hypothesis that ALA is not the sole inducer of EGF-caused sleep, as previously reported (Hill et al., 2014; Nath et al., 2016; Nelson et al., 2014). To test this hypothesis, I heat shocked worms for 20 minutes at 37°C in a functionally ablated background of RIS, ALA, or both. RIS functionally ablation was caused by the mutated AP2 transcription factor *aptf-1* (Turek et al., 2013). The heat shock was applied via a Peltier element to young adult worms in agarose microchambers. This setup allowed the quantification of sleep behavior before, during, and after the heat shock.

Wild-type worms showed no sleep before the heat shock, complete immobility during, and rhythmic bouts of quiescence until one hour after the heat shock. In the *aptf-1(-)* mutant, the number of worms quiescent during the heat shock was reduced by at least 20%, and worms showed almost none quiescence after it. Worms with *ceh-17(-)* immobilized slower during the heat shock and had fewer sleep bouts after it. While wild-type worms showed SIS for around 40% of the first half hour after the heat shock, worms with an functionally ablated ALA showed less than 10% SIS and functionally ablated RIS had almost no SIS during that period. The *ceh-17(-)* and *aptf-1(-)* double mutant showed quiescence levels between the levels of the two alleles alone. Although a part of this quiescence seemed to come from an extension of the immobility caused by the heat shock, suggesting that double ablation perhaps caused some unspecific quiescence (Figure 10B-G). The experiment confirmed the previously reported influence of ALA on SIS (Goetting, Soto, & Van Buskirk, 2018; Hill et al., 2014; Cheryl Van Buskirk & Sternberg, 2007). Additionally, it was shown that RIS also takes a vital role in controlling SIS by being responsible for the induction of sleep bouts.

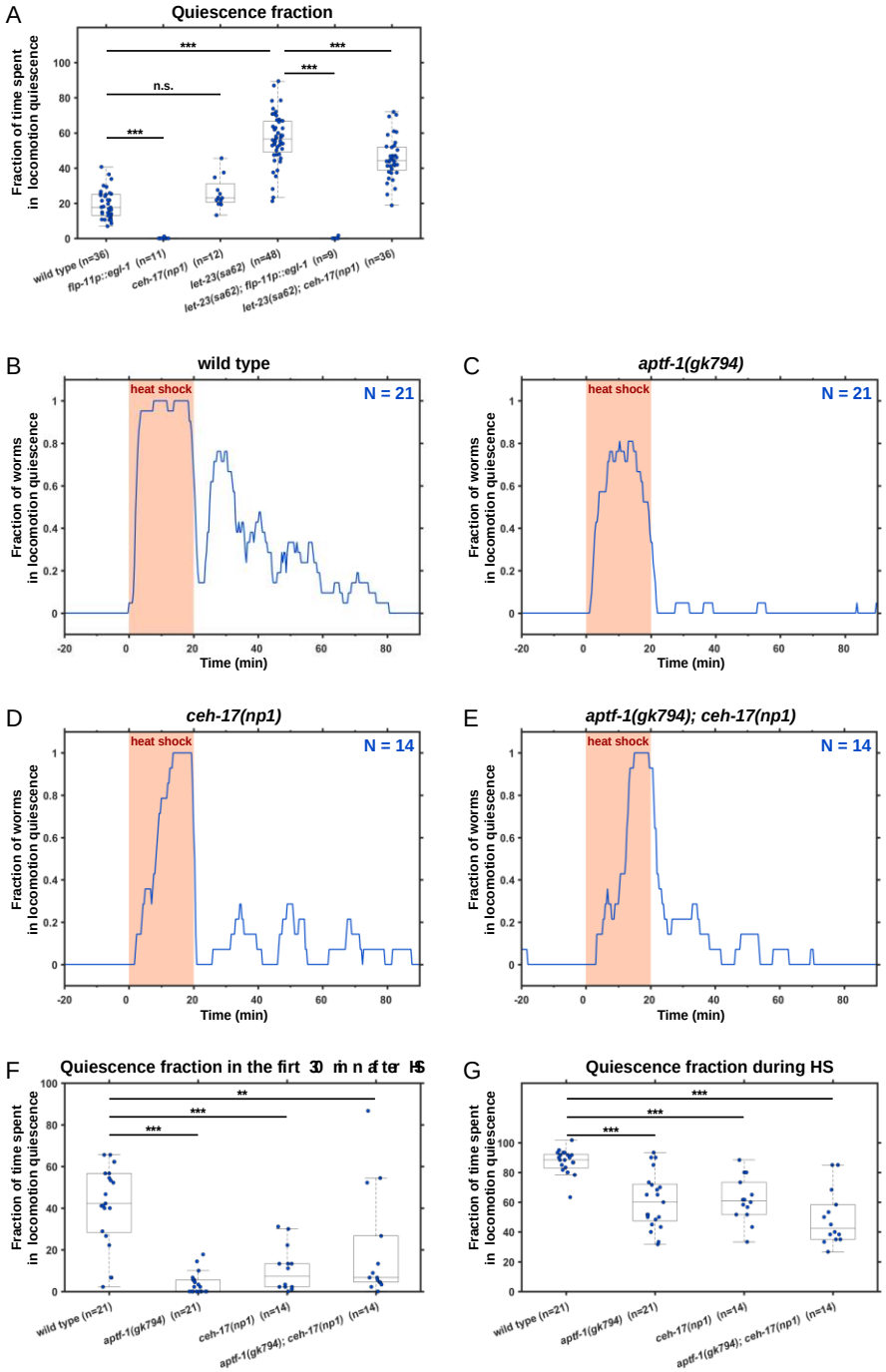

Figure 10 – ALA and RIS are required for sleep after EGFR activation and cellular stress

(A) ALA and RIS are required for sleep caused by *let-23gf* during L1 arrest. Fraction of time spent in sleep during L1 arrest was measured by quantifying locomotion quiescence. *ceh-17(-)* partially suppressed the increase of sleep caused by *let-23gf*. RIS-ablation suppressed virtually all sleeping behavior.
(B-E) ALA and RIS are required for sleep induced by cellular stress. The fraction of worms is shown vs. time, with the time during which the heat shock (37°C) was applied is indicated in orange. N is number of worms; three biological replicates were performed for each genotype. (B) Wild type worms immobilized during heat shock and showed a series of consecutive quiescence bouts during the 60 minutes after the heat shock. (C) *aptf-1(-)* showed reduced movement quiescence during the heat shock and almost no quiescence was seen following the heat shock. (D) *ceh-17(-)* mutants took longer to immobilize during the heat shock and sleep bouts were reduced following the heat shock. (E) *aptf-1(-)*; *ceh-17(-)* double mutation reduced quiescence, albeit not as strongly as *aptf-1(-)* alone.
(F-G) Quantification of locomotion quiescence. *** denotes statistical significance with $p < 0.001$, ** denotes statistical significance with $p < 0.01$, Wilcoxon signed-rank test.

The neuronal ablation experiments showed that both ALA and RIS are required to promote sleep following EGFR activation. The question was if EGFR signaling was needed for SIS in RIS, like it was reported for ALA (Cheryl Van Buskirk & Sternberg, 2007). This was checked via a specific knock-out of the EGFR gene *let-23* in RIS. I used a conditional allele *zh131* of *let-23*, in which a critical exon is flanked by *frt* sites and can thus be removed through FLPase-induced recombination (Davis, Morton, Carroll, & Jorgensen, 2008; Hubbard, 2014; Voutev & Hubbard, 2008). Besides the *frt* sites, a *gfp* gene was incorporated close to the 3' end of the *let-23* gene, so a LET-23::GFP fusion protein was produced. The FLPase expression in my experiments was driven by the *unc-47* promoter, which expresses in RIS but not ALA. Via microscopy imaging, I could confirm that the fluorescent LET-23::GFP was present in ALA and RIS, while being absent in RIS in worms with *unc-47p::FLP* background (data not shown). Applying a heat shock (37°C, 20 min) to worms carrying both, *frt*-flanked *let-23* and *unc-47::FLP*, reduced SIS to roughly 50% compared to the parental strains (Figure 11). Thus, EGF signaling is required in both ALA and RIS to promote sleep following heat shock. These results suggest a model in which EGF is released following cellular stress and activates both ALA and RIS, which act concertedly to induce sleep. The consistently stronger effect of RIS impairment on sleep bouts compared with ALA impairment suggests that ALA might act upstream of RIS.

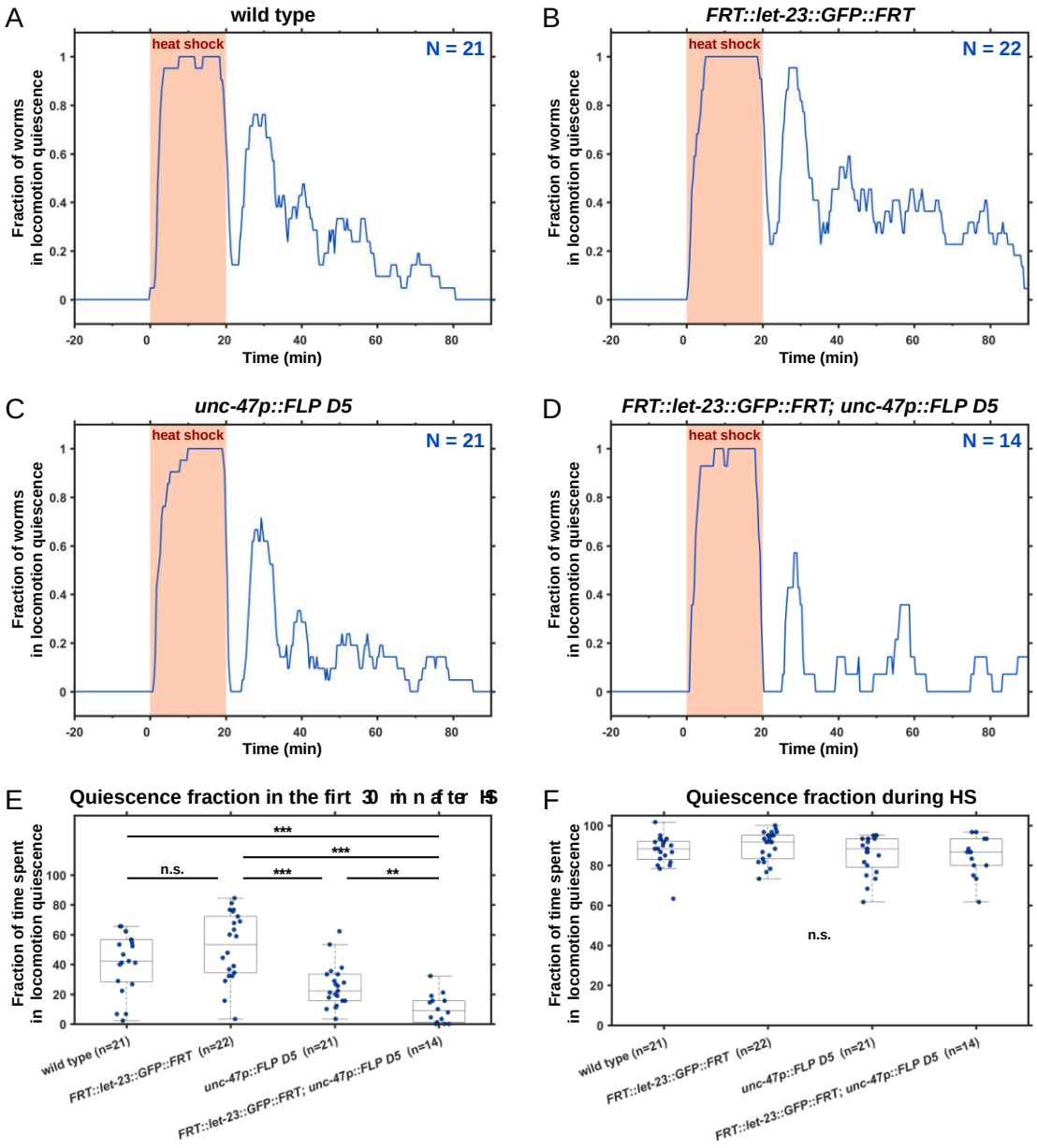

Figure 11 – EGFR is required in RIS to increase sleep after cellular stress

(A-D) RIS-specific knockdown of let-23 reveals a role for EGFR in RIS following cellular stress, in addition to the known role of EGFR in ALA (Cheryl Van Buskirk and Sternberg 2007). The heat shock (37°C) is indicated in orange. N indicates number of worms; three biological replicates were performed for each genotype. (A) is the same data as in Fig.3B. (B-C) behavior of the parental strains following a heat shock. (B) The conditional allele of let-23, FRT::let-23::GFP::FRT, was created using CRISPR/Cas9.
(C) The recombinase (FLPase) was expressed in GABAergic neurons, unc-47p::FLP D5, which include RIS, but no expression was detectable in ALA with this promoter (data not shown).
(D) Worms with a conditional knockdown of let-23 in RIS, unc-47p::FLP D5; FRT::let 23::GFP::FRT, displayed reduced quiescence. (E-F) Quantification of locomotion quiescence during and after the heat shock in the conditional strain and in the parental controls. *** denotes statistical significance with $p < 0.001$, Wilcoxon signed-rank test.

4.4. Cellular stress and EGF signaling depolarize ALA and RIS

Calcium imaging and optogenetic manipulation of RIS and ALA have suggested that these neurons act through depolarization (Nelson et al., 2014; Turek et al., 2013). To test whether cellular stress and EGF depolarizes RIS and ALA, I measured calcium activity in these neurons after heat shock or overexpression of the EGF gene *lin-3*.

First, I measured the RIS activity with AMI in young adult, which were exposed to a 37°C 20 min heat shock. RIS also showed an activity peak at the onset of the heat shock, which was reported before. Upon temperature increase, RIS activated strongly while the animal immobilized, which is consistent with a previously identified increase of RIS during temperature increase (Kotera et al., 2016). Following that, RIS showed rhythmic transients of around 10 minutes, which also highly correlated with worm quiescence bouts (Figure 12A). Typically, three to four consecutive RIS transients and sleep bouts lasting each for about 12 minutes were observed, with the first transient being the strongest and subsequent transients displaying reduced intensity until the succession of transients ceased after about one hour. RIS transients and behavioral quiescence correlation were already shown in lethargus and L1 arrest sleep (Turek et al., 2013; Wu et al., 2018). ALA ablation resulted in a strong reduction of RIS activity, hinting again that ALA might act upstream of RIS (Figure 12B).

To test for the effects of EGF upon RIS activation, I overexpressed this signaling protein using a heat-shock promoter. I induced expression with a temperature increase that is not sufficient to trigger subsequent sleep. Overexpression of EGF induced immobility and led to a strong increase of RIS calcium activity (Figure 12C). Immobilization of the worms after LIN-3 overexpression was reported before (Cheryl Van Buskirk & Sternberg, 2007). RIS calcium imaging in *let-23(gf)* mutant animals showed that RIS is already active during baseline condition and cannot be activated much further following EGF overexpression (Figure 12D).

Next, I used calcium imaging in ALA, by expressing the calcium sensor GCaMP under the *flp-24* promoter. After a 37°C 20 min heat shock, ALA activated to roughly 150% and slowly dropped again to baseline levels. Although the time ALA was active

corresponded to the period worms showed quiescence bouts, ALA activity did not correlate well with the sleep state of the animal, i.e. correlation analysis showed that ALA did not activate specifically during sleep bouts but are more broadly associated with the time during which sleep bouts occur (Figure 12E). Overexpression of EGF increased the calcium activity of ALA substantially, the calcium increase was even much stronger than that following a heat shock (Figure 12F).

These results show that cellular stress and EGF increase calcium activity of RIS and ALA. Intriguingly, the activation kinetics of these neurons differed. ALA activity correlated with the time during which sleep bouts occurred, but calcium activity did not correlate strongly with the actual sleep state. By contrast, RIS activation transients directly correlated with the occurrence of sleep bouts. The different calcium kinetics of ALA and RIS suggest that these neurons act by different mechanisms, with ALA inducing sleep bouts indirectly and RIS inducing sleep bouts directly. Together with the reduction of RIS calcium transients in the absence of ALA these kinetic changes suggest that ALA activates RIS to induce sleep bouts. ALA activating RIS could be a second pathway to induce sleep next to RIS independent quiescence induction (Trojanowski, Nelson, Flavell, Fang-Yen, & Raizen, 2015).

ALA has been proposed to induce sleep by calcium-induced secretion of multiple neuropeptides that may act by a diffusional mechanism, but ALA also has been shown to control locomotion behavior and sleep through synaptic mechanisms (Fry, Laboy, & Norman, 2014; M. Katz, Corson, Iwanir, Biron, & Shaham, 2018; Nath et al., 2016; Nelson et al., 2014). To test whether ALA activates RIS, I optogenetically activated ALA and recorded RIS depolarization via GCaMP activity. The red-shifted variant of the light-activated channelrhodopsin ReaChR was expressed via the *flp-24* promotor specifically in ALA. ReaChR in ALA was activated by green light in the presence of retinal for 5 minutes. RIS depolarized during ALA activation, which dropped to baseline levels after the stimuli had stopped (Figure 12G). This showed RIS could be activated by ALA.

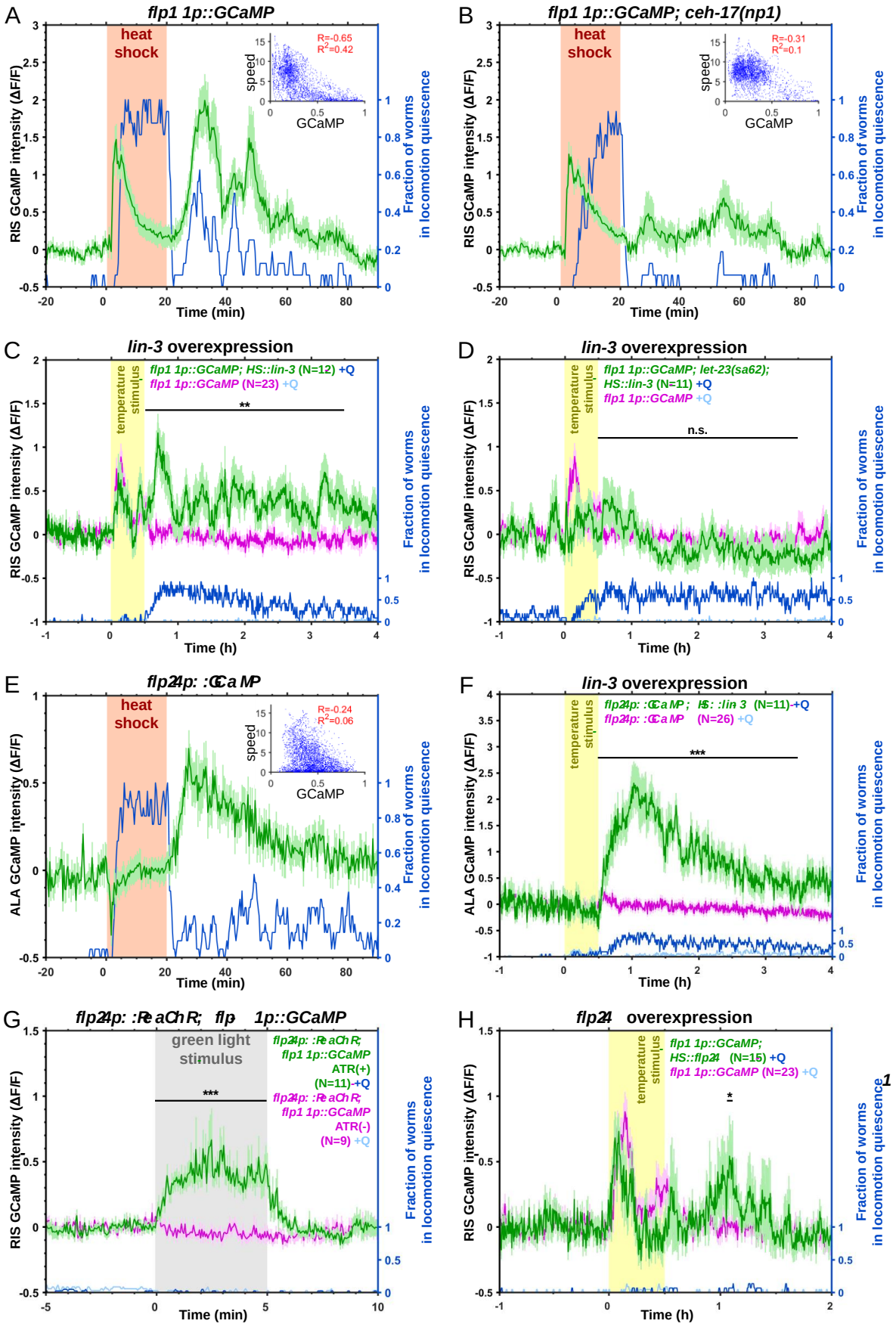
A
flp1 1p::GCaMP
heat shock
R=-0.65
R²=0.42
speed
GCaMP
RIS GCaMP intensity (ΔF/F)
Fraction of worms in locomotion quiescence
Time (min)
B
flp1 1p::GCaMP; ceh-17(np1)
heat shock
R=-0.31
R²=0.1
speed
GCaMP
RIS GCaMP intensity (ΔF/F)
Fraction of worms in locomotion quiescence
Time (min)
C
lin-3 overexpression
temperature stimulus
flp1 1p::GCaMP; HS::lin-3 (N=12) +Q
flp1 1p::GCaMP (N=23) +Q
**
RIS GCaMP intensity (ΔF/F)
Fraction of worms in locomotion quiescence
Time (h)
D
lin-3 overexpression
temperature stimulus
flp1 1p::GCaMP; let-23(sa62); HS::lin-3 (N=11) +Q
flp1 1p::GCaMP +Q
n.s.
RIS GCaMP intensity (ΔF/F)
Fraction of worms in locomotion quiescence
Time (h)
E
flp24p::GCaMP
heat shock
R=-0.24
R²=0.06
speed
GCaMP
ALA GCaMP intensity (ΔF/F)
Fraction of worms in locomotion quiescence
Time (min)
F
lin-3 overexpression
temperature stimulus
flp24p::GCaMP; HS::lin-3 (N=11) +Q
flp24p::GCaMP (N=26) +Q
***
ALA GCaMP intensity (ΔF/F)
Fraction of worms in locomotion quiescence
Time (h)
G
flp24p::ReaChR; flp1p::GCaMP
green light stimulus
***
flp24p::ReaChR; flp1 1p::GCaMP ATR(+) (N=11) +Q
flp24p::ReaChR; flp1 1p::GCaMP ATR(-) (N=9) +Q
RIS GCaMP intensity (ΔF/F)
Fraction of worms in locomotion quiescence
Time (min)
H
flp24 overexpression
temperature stimulus
flp1 1p::GCaMP; HS::flp24 (N=15) +Q
flp1 1p::GCaMP (N=23) +Q
*
RIS GCaMP intensity (ΔF/F)
Fraction of worms in locomotion quiescence
Time (h)

Figure 12 – Heat shock and EGF activate RIS and ALA, and ALA acts upstream of RIS

(A) Calcium activity of RIS following a heat shock (37°C, orange). *flp-11p::GCaMP* intensities are shown in green, and the fraction of worms in locomotion quiescence is shown in blue. The insert shows a correlation of normalized, smoothed GCaMP intensities with speed (µm/s) for the first 60 min after the heat shock, with Spearman's rank correlation coefficient. Calcium activity peaks during the first part of the heat shock and shows several transients following the heat shock. RIS calcium transients correlate with locomotion quiescence.
(B) *ceh-17(-)* reduces RIS calcium activity following the heat shock.
(C) EGF over expression induces RIS calcium activity. Overexpression is induced by a temperature increase (30°C, yellow). Control *flp-11p::GCaMP* (without EGF overexpression transgene) intensity (magenta) ±SEM, according fraction of worms in movement quiescence (light blue).
(D) EGF over expression in *let-23(gf)* does not further increase RIS calcium activity. *let-23(gf)* leads to movement quiescence already before the heat shock, while no increase in GCaMP activity can be seen.
(E) A heat shock causes subsequent ALA calcium activation. GCaMP activity does not increase during the heat shock but after the heat shock. Neural activity and locomotion quiescence do not correlate well.
(F) EGF overexpression by temperature increase induces massive ALA activation.
(G) Optogenetic activation of ALA by green light (indicated in grey) causes RIS calcium activation (green). Control (without retinal) *flp-11p::GCaMP* intensity (magenta). Movement quiescence is shown in light blue.
(H) Overexpression of *flp-24* by a heat shock promoter and temperature increase (30°C, yellow) induces RIS calcium transients.
Error is ± SEM, *** denotes statistical significance with $p < 0.001$, ** denotes statistical significance with $p < 0.01$, * denotes statistical significance with $p < 0.05$, Wilcoxon signed-rank test.

As ALA releases sleep-inducing neuropeptides upon activation, I checked if overexpression of one of the most prominent neuropeptide genes in ALA, *flp-24*, could activate RIS. A heat shock promoter-driven overexpression of *flp-24* was used. Overexpression was again achieved by a 30°C 30 min temperature stimulus, which did not trigger endogenous heat shock responses. RIS showed a modest but significant GCaMP activation after *flp-24* overexpression in the worm (Figure 12H).

I demonstrated, ALA can act upstream of RIS to induce SIS via the neuropeptide FLP-24. Although ALA activation strongly increases RIS activation during SIS, RIS is also able to induce SIS quiescence after EGF/LIN-3 activation by itself. Thus, a model emerges in which EGF activates both ALA and RIS, with ALA inducing behavioral quiescence that includes the promotion of RIS activation, which induces sleep bouts.

4.5. ALA rather than RIS support survival after stress

ALA and RIS seemed to trigger SIS through two distinct mechanisms and ALA dependent SIS was shown to be beneficial for survival after cellular stress (Goetting et al., 2018; Hill et al., 2014). This raised the question if RIS dependent SIS is also beneficial for the lifespan of the worm after cellular stress. Worms carrying either the *ceh-17(-)*, the *aptf-1(-)*, or both mutations were heat shocked in a 40°C water bath for 20 minutes, and their survival was tracked. Worms with the *ceh-17(-)* or the double mutant died around 2 days earlier than wild type worms (Figure 13). The lifespan data of the *ceh-17(-)*mutation was in line with the literature (Hill et al., 2014). *Aptf-1(-)* mutant was indistinguishable from the wild type. ALA activity seemed to mediate protective functions for cellular stress independent of RIS and its acute quiescence bouts. ALA seemed to have a rather sedating effect compared to RIS induced acute sleep bouts. Although the function of those acute sleep bouts in the event of cellular stress is unknown so far, it was shown now that RIS is also an important player in SIS. Cellular stress causes two different types of behavioral quiescence via two different neurons with distinct mechanistic properties and functions.

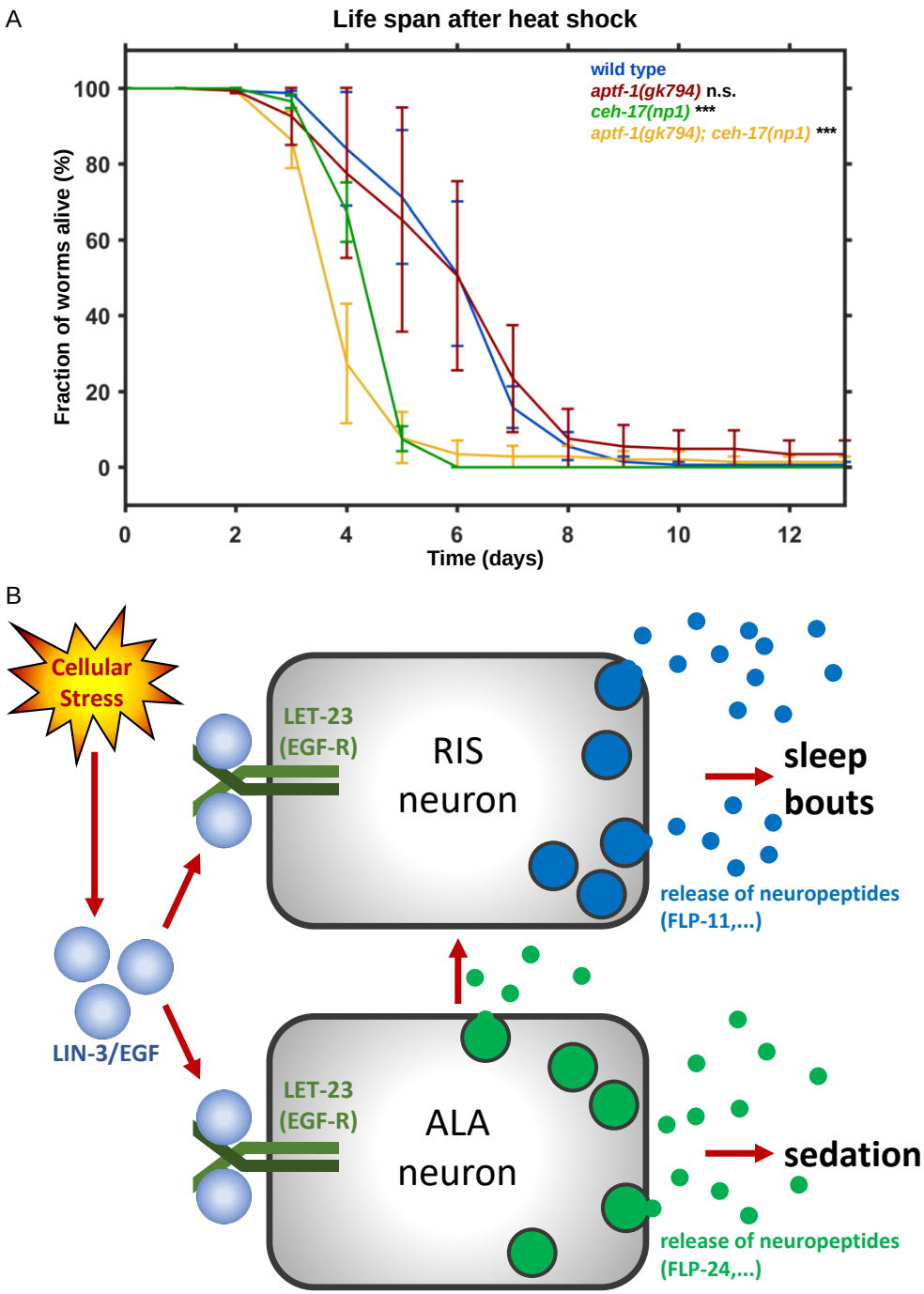

Figure 13 – ALA rather than RIS is required for survival following heat stress

(A) Survival of ALA and RIS mutants after heat shock (40°C, 20 min). *aptf-1(-)* (red) did not show a different survival rate after the heat shock. *ceh-17(-)* and the *ceh-17(-)*; *aptf-1(-)* double mutant died earlier than wild-type worms. Three biological replicates were performed, with N = 50 worms per allele per replicate. *** denotes statistical significance with $p < 0.001$, Cox proportional hazards regression.
(B) Model for EGF-induced sedation and sleep through ALA and RIS neurons. Cellular stress leads to EGF release, which activates the RIS and ALA neurons via the EGF receptor. Both neurons release neuropeptides. ALA induces sedation and activates RIS. RIS induces sleep bouts.

5. Discussion

The sections “ALA is a sedating and sleep-promoting neuron”, “EGFR activates RIS to induce sleep bouts following cellular stress”, and “Sedation is protective after cellular stress rather than sleep bouts” of this discussion are part of the manuscript we are currently writing, which is entitled “Epidermal Growth Factor signaling promotes sleep-active neuron depolarization to increase sleep following cellular stress”.

5.1. The starting point of this thesis

Sleep is an essential biological process in all organism with a nervous system, although its basic function is still unknown. It exists in humans with a highly complex nervous system as well as in cnidarians with a rather simple and diffuse nervous system (Nath et al., 2017). Also, the nematode *C. elegans*, with a minimalistic nervous system of exactly 302 neurons in the adult hermaphrodite, shows different types of sleep. They range from developmental-controlled, over environment-stimulated to stress-induced sleep (Hill et al., 2014; Raizen et al., 2008; Wu et al., 2018). Two neurons controlling these sleep-types had been discovered in *C. elegans* so far.

On the one hand is the sleep-active neuron RIS, which is active during lethargus and L1 arrest sleep, and on the other hand the neuron ALA, which was known for its role in SIS (Hill et al., 2014). Former colleagues of me discovered that RIS expresses the transcription factor APTF-1, which controls the expression of the neuropeptides encoded by the *flp-11* gene (Turek et al., 2016, 2013). The release of FLP-11 neuropeptides induces sleep in the worm. Further molecular mechanism of RIS had been unknown so far. I obtained three RIS transcriptomes to unravel what differs the sleep-active RIS from other neurons and cells in the worm.

5.2. Genes enriched in the sleep-active neuron RIS

The RIS transcriptomes I obtained differed largely in the way they were produced. The first transcriptome was based on RNA sequencing of FACS-sorted RIS neurons. The RNA-seq data was compared to an RNA-seq data set of all L2 cells. It revealed 4’371

significant differentially expressed genes, with 1’188 enriched and 3’183 de-enriched genes in RIS. This was a quite high-number compared to the 66 (RIS vs. neurons) or 381 (RIS vs. all) significant differentially expressed genes of the transcriptomes, which were obtained by the second method: sci-RNA-seq. The high number of enriched genes in the FACS/RNA-seq transcriptome indicate a good sensitivity but might also mean genes were covered, which are more broadly expressed and so less specific for RIS.

For the second method, a published data set of 42’035 single-cell transcriptomes were used to identify one cluster with 44 cells as RIS (Cao et al., 2017). The single-cell transcriptomes had been gathered by sci-RNA-seq on L2 larval cells. Transcripts found in this cluster were either compared to transcripts of all other neurons or all other cells. The lower amount of enriched genes in RIS via sci-RNA-seq can be explained by the large amount of total analyzed cells, which vice versa led to less identified transcripts per individual cell. As every worm cell is sampled several times, e.g., 44 times for RIS and 22 times for ALA, the expression profile should cover the most abundant transcripts and be highly representative for the given cell type (Cao et al., 2017).

To confirm the validity of the transcriptomes, reporter strains for 20 significant enriched genes in RIS in at least one of the transcriptome were used to confirm their expression in RIS. Seven of these strains had been confirmed to express in RIS before. They included *unc-47*, *unc-25*, *lim-6*, *aptf-1*, *flp-11*, *C10C6.7* and *srd-32* (Hobert et al., 1999; Jin et al., 1999; McIntire et al., 1997; Turek et al., 2016, 2013; Vidal et al., 2018). Six reporters did not express in RIS. It is noteworthy that four were a reporter for neuropeptide encoding genes: *nlp-8*, *nlp-13*, *nlp-37*, and *flp-1*. The other two were insulin-related genes: *ins-24* and *ins-27*. Their belonging to those two signal peptide groups could indicate a mechanistic problem with a reporter for those genes, and the missing expression is a false-negative result. At least *nlp-8* and *nlp-13* might be candidates for false-negative expression, as they are highly enriched in all three RIS transcriptomes. Still, there is the other possibility of false-positive transcriptome enrichment for those six genes.

Finally, there were seven reporters, which were suspected to express in RIS by the transcriptomes and were newly confirmed by co-localization with RIS specific mKate2 expression. The seven genes were: *let-23*, *plc-3*, *ilys-4*, *sbt-1*, *nlp-11*, *ser-7*, and *zig-2*. The three genes *let-23*, *plc-3*, and *ilys-4*, had been previously described to also express in

ALA (Gravato-Nobre et al., 2016; C. Van Buskirk & Sternberg, 2010; Cheryl Van Buskirk & Sternberg, 2007). With 14 gene-reporters expressing in RIS and just six not expressing, the transcriptomes seemed to be reasonably accurate to represent the molecular-intracellular environment of RIS. To increase their informative value, an overlap list was produced, with all genes significantly enriched in RIS in all three transcriptomes.

5.3. L1 arrest sleep screen

As I was interested in the difference of RIS compared to other neurons, I used the sci-RNA-seq RIS versus pan-neuronal cells transcriptome. To screen for RIS-dependent sleep phenotypes, lethargus and L1 arrest sleep would have been an option. L1 arrest sleep seemed more suitable as it is independent of developmental regulation (Wu et al., 2018).

In theory for each gene in *C. elegans* a mutated allele exists, which is available for research. However, not every mutation is severe and inhibits protein function. The best options for functional null alleles are mutations, which cause an early stop codon or a frameshift in the genetic code. Deletions of nucleotides or mutations which affect splice sites can also disturb proper protein work. In contrast, single nucleotide changes might affect the translation of single amino acid but could be even silent mutations and hence have a low chance to produce an obvious phenotype. Therefore, for screening, only alleles with a given chance to produce an altered sleep phenotypes had been used. Alleles with early stop codons, frameshift mutation or affected splice sites covered around 2/3 of all genes. Excluding 16 alleles, because of severe developmental problems in the strain, 87 genes have been screened for L1 arrest.

Of 89 screened alleles, two genes were covered by two different alleles, over 90%, did not produce any significant sleep phenotype in the end. One group of strains, mainly coming from the MMP, had an initially increased sleep fraction. When these strains were crossed back against wild type worms and selected for the allele of interest the sleep phenotype was no longer present. Also, 12 of the 16 excluded strains derived from the MMP.

The main issue with strains of the MMP is that they often carry over 400 mutations per strain if compared to wild type N2 strain (Thompson et al., 2013). Many of these are in non-coding regions or if they are actually in coding regions are just missense mutations. For two strains in which I lost a promising sleep phenotype after backcrossing, I went back and checked in the database which other genes were affected. In both strains, six other genes had nonsense mutations by early stop codons. I crossed both strains back against the wild type and selected in the offspring for each of the different nonsense mutations respectively. None of the backcrossed strains showed the sleep phenotype of the parental strain (data not shown). The phenotype might have come from one of the missense mutations, a non-coding but regulating gene region or maybe even from an interaction of several mutations. As there were at this point countless possibilities causing the phenotypes and no proof that they were RIS dependent it was not feasible to track them further down.

Two alleles produced a decreased sleep fraction phenotype in the L1 arrest screen. One gene was *goa-1*, the ortholog of human G protein subunit alpha o1. The allele *goa-1(sa734)* was a nonsense mutation by an early stop codon. It is known to produce a hyperactivity phenotype in the worm, and so the decreased L1 arrest sleep phenotype would fit to it (Robatzek & Thomas, 2000).

The second allele with less L1 arrest sleep was *sbt-1(ok901)*, which was additionally confirmed to express in RIS via my reporter analysis. SBT-1 is the ortholog of the human neuroendocrine chaperone 7B2, which binds to the prohormone convertase 2 and is needed for cleavage of larger peptide precursors (Lindberg, Tu, Muller, & Dickerson, 1998). Worms carrying the *sbt-1(ok901)* allele were completely missing some of their neuropeptides, which are present in the wild type. Present neuropeptides in *sbt-1(ok901)* worms, were less abundant compared to the wild type (Husson & Schoofs, 2007). A conclusion from this could be, RIS is expressing *sbt-1* to process FLP-11. Missing SBT-1 might lead to less matured FLP-11 neuropeptides which could be released upon RIS activation, and thus less sleep would be induced.

One mutated gene which produced an increased L1 arrest sleep phenotype was *ilys-4*. The increased quiescence of the MMP allele *ilys-4(gk402093)* persisted after four times backcrossing against the wild type. The *ilys-4p::GFP* reporter also expressed in RIS. A

sleep phenotype and confirmed expression in RIS made *ilys-4* an interesting target for further analysis. A complete genetic deletion of *ilys-4* was produced via CRISPR-Cas9 gene editing, which also reproduced the increased L1 arrest sleep phenotype.

ILYS-4 belongs to the invertebrate-type lysozyme family, which covers six known proteins in *C. elegans*. They are expressed in various tissues, like pharynx, intestine, excretory system, coelomocytes, or the nervous system. Their function is thought to be a defense against pathogens and also being related to digestion (Schulenburg & Boehnisch, 2008). ILYS-4 differs from the five other ILYS proteins, because it has 14 instead of 16 cysteines and is presumably the only ILYS protein with intact isopeptidase functionality (Gravato-Nobre et al., 2016). In a maximum likelihood analysis, *ilys-4* seems more closely related to *ilys-4* genes of other nematodes, e.g., *Caenorhabditis remanei* and *Caenorhabditis briggsae*, than the other *ilys* genes of *C. elegans* itself. It indicates a specialized function for *ilys-4* (Schulenburg & Boehnisch, 2008). The fact, it is not only expressed in RIS, but also in ALA, like the EGF receptor signaling pathway makes it an interesting target for further analysis in the future.

The most strong increased sleep phenotype coming out from the L1 arrest screen was a gain-of-function allele of *let-23*. A gene, which I showed to be expressed in both sleep-related neurons, RIS and ALA. LET-23 is the *C. elegans* homologue of the EGF receptor. The gain-of-function allele *let-23(sa62)* is caused by a single point mutation which converts cysteine 359 to tyrosine and is close to the extracellular major ligand-binding domain of LET-23. So far, it was known for producing a ligand-independent, but semi-dominant multi-vulva phenotype (W. S. Katz et al., 1996). Homozygous null alleles for let-23, e.g., *mn23* and *sy10*, are lethal (Aroian, Lesa, & Sternberg, 1994). Worms die already as embryos in the eggs or shortly after hatching and therefore could not be screened in L1 arrest sleep. Tissue-specific rescue of $let\text{-}23_{null}$ by expressing exogenous *let-23* under the *dpy-7* promoter did not recover the lethal phenotype (data not shown).

As *let-23* is expressed in ALA and RIS, it was of interest which neuron caused the increased L1 arrest sleep phenotype. To check ALA dependency, *let-23(gf)* was crossed with *ceh-17(np1)* a loss-of-function allele, which causes a non-functional ALA (C. Van Buskirk & Sternberg, 2010). RIS dependency was checked by crossing *let-23(gf)* with a RIS specific expression of an apoptosis activator construct, *flp-11p::egl-1* (Conradt &

Horvitz, 1998). *Let-23(gf)* in the *ceh-17(-)* background reduced the increased L1 arrest sleep phenotype, but the worms were still sleeping more than wild-type ones. In the *flp-11p::egl-1* background, L1 arrest sleep was almost completely gone, similar to *flp-11p::egl-3* alone. This showed a partial influence of ALA on the *let-23(gf)* phenotype but also the dependency of L1 arrest sleep on RIS at all.

It raised two questions, (1) if ALA and RIS have more in common on the molecular level than the EGF receptor and (2) if RIS also plays a role in SIS, which was just linked to ALA in the literature (Hill et al., 2014; Nath et al., 2016; Nelson et al., 2014).

5.4. RIS vs. ALA transcriptome

It was interesting to find the EGF receptor enriched in RIS, which was known for its role in SIS via ALA. It was shown before that SIS was linked to ALA, and L1 arrest and lethargus sleep were linked to RIS without any report of interaction so far (Hill et al., 2014; Turek et al., 2013). The enrichment of the EGF receptor worm homologue LET-23 and the downstream phospholipase PLC-3, as well as the confirmed gene expression via reporter of *let-23* and *plc-3*, raised the question if the sleep controlling neurons RIS and ALA are more similar than thought before. With the massive sci-RNA-seq data set available it was possible to also extract an ALA transcriptome from it.

The comparison of the sci-RNA-seq transcriptomes of RIS and ALA, each vs. neurons, revealed an overlap of 4 enriched genes. One neurotransmitter encoding genge, *nlp-8*, and the worm homologue of the peptidylglycine alpha-amidating monooxygenase(PAM), *pgal-1*. PAM modifies post-translational many signaling peptides (Glauder, Ragg, Rauch, & Engels, 1990; Shaye & Greenwald, 2011). The other two overlapping genes were part of the EGF signaling pathway, *let-23*, and *plc-3*. An additional pairwise correlation confirmed the general difference in gene expression between RIS and ALA. Apart from the interneuron RIC, RIS does not cluster well in the pairwise correlation with any other neuron, highlighting the peculiarity of RIS.
The expression of the EGF receptor machinery in RIS indicated that this sleep-active neuron also plays a role in SIS. It would mean that RIS is involved in all known types of sleep in the worm and hence increase its significance in sleep control even more.

5.5. EGF receptor signaling in RIS and ALA

The EGF receptor has two major intracellular downstream signaling pathways. The first induces gene expression via the Ras/ERK pathway and includes in *C. elegans* the proteins SEM-5(Grb2), LET-341(mSOS), LET-60(Ras), LIN-45(Raf), MEK-2(MEK) and MPK-1(MAPK,ERK) (Rongo, 2011). Most of these genes were significantly enriched in RIS in the three different transcriptomes but surprisingly not in the ALA sci-RNA-seq transcriptome. In the second pathway, the EGF receptor LET-23 activates the phospholipase PLC-3, which uses phosphatidylinositol 4,5-bisphosphate (PIP2) to produce diacylglycerol (DAG) and inositol 1,4,5-trisphosphate (IP3). IP3 binds to the IP3 receptor ITR-1 at the endoplasmatic reticulum to release Ca^{2+} into the cytosol (Iwasa, Yu, Xue, & Driscoll, 2010). *let-23* and *plc-3* were both enriched in the ALA transcriptome and RIS transcriptomes. *itr-1* was de-enriched in the FACS/RNAseq RIS transcriptome while not significantly changed in the other transcriptomes, which is of no surprise as it is widely expressed throughout various tissues in the worm (Baylis, Furuichi, Yoshikawa, Mikoshiba, & Sattelle, 1999).

The expression of several EGF receptor signaling pathway components in RIS and ALA suggested that both neurons can be activated by EGF. However, their general difference in gene expression although indicated that they might inherit different mechanistic properties and show a different cellular response.

5.6. ALA is a sedating and sleep-promoting neuron

ALA expresses the EGF receptor machinery and was shown to release a cocktail of neuropeptides upon activation by EGF, including those encoded by the *flp-13*, *nlp-8*, and *nlp-24* neuropeptide genes. The peptides encoded by these genes act in parallel to induce sleep behavior and inhibit specific behaviors such as feeding (Nath et al., 2016; Nelson et al., 2014; Cheryl Van Buskirk & Sternberg, 2007). Without a functioning ALA, fewer worms showed sleep bouts after a heat shock, but some sleep bouts were still present. In contrast, if RIS was missing, almost no sleep was present any more after the heat shock. ALA activity increased rapidly to a plateau in the experiments after EGF signaling, either via noxious heat shock or EGF/LIN-3 overexpression, and then slowly dropped over time

to wild-type levels again. During that time worms showed bouts of behavioral quiescence, although they did not directly correlate with ALA activity. ALA seemed to be a sedating and sleep promoting neuron.

It looks like the sedating and sleep promoting property are achieved by two parallel pathways. For the first pathway, it was shown, that neuropeptides, which were released by ALA in case of cellular stress, caused inhibition of behavioral activities like feeding, independently of RIS (Trojanowski et al., 2015). This might work via inhibition of wake-promoting neurons directly and thus inhibiting active behaviors over prolonged time periods causing sedation or lethargy (Nath et al., 2016; Nelson et al., 2014). It was shown, that ALA is able to inhibit AVE and other command interneurons for example (Fry et al., 2014; M. Katz et al., 2018).

In the second pathway, ALA activates or boosts RIS activity, which then causes sleep in the worm. I showed that stress-caused RIS activation was decreased in the absence of ALA and also, that optogenetic ALA activation was able to stimulate RIS.

In general, sedation has some similarities to sleep, such as reduced voluntary movement and reduced responsiveness to stimulation. It differs from sleep by not displaying the fast switching properties that cause the succession of sleep bouts as well as quick reversibility. Nevertheless, sedation is associated with increased sleep, indicating that these two behaviors are causally linked.

5.7. EGFR activates RIS to induce sleep bouts following cellular stress

Stress-induced EGF signaling does not only work via ALA but also via the sleep-active neuron RIS. The EGF receptor LET-23 was found to be expressed in RIS just as the *C. elegans* homologue of the LET-23 downstream target, PLC-3. It is the worm homologue of the phospholipase C gamma. Activation of LET-23 leads via PLC-3 to an increase of intracellular Ca^{2+} concentration (Cheryl Van Buskirk & Sternberg, 2007). This is presumably also true in RIS, where increased excitability could lead to an increase in the probability of strong RIS calcium transients. Experiments supporting this hypothesis showed an increase in Ca^{2+} in RIS after heat shock stress or EGF overexpression,

indicated via the calcium sensor GCaMP. In the *let-23(gf)* background RIS could not be activated further via EGF overexpression, which is in agreement with literature as the LET-23(gf) functions ligand-independent (W. S. Katz et al., 1996).

In contrast to ALA, RIS activated already during the onset of a noxious heat shock. Activation dropped to wild-type levels again, if the heat shock continued longer than a few minutes. RIS activation during the onset of a heat shock was shown before (Kotera et al., 2016). Quiescence during the heat shock was to some extend RIS dependent, but not all of it. This suggested a second pathway paralyzing the worm during a continued heat shock.

After the end of the heat shock, RIS showed around one to four short but strong transients which highly correlated with movement quiescence bouts in each worm. This correlation of RIS and quiescence was in line with the results for other types of sleep in the worm (Turek et al., 2013; Wu et al., 2018). It verified, RIS is a sleep-active neuron during SIS and thus in all known types of sleep in *C. elegans*.

The induction of SIS via EGF receptor signaling in ALA was previously known (Hill et al., 2014). However, I was able to show, that EGF acts via two parallel pathways to induce SIS. The EGF activation of ALA causes inhibition of specific behaviors over longer time scales and can additionally amplify the probability of RIS activity. RIS can also be activated by EGF itself and inhibits systemic behaviors on short time scales. Two different pathways via two neurons allow the organism to orchestrate the physiological response on different levels of specificity and time scales. In the end, all known types of sleep in *C. elegans* are controlled by RIS activity.

5.8. Sedation is protective after cellular stress rather than sleep bouts

One of the assumed functions of sleep is to be protective or respectively allow the organism to recover, e.g., in the case of stress. Lifespan measurements of *C. elegans* worms after a heat shock showed a drop in longevity in the absence of a functional ALA (Hill et al., 2014). I reproduced these results but could not find an effect vice versa in the absence of a functional RIS. It rather seemed sedation via ALA was necessary for survival after several days, more than RIS dependent sleep. ALA has been shown to inhibit feeding

independently of RIS (Trojanowski et al., 2015). Reduced food intake increases health and longevity, suggesting that ALA might, at least in part, act by reducing food intake following cellular stress (Kapahi, Kaeberlein, & Hansen, 2017). RIS on the other hand might have a beneficial effect on the nervous system at the onset and after the heat shock, which does not translate in life span effects after several days.

This would mean EGF receptor signaling activates two different parallel pathways to cope with cellular stress. EGF receptor signaling is already known to promote healthy aging via *plc-3* and *itr-1* on the one hand, and regulating lifespan via the Ras-MAPK pathway and the PLZF transcription factors EOR-1 and EOR-2 on the other hand (Iwasa et al., 2010; Liu, Rogers, Murphy, & Rongo, 2011; Yu & Driscoll, 2011). This is even more relevant as EGF signaling is highly conserved across all animal phyla and was also shown to promote sleep in other species, like fruit flies and rabbits (Foltenyi et al., 2007; Kushikata et al., 1998). It seems that EGF signaling is highly involved in various pathways and species promoting a healthy organism.

Stress-induced EGF receptor signaling in *C. elegans* hinted an interesting interaction of ALA-dependent sedation and RIS-induced sleep. In general, there might be distinct protective functions for sedation and sleep, not only in worms but also other complex organism.

6. References

Ahringer, J. (Ed.). (2006). *Reverse genetics*. Retrieved from http://www.wormbook.org

Alam, Md. A., Kumar, S., McGinty, D., Alam, Md. N., & Szymusiak, R. (2014). Neuronal activity in the preoptic hypothalamus during sleep deprivation and recovery sleep. *Journal of Neurophysiology*, *111*(2), 287–299. https://doi.org/10.1152/jn.00504.2013

Albrecht, U., Zheng, B., Larkin, D., Sun, Z. S., & Lee, C. C. (2001). MPer1 and mper2 are essential for normal resetting of the circadian clock. *Journal of Biological Rhythms*, *16*(2), 100–104. https://doi.org/10.1177/074873001129001791

Allada, R., & Siegel, J. M. (2008). Unearthing the Phylogenetic Roots of Sleep. *Current Biology*, *18*(15), R670–R679. https://doi.org/10.1016/j.cub.2008.06.033

Altun, Z. F., & Hall, D. H. (2009). INTRODUCTION TO *C. elegans* ANATOMY. In L. A. Herndon (Ed.), *WormAtlas*.

Aroian, R. V., Lesa, G. M., & Sternberg, P. W. (1994). Mutations in the *Caenorhabditis elegans* let-23 EGFR-like gene define elements important for cell-type specificity and function. *The EMBO Journal*, *13*(2), 360–366.

Baylis, H. A., Furuichi, T., Yoshikawa, F., Mikoshiba, K., & Sattelle, D. B. (1999). Inositol 1,4,5-trisphosphate receptors are strongly expressed in the nervous system, pharynx, intestine, gonad and excretory cell of Caenorhabditis elegans and are encoded by a single gene (itr-1). *Journal of Molecular Biology*, *294*(2), 467–476. https://doi.org/10.1006/jmbi.1999.3229

Brenner, S. (1974). The genetics of *Caenorhabditis elegans*. *Genetics*, *77*(1), 71–94.

Bringmann, H. (2011). Agarose hydrogel microcompartments for imaging sleep- and wake-like behavior and nervous system development in *Caenorhabditis elegans* larvae. *Journal of Neuroscience Methods*, *201*(1), 78–88. https://doi.org/10.1016/j.jneumeth.2011.07.013

Bringmann, H. (2018). Sleep-Active Neurons: Conserved Motors of Sleep. *Genetics*, *208*(4), 1279–1289. https://doi.org/10.1534/genetics.117.300521

Bryant, P. A., Trinder, J., & Curtis, N. (2004). Sick and tired: Does sleep have a vital role in the immune system? *Nature Reviews. Immunology*, *4*(6), 457–467. https://doi.org/10.1038/nri1369

Campbell, S. S., & Tobler, I. (1984). Animal sleep: A review of sleep duration across phylogeny. *Neuroscience & Biobehavioral Reviews*, *8*(3), 269–300. https://doi.org/10.1016/0149-7634(84)90054-X

Cao, J., Packer, J. S., Ramani, V., Cusanovich, D. A., Huynh, C., Daza, R., … Shendure, J. (2017). Comprehensive single-cell transcriptional profiling of a multicellular organism. *Science*, *357*(6352), 661–667. https://doi.org/10.1126/science.aam8940

Chapman, E. R. (2008). How Does Synaptotagmin Trigger Neurotransmitter Release? *Annual Review of Biochemistry*, *77*(1), 615–641. https://doi.org/10.1146/annurev.biochem.77.062005.101135

Conradt, B., & Horvitz, H. R. (1998). The *C. elegans* protein EGL-1 is required for programmed cell death and interacts with the Bcl-2-like protein CED-9. *Cell*, *93*(4), 519–529.

Corsi, A. K. (2015). A Transparent window into biology: A primer on *Caenorhabditis elegans*. *WormBook*, 1–31. https://doi.org/10.1895/wormbook.1.177.1

Davis, M. W., Morton, J. J., Carroll, D., & Jorgensen, E. M. (2008). Gene activation using FLP recombinase in *C. elegans*. *PLoS Genetics*, *4*(3), e1000028. https://doi.org/10.1371/journal.pgen.1000028

Diekelmann, S., & Born, J. (2010). The memory function of sleep. *Nature Reviews Neuroscience, 11*(2), 114–126. https://doi.org/10.1038/nrn2762

Dobin, A., Davis, C. A., Schlesinger, F., Drenkow, J., Zaleski, C., Jha, S., … Gingeras, T. R. (2013). STAR: ultrafast universal RNA-seq aligner. *Bioinformatics (Oxford, England), 29*(1), 15–21. https://doi.org/10.1093/bioinformatics/bts635

Ewels, P., Magnusson, M., Lundin, S., & Käller, M. (2016). MultiQC: summarize analysis results for multiple tools and samples in a single report. *Bioinformatics (Oxford, England), 32*(19), 3047–3048. https://doi.org/10.1093/bioinformatics/btw354

Foltenyi, K., Greenspan, R. J., & Newport, J. W. (2007). Activation of EGFR and ERK by rhomboid signaling regulates the consolidation and maintenance of sleep in Drosophila. *Nature Neuroscience, 10*(9), 1160–1167. https://doi.org/10.1038/nn1957

Franken, P., & Dijk, D.-J. (2009). Circadian clock genes and sleep homeostasis. *European Journal of Neuroscience, 29*(9), 1820–1829. https://doi.org/10.1111/j.1460-9568.2009.06723.x

Fry, A. L., Laboy, J. T., & Norman, K. R. (2014). VAV-1 acts in a single interneuron to inhibit motor circuit activity in *Caenorhabditis elegans*. *Nature Communications, 5*, 5579. https://doi.org/10.1038/ncomms6579

Glauder, J., Ragg, H., Rauch, J., & Engels, J. W. (1990). Human peptidylglycine alpha-amidating monooxygenase: cDNA, cloning and functional expression of a truncated form in COS cells. *Biochemical and Biophysical Research Communications, 169*(2), 551–558.

Goetting, D. L., Soto, R., & Van Buskirk, C. (2018). Food-Dependent Plasticity in *Caenorhabditis elegans* Stress-Induced Sleep Is Mediated by TOR–FOXA and TGF-β Signaling. *Genetics, 209*(4), 1183–1195. https://doi.org/10.1534/genetics.118.301204

Gravato-Nobre, M. J., Vaz, F., Filipe, S., Chalmers, R., & Hodgkin, J. (2016). The Invertebrate Lysozyme Effector ILYS-3 Is Systemically Activated in Response to Danger Signals and Confers Antimicrobial Protection in *C. elegans*. *PLOS Pathogens, 12*(8), e1005826. https://doi.org/10.1371/journal.ppat.1005826

Hakim, F., Wang, Y., Zhang, S. X. L., Zheng, J., Yolcu, E. S., Carreras, A., … Gozal, D. (2014). Fragmented Sleep Accelerates Tumor Growth and Progression through Recruitment of Tumor-Associated Macrophages and TLR4 Signaling. *Cancer Research, 74*(5), 1329–1337. https://doi.org/10.1158/0008-5472.CAN-13-3014

Herman, M. (2006). Hermaphrodite cell-fate specification. *WormBook*. https://doi.org/10.1895/wormbook.1.39.1

Hill, A. J., Mansfield, R., Lopez, J. M. N. G., Raizen, D. M., & Van Buskirk, C. (2014). Cellular Stress Induces a Protective Sleep-like State in *C. elegans*. *Current Biology, 24*(20), 2399–2405. https://doi.org/10.1016/j.cub.2014.08.040

Hobert, O., Tessmar, K., & Ruvkun, G. (1999). The *Caenorhabditis elegans* lim-6 LIM homeobox gene regulates neurite outgrowth and function of particular GABAergic neurons. *Development (Cambridge, England), 126*(7), 1547–1562.

Hubbard, E. J. A. (2014). FLP/FRT and Cre/lox recombination technology in *C. elegans*. *Methods (San Diego, Calif.), 68*(3), 417–424. https://doi.org/10.1016/j.ymeth.2014.05.007

Husson, S. J., & Schoofs, L. (2007). Altered neuropeptide profile of *Caenorhabditis elegans* lacking the chaperone protein 7B2 as analyzed by mass spectrometry. *FEBS Letters, 581*(22), 4288–4292. https://doi.org/10.1016/j.febslet.2007.08.003

Hutter, H., & Suh, J. (2016). GExplore 1.4: An expanded web interface for queries on *Caenorhabditis elegans* protein and gene function. *Worm*, *5*(4), e1234659. https://doi.org/10.1080/21624054.2016.1234659

Iber, C., Ancoli-Israel, S., Chesson, A., & Quan, S. (2007). *The AASM Manual for the Scoring of Sleep and Associated Events: Rules, Terminology, and Technical Specifications. III*. Presented at the Westchester. Westchester.

Iwasa, H., Yu, S., Xue, J., & Driscoll, M. (2010). Novel EGF pathway regulators modulate *C. elegans* healthspan and lifespan via EGF receptor, PLC-gamma, and IP3R activation. *Aging Cell*, *9*(4), 490–505. https://doi.org/10.1111/j.1474-9726.2010.00575.x

Jeon, M. (1999). Similarity of the *C. elegans* Developmental Timing Protein LIN-42 to Circadian Rhythm Proteins. *Science*, *286*(5442), 1141–1146. https://doi.org/10.1126/science.286.5442.1141

Jin, Y., Jorgensen, E., Hartwieg, E., & Horvitz, H. R. (1999). The *Caenorhabditis elegans* Gene *unc-25* Encodes Glutamic Acid Decarboxylase and Is Required for Synaptic Transmission But Not Synaptic Development. *The Journal of Neuroscience*, *19*(2), 539–548. https://doi.org/10.1523/JNEUROSCI.19-02-00539.1999

Kaeberlein, T. L., Smith, E. D., Tsuchiya, M., Welton, K. L., Thomas, J. H., Fields, S., … Kaeberlein, M. (2006). Lifespan extension in *Caenorhabditis elegans* by complete removal of food. *Aging Cell*, *5*(6), 487–494. https://doi.org/10.1111/j.1474-9726.2006.00238.x

Kapahi, P., Kaeberlein, M., & Hansen, M. (2017). Dietary restriction and lifespan: Lessons from invertebrate models. *Ageing Research Reviews*, *39*, 3–14. https://doi.org/10.1016/j.arr.2016.12.005

Katz, M., Corson, F., Iwanir, S., Biron, D., & Shaham, S. (2018). Glia Modulate a Neuronal Circuit for Locomotion Suppression during Sleep in *C. elegans*. *Cell Reports*, *22*(10), 2575–2583. https://doi.org/10.1016/j.celrep.2018.02.036

Katz, W. S., Lesa, G. M., Yannoukakos, D., Clandinin, T. R., Schlessinger, J., & Sternberg, P. W. (1996). A point mutation in the extracellular domain activates LET-23, the *Caenorhabditis elegans* epidermal growth factor receptor homolog. *Molecular and Cellular Biology*, *16*(2), 529–537.

Kotera, I., Tran, N. A., Fu, D., Kim, J. H., Byrne Rodgers, J., & Ryu, W. S. (2016). Pan-neuronal screening in *Caenorhabditis elegans* reveals asymmetric dynamics of AWC neurons is critical for thermal avoidance behavior. *ELife*, *5*. https://doi.org/10.7554/eLife.19021

Krueger, J. M., Frank, M. G., Wisor, J. P., & Roy, S. (2016). Sleep function: Toward elucidating an enigma. *Sleep Medicine Reviews*, *28*, 46–54. https://doi.org/10.1016/j.smrv.2015.08.005

Kushikata, T., Fang, J., Chen, Z., Wang, Y., & Krueger, J. M. (1998). Epidermal growth factor enhances spontaneous sleep in rabbits. *American Journal of Physiology-Regulatory, Integrative and Comparative Physiology*, *275*(2), R509–R514. https://doi.org/10.1152/ajpregu.1998.275.2.R509

Lewis, J. A., & Fleming, J. T. (1995). Basic culture methods. *Methods in Cell Biology*, *48*, 3–29.

Li, B., & Dewey, C. N. (2011). RSEM: accurate transcript quantification from RNA-Seq data with or without a reference genome. *BMC Bioinformatics*, *12*, 323. https://doi.org/10.1186/1471-2105-12-323

Lim, M. A., Chitturi, J., Laskova, V., Meng, J., Findeis, D., Wiekenberg, A., … Zhen, M. (2016). Neuroendocrine modulation sustains the *C. elegans* forward motor state. *ELife*, *5*. https://doi.org/10.7554/eLife.19887

Lin, J. Y., Knutsen, P. M., Muller, A., Kleinfeld, D., & Tsien, R. Y. (2013). ReaChR: a red-shifted variant of channelrhodopsin enables deep transcranial optogenetic excitation. *Nature Neuroscience*, *16*(10), 1499–1508. https://doi.org/10.1038/nn.3502

Lindberg, I., Tu, B., Muller, L., & Dickerson, I. M. (1998). Cloning and functional analysis of *C. elegans* 7B2. *DNA and Cell Biology*, *17*(8), 727–734. https://doi.org/10.1089/dna.1998.17.727

Liu, G., Rogers, J., Murphy, C. T., & Rongo, C. (2011). EGF signalling activates the ubiquitin proteasome system to modulate *C. elegans* lifespan. *The EMBO Journal*, *30*(15), 2990–3003. https://doi.org/10.1038/emboj.2011.195

Lockery, S. R., Goodman, M. B., & Faumont, S. (2009). First report of action potentials in a *C. elegans* neuron is premature. *Nature Neuroscience*, *12*(4), 365–366; author reply 366. https://doi.org/10.1038/nn0409-365

Lu, J., Sherman, D., Devor, M., & Saper, C. B. (2006). A putative flip-flop switch for control of REM sleep. *Nature*, *441*(7093), 589–594. https://doi.org/10.1038/nature04767

Maquet. (2000). Functional neuroimaging of normal human sleep by positron emission tomography. *Journal of Sleep Research*, *9*(3), 207–231. https://doi.org/10.1046/j.1365-2869.2000.00214.x

McIntire, S. L., Reimer, R. J., Schuske, K., Edwards, R. H., & Jorgensen, E. M. (1997). Identification and characterization of the vesicular GABA transporter. *Nature*, *389*(6653), 870–876. https://doi.org/10.1038/39908

Merritt, C., & Seydoux, G. (2010). Transgenic solutions for the germline. *WormBook: The Online Review of C. Elegans Biology*, 1–21. https://doi.org/10.1895/wormbook.1.148.1

Mitani, S. (2009). Nematode, an Experimental Animal in the National BioResource Project. *Experimental Animals*, *58*(4), 351–356. https://doi.org/10.1538/expanim.58.351

Miyabayashi, T., Palfreyman, M. T., Sluder, A. E., Slack, F., & Sengupta, P. (1999). Expression and Function of Members of a Divergent Nuclear Receptor Family in *Caenorhabditis elegans*. *Developmental Biology*, *215*(2), 314–331. https://doi.org/10.1006/dbio.1999.9470

Moghal, N., & Sternberg, P. W. (2003). The epidermal growth factor system in *Caenorhabditis elegans*. *Experimental Cell Research*, *284*(1), 150–159.

Monsalve, G. C., Van Buskirk, C., & Frand, A. R. (2011). LIN-42/PERIOD Controls Cyclical and Developmental Progression of *C. elegans* Molts. *Current Biology*, *21*(24), 2033–2045. https://doi.org/10.1016/j.cub.2011.10.054

Moore, R. Y., & Eichler, V. B. (1972). Loss of a circadian adrenal corticosterone rhythm following suprachiasmatic lesions in the rat. *Brain Research*, *42*(1), 201–206. https://doi.org/10.1016/0006-8993(72)90054-6

Nagy, S., Raizen, D. M., & Biron, D. (2014). Measurements of behavioral quiescence in *Caenorhabditis elegans*. *Methods*, *68*(3), 500–507. https://doi.org/10.1016/j.ymeth.2014.03.009

Nath, R. D., Bedbrook, C. N., Abrams, M. J., Basinger, T., Bois, J. S., Prober, D. A., … Goentoro, L. (2017). The Jellyfish *Cassiopea* Exhibits a Sleep-like State. *Current Biology*, *27*(19), 2984-2990.e3. https://doi.org/10.1016/j.cub.2017.08.014

Nath, R. D., Chow, E. S., Wang, H., Schwarz, E. M., & Sternberg, P. W. (2016). *C. elegans* Stress-Induced Sleep Emerges from the Collective Action of Multiple Neuropeptides. *Current Biology*, *26*(18), 2446–2455. https://doi.org/10.1016/j.cub.2016.07.048

Nelson, M. D., Lee, K. H., Churgin, M. A., Hill, A. J., Van Buskirk, C., Fang-Yen, C., & Raizen, D. M. (2014). FMRFamide-like FLP-13 Neuropeptides Promote Quiescence following Heat Stress in *Caenorhabditis elegans*. *Current Biology*, *24*(20), 2406–2410. https://doi.org/10.1016/j.cub.2014.08.037

Parmeggiani, P. L. (2003). *THERMOREGULATION AND SLEEP*. 11.

Pearlmutter, B. A., & Houghton, C. J. (2009). A New Hypothesis for Sleep: Tuning for Criticality. *Neural Computation*, *21*, 1622–1641.

Porkka-Heiskanen, T., & Kalinchuk, A. V. (2011). Adenosine, energy metabolism and sleep homeostasis. *Sleep Medicine Reviews*, *15*(2), 123–135. https://doi.org/10.1016/j.smrv.2010.06.005

Praitis, V., Casey, E., Collar, D., & Austin, J. (2000). Creation of Low-Copy Integrated Transgenic Lines in *Caenorhabditis elegans*. *Genetics*, 157(3)1217-1226.

Raizen, D. M., Zimmerman, J. E., Maycock, M. H., Ta, U. D., You, Y., Sundaram, M. V., & Pack, A. I. (2008). Lethargus is a *Caenorhabditis elegans* sleep-like state. *Nature*, *451*(7178), 569–572. https://doi.org/10.1038/nature06535

Ralph, M. R., Foster, R. G., Davis, F. C., & Menaker, M. (1990). Transplanted suprachiasmatic nucleus determines circadian period. *Science (New York, N.Y.)*, *247*(4945), 975–978.

Rechtschaffen, A., & Bergmann, B. M. (2002). Sleep Deprivation in the Rat: An Update of the 1989 Paper. *Sleep*, *25*(1), 18–24. https://doi.org/10.1093/sleep/25.1.18

Redemann, S., Schloissnig, S., Ernst, S., Pozniakowsky, A., Ayloo, S., Hyman, A. A., & Bringmann, H. (2011). Codon adaptation-based control of protein expression in *C. elegans*. *Nature Methods*, *8*(3), 250–252. https://doi.org/10.1038/nmeth.1565

Robatzek, M., & Thomas, J. H. (2000). Calcium/calmodulin-dependent protein kinase II regulates *Caenorhabditis elegans* locomotion in concert with a G(o)/G(q) signaling network. *Genetics*, *156*(3), 1069–1082.

Robinson, M. D., McCarthy, D. J., & Smyth, G. K. (2010). edgeR: a Bioconductor package for differential expression analysis of digital gene expression data. *Bioinformatics (Oxford, England)*, *26*(1), 139–140. https://doi.org/10.1093/bioinformatics/btp616

Rongo, C. (2011). Epidermal growth factor and aging: a signaling molecule reveals a new eye opening function. *Aging*, *3*(9), 896–905. https://doi.org/10.18632/aging.100384

Ruiz, F. S., Andersen, M. L., Guindalini, C., Araujo, L. P., Lopes, J. D., & Tufik, S. (2017). Sleep influences the immune response and the rejection process alters sleep pattern: Evidence from a skin allograft model in mice. *Brain, Behavior, and Immunity*, *61*, 274–288. https://doi.org/10.1016/j.bbi.2016.12.027

Saper, Chou, T. C., & Scammell, T. E. (2001). The sleep switch: hypothalamic control of sleep and wakefulness. *Trends in Neurosciences*, *24*(12), 726–731.

Saper, Fuller, P. M., Pedersen, N. P., Lu, J., & Scammell, T. E. (2010). Sleep State Switching. *Neuron*, *68*(6), 1023–1042. https://doi.org/10.1016/j.neuron.2010.11.032

Saper, Scammell, T. E., & Lu, J. (2005). Hypothalamic regulation of sleep and circadian rhythms. *Nature*, *437*(7063), 1257–1263. https://doi.org/10.1038/nature04284

Schulenburg, H., & Boehnisch, C. (2008). Diversification and adaptive sequence evolution of *Caenorhabditis* lysozymes (Nematoda: Rhabditidae). *BMC Evolutionary Biology*, *8*(1), 114. https://doi.org/10.1186/1471-2148-8-114

Shaye, D. D., & Greenwald, I. (2011). OrthoList: a compendium of *C. elegans* genes with human orthologs. *PloS One*, *6*(5), e20085. https://doi.org/10.1371/journal.pone.0020085

Shine, R. (1984). Reproductive Biology and Food Habits of the Australian Elapid Snakes of the Genus *Cryptophis*. *Journal of Herpetology*, *18*(1), 33. https://doi.org/10.2307/1563669

Siegel, J. M. (2008). Do all animals sleep? *Trends in Neurosciences*, *31*(4), 208–213. https://doi.org/10.1016/j.tins.2008.02.001

Soneson, C., Love, M. I., & Robinson, M. D. (2015). Differential analyses for RNA-seq: transcript-level estimates improve gene-level inferences. *F1000Research*, *4*, 1521. https://doi.org/10.12688/f1000research.7563.2

Spencer, W. C., McWhirter, R., Miller, T., Strasbourger, P., Thompson, O., Hillier, L. W., … Miller, D. M. (2014). Isolation of Specific Neurons from *C. elegans* Larvae for Gene Expression Profiling. *PLoS ONE*, *9*(11), e112102. https://doi.org/10.1371/journal.pone.0112102

Steriade, M., Timofeev, I., & Grenier, F. (2001). Natural Waking and Sleep States: A View From Inside Neocortical Neurons. *Journal of Neurophysiology*, *85*(5), 1969–1985. https://doi.org/10.1152/jn.2001.85.5.1969

Stiernagle, T. (2006). *Maintenance of C. elegans*. Retrieved from http://www.wormbook.org

Sulston, J. E., & Horvitz, H. R. (1977). Post-embryonic cell lineages of the nematode, *Caenorhabditis elegans*. *Developmental Biology*, *56*(1), 110–156. https://doi.org/10.1016/0012-1606(77)90158-0

Takahashi, K., Kayama, Y., Lin, J. S., & Sakai, K. (2010). Locus coeruleus neuronal activity during the sleep-waking cycle in mice. *Neuroscience*, *169*(3), 1115–1126. https://doi.org/10.1016/j.neuroscience.2010.06.009

The *C. elegans* Sequencing Consortium. (1998). Genome Sequence of the Nematode *C. elegans*: A Platform for Investigating Biology. *Science*, *282*(5396), 2012–2018. https://doi.org/10.1126/science.282.5396.2012

Thompson, O., Edgley, M., Strasbourger, P., Flibotte, S., Ewing, B., Adair, R., … Waterston, R. H. (2013). The million mutation project: A new approach to genetics in *Caenorhabditis elegans*. *Genome Research*, *23*(10), 1749–1762. https://doi.org/10.1101/gr.157651.113

Tian, L., Hires, S. A., Mao, T., Huber, D., Chiappe, M. E., Chalasani, S. H., … Looger, L. L. (2009). Imaging neural activity in worms, flies and mice with improved GCaMP calcium indicators. *Nature Methods*, *6*(12), 875–881. https://doi.org/10.1038/nmeth.1398

Trojanowski, N. F., Nelson, M. D., Flavell, S. W., Fang-Yen, C., & Raizen, D. M. (2015). Distinct Mechanisms Underlie Quiescence during Two *Caenorhabditis elegans* Sleep-Like States. *The Journal of Neuroscience: The Official Journal of the Society for Neuroscience*, *35*(43), 14571–14584. https://doi.org/10.1523/JNEUROSCI.1369-15.2015

Turek, M., Besseling, J., & Bringmann, H. (2015). Agarose Microchambers for Long-term Calcium Imaging of *Caenorhabditis elegans*. *Journal of Visualized Experiments: JoVE*, (100), e52742. https://doi.org/10.3791/52742

Turek, M., Besseling, J., Spies, J.-P., König, S., & Bringmann, H. (2016). Sleep-active neuron specification and sleep induction require FLP-11 neuropeptides to systemically induce sleep. *ELife*, *5*. https://doi.org/10.7554/eLife.12499

Turek, M., Lewandrowski, I., & Bringmann, H. (2013). An AP2 Transcription Factor Is Required for a Sleep-Active Neuron to Induce Sleep-like Quiescence in *C. elegans*. *Current Biology*, *23*(22), 2215–2223. https://doi.org/10.1016/j.cub.2013.09.028

Van Buskirk, C., & Sternberg, P. W. (2010). Paired and LIM class homeodomain proteins coordinate differentiation of the *C. elegans* ALA neuron. *Development*, *137*(12), 2065–2074. https://doi.org/10.1242/dev.040881

Van Buskirk, Cheryl, & Sternberg, P. W. (2007). Epidermal growth factor signaling induces behavioral quiescence in *Caenorhabditis elegans*. *Nature Neuroscience*, *10*(10), 1300–1307. https://doi.org/10.1038/nn1981

Vidal, B., Aghayeva, U., Sun, H., Wang, C., Glenwinkel, L., Bayer, E. A., & Hobert, O. (2018). An atlas of *Caenorhabditis elegans* chemoreceptor expression. *PLOS Biology*, *16*(1), e2004218. https://doi.org/10.1371/journal.pbio.2004218

Voutev, R., & Hubbard, E. J. A. (2008). A "FLP-Out" system for controlled gene expression in *Caenorhabditis elegans*. *Genetics*, *180*(1), 103–119. https://doi.org/10.1534/genetics.108.090274

Vyazovskiy, V., Borbély, A. A., & Tobler, I. (2000). Unilateral vibrissae stimulation during waking induces interhemispheric EEG asymmetry during subsequent sleep in the rat. *Journal of Sleep Research*, *9*(4), 367–371.

White, J. G., Southgate, E., Thomson, J. N., & Brenner, S. (1986). The Structure of the Nervous System of the Nematode *Caenorhabditis elegans*. *Philosophical Transactions of the Royal Society of London. Series B, Biological Sciences*, *314*(1165,), 1–340.

Wilm, T., Demel, P., Koop, H. U., Schnabel, H., & Schnabel, R. (1999). Ballistic transformation of *Caenorhabditis elegans*. *Gene*, *229*(1–2), 31–35.

Wright, K. P., Badia, P., & Wauquier, A. (1995). Topographical and Temporal Patterns of Brain Activity During the Transition From Wakefulness to Sleep. *Sleep*, *18*(10), 880–889. https://doi.org/10.1093/sleep/18.10.880

Wu, Y., Masurat, F., Preis, J., & Bringmann, H. (2018). Sleep Counteracts Aging Phenotypes to Survive Starvation-Induced Developmental Arrest in *C. elegans*. *Current Biology*, *28*(22), 3610-3624.e8. https://doi.org/10.1016/j.cub.2018.10.009

Xie, L., Kang, H., Xu, Q., Chen, M. J., Liao, Y., Thiyagarajan, M., … Nedergaard, M. (2013). Sleep Drives Metabolite Clearance from the Adult Brain. *Science*, *342*(6156), 373–377. https://doi.org/10.1126/science.1241224

Ye, S. (2001). An efficient procedure for genotyping single nucleotide polymorphisms. *Nucleic Acids Research*, *29*(17), 88e–888. https://doi.org/10.1093/nar/29.17.e88

Yu, S., & Driscoll, M. (2011). EGF signaling comes of age: promotion of healthy aging in C. elegans. *Experimental Gerontology*, *46*(2–3), 129–134. https://doi.org/10.1016/j.exger.2010.10.010

7. Abbreviations

AMI	Agarose microchamber imaging
ATR	All-trans-retinal
CPM	Counts per million
CLOCK	Circadian Locomotor Output Cycles Kaput
DIC	Differential interference contrast
EEG	Electroencephalogram
EGF	Epidermal growth factor
EGFR	EGF receptor
EMG	Electromyogram
FACS	Fluorescence-activated cell sorting
GABA	γ-aminobutyric acid
L1/L2/L3/L4	Larval state 1/2/3/4
MMP	Million mutation project
NREM	Non rapid eye movement sleep
NGM	Nematode growth medium
PCA	Principal component analysis
PDMS	Polydimethylsiloxane
POA	Preoptic area
ReaChR	Red-shifted variant of channelrhodopsin
REM	Rapid eye movement sleep
RNA-seq	RNA sequencing
SCT	Single cell transcriptome
SIS	Stress-induced sleep
sci-RNA-seq	single-cell combinatorial indexing RNA sequencing

8. List of figures

Figure 1 – Interneuron RIS 7
Figure 2 – C. elegans life cycles 8
Figure 3 – Interneuron ALA 9
Figure 4 – CRISPR/Cas9-based editing of the let-23 locus 16
Figure 5 – Heat control device 25
Figure 6 – Sleep-active RIS neuron transcriptome computed from single-cell data 34
Figure 7 – RIS enriched genes for which fluorescence transgene reporters are expressed in RIS 35
Figure 8 – RIS enriched genes for which fluorescent transgene reporters do not show RIS expression 36
Figure 9 – The EGFR signaling machinery is expressed in both ALA and RIS neurons 40
Figure 10 – ALA and RIS are required for sleep after EGFR activation and cellular stress 42
Figure 11 – EGFR is required in RIS to increase sleep after cellular stress 44
Figure 12 – Heat shock and EGF activate RIS and ALA, and ALA acts upstream of RIS 48
Figure 13 – ALA rather than RIS is required for survival following heat stress 50

9. List of tables

Table 1 – Constructs created and used for transgenic strain generation..... 14
Table 2 – C. elegans strains used throughout all experiments in this thesis. 71
Table 3 – All primers used throughout this thesis and the regarding band sizes..... 75
Table 4 – All significantly differentially expressed genes of the "FACS/RNA-seq RIS vs. all" transcriptome and their logFC..... 76
Table 5 – All significantly differentially expressed genes of the "sci-RNA-seq RIS vs. all" transcriptome and their logFC 96
Table 6 – All significantly differentially expressed genes of the "sci-RNA-seq RIS vs. neurons" transcriptome and their logFC..... 98
Table 7 – All significantly differentially expressed genes of the "sci-RNA-seq ALA vs. neurons" transcriptome and their logFC..... 99
Table 8 – Genes enriched in all three RIS transcriptomes..... 100

10. Appendix

10.1. Supplementary tables

Table 2 – C. elegans strains used throughout all experiments in this thesis.

strain	genotype	backcrossed
AH12	*gap-1(ga133) X.*	x4
AH5059	*let-23(zh131[FRT::let-23::FRT::GFP::LoxP::FLAG::let-23]) II.*	
AQ866	*ser-4(ok512) III.*	x5
BC16236	*dpy-5(e907) I; sEx16236[rCesT17E9.2a::GFP + pCeh361].*	x0
CB30	*sma-1(e30) V.*	x1
CB6785	*unc-119(ed3) III; eEx650[ilys-4p::GFP + unc-119(+)].*	x2
CG625	*unc-103(n1213) pha-1(e2123) III; him-5(e1490) V; rgEx235[plc-3p::YFP + pha-1(+)].*	
DA1641	*lin-15B&lin-15A(n765) X; adEx1641[C09B7.1::GFP + lin-15(+)].*	
FX01512	*rabx-5(tm1512) III.*	x0
FX01556	*tiam-1(tm1556) I.*	x0
FX02304	*ssup-72(tm2304) II.*	x0
FX02584	*mct-6(tm2584) X.*	x0
FX02735	*T21F2.1(tm2735) X.*	x0
FX03878	*pkg-2(tm3878) IV.*	x0
FX04341	*F57A8.4(tm4341) V.*	x0
FX04393	*nlp-37(tm4393) X.*	x0
FX04503	*kin-15(tm4503) II.*	x0
FX05049	*R11F4.2(tm5049) II.*	x0
FX05160	*F38B6.6(tm5160) X.*	x0
FX05990	*F40A3.7(tm5990) V.*	x0
FX06682	*C49H3.3(tm6682) IV.*	x0
FX17081	*cyn-10(tm6703) II.*	x0
FX18630	*mrpl-19(tm4843) I.*	x0
FX30291	*unc-25(tm2727) III.*	x0
HA328	*lin-15B&lin-15A(n765) X; rtEx233[nlp-11p::GFP + lin-15(+)].*	
HA329	*lin-15B&lin-15A(n765) X; rtEx234[nlp-13p::GFP + lin-15(+)].*	
HBR1261	*goeIs288[flp-11p::mKate2::unc-54-3'utr,unc-119(+)].*	x2
HBR1361	*goeIs304[flp-11p::SL1-GCaMP3.35-SL2::mKate2-unc-54-3'UTR, unc-119(+)].*	x2
HBR1777	*goeIs384 [flp-11p::egl-1::SL2-mKate2-flp-11-3'UTR, unc-119(+)].*	x0

strain	genotype	backcrossed
HBR183	*cca-1(ad1650) X.*	x0
HBR1857	*ceh-17(np1) I; goeIs304[flp-11p::SL1-GCaMP3.35-SL2::mKate2-unc-54-3'UTR, unc-119(+)].*	x0
HBR2026	*C50F7.6(gk744131) IV.*	x4
HBR2040	*ckr-1(ok2502) I.*	x2
HBR2043	*R09F10.1(ok3119) X.*	x1
HBR2047	*zig-2(ok696) X.*	x1
HBR2066	*R02F2.4(gk382575) III.*	x2
HBR2067	*F32D1.3(gk232755) V.*	x4
HBR2068	*ncs-6(gk138627) II.*	x2
HBR2073	*gei-1(gk170616) III.*	x2
HBR2086	*srx-2(gk242439) V.*	x2
HBR2088	*ceh-17(np1) I; aptf-1(gk794) II.*	x0
HBR2107	*ilys-4(gk402093) IV.*	x4
HBR2108	*srd-32(gk468949) V.*	x2
HBR2193	*goeEx727[flp-24p::ReaChR::mKate2-unc-54 3'UTR, unc-122p::dsRed]; goeIs304[flp-11p::SL1-GCaMP3.35-SL2::mKate2-unc-54-3'UTR, unc-119(+)].*	x0
HBR2195	*let-23(sa62) II; goeIs304[flp-11p::SL1-GCaMP3.35-SL2::mKate2-unc-54-3'UTR, unc-119(+)]; him-5(e1490) V; syIs197[hs::LIN-3C(cDNA) + myo-2p::dsRed + pha-1(+)].*	x0
HBR2205	*syEx1286[hsp16-41p::flp-24, myo-2p::dsRed, KS+]; goeIs304[pflp-11::SL1-GCaMP3.35-SL2::mKate2-unc-54-3'UTR, unc-119(+)].*	x0
HBR2238	*bqSi542[unc-47p::FLP D5 + unc-119(+)]; let-23(zh131[FRT::let-23::FRT::GFP::LoxP::FLAG::let-23] II.*	x0
HBR2239	*bqSi542[unc-47p::FLP D5 + unc-119(+)]*	x2
HBR2256	*goeEx737[flp-24p::SL1-GCaMP3.35-SL2::SL2-mKate2::unc-54 3'UTR, unc-119(+)].*	x0
HBR2257	*goeEx737[flp-24p::SL1-GCaMP3.35-SL2::SL2-mKate2::unc-54 3'UTR, unc-119(+)]; him-5(e1490) V; syIs197 [hs::LIN-3C(cDNA) + myo-2p::dsRed + pha-1(+)].*	x0
HBR227	*aptf-1(gk794) II.*	x10
HBR507	*flp-11(tm2706) X.*	x7
HBR763	*C10C6.7(goe4) IV.*	x0
HT1757	*unc-119(ed3) III; wwIs34[ins-24p::GFP + unc-119(+)].*	x0
HT1768	*unc-119(ed3) III; wwIs35[ins-27p::GFP + unc-119(+)].*	x0
IB16	*ceh-17(np1) I.*	x0
JD596	*avr-15(vu227) V.*	x2
JT734	*goa-1(sa734) I.*	x3
KJ355	*csq-1(jh109) X.*	x6

strain	genotype	backcrossed
LSC1264	*sprr-1(ok3685) IV.*	x4
LSC87	*lstEx6[pdf-2p::GFP + myo-3p::mCherry]. (pdf-2 = nlp-37)*	
MB5	*lin-15(ts); him5(e1490); rtEx277[Pnlp-8::GFP+lin-15(+)].*	
MT4433	*ced-6(n1813) III.*	
MU1255	*nhr-67(tm2217) IV.*	x2
N2	*wild type*	
NY2072	*ynIs72[flp-1p::GFP].*	x0
OH14368	*pha-1(e1323) III; him-5(e1490) V; otEx6710[srd-32p::GFP + pha-1(+)].*	
OH4836	*otIs7[zig-2::GFP + rol-6(su1006)].*	x2
PHX530	*nlp-11(syb530) II.*	x0
PHX700	*ilys-4(syb700) IV.*	x0
PS1839	*let-23(sa62) II.*	
PS2746	*dpy-20(e1282) IV; syEx234[let-23::GFP + pBS + (pMH86) dpy-20(+)].*	
PS4886	*plc-3(tm1340) II.*	
RB1001	*cpna-3(ok922) IV.*	x0
RB1136	*R05G6.10(ok1159) IV.*	x0
RB1151	*cft-1(ok1180) V.*	x0
RB1245	*rga-1(ok204) II.*	x0
RB1399	*T01H8.2(ok340) I.*	x0
RB1431	*mps-2(ok1631) II.*	x0
RB1468	*dkf-2(ok1704) V.*	x0
RB1512	*Y57A10A.24(ok1803) II.*	x0
RB1523	*C24G7.1(ok1822) I.*	x0
RB1911	*ins-27(ok2474) I.*	x0
RB2110	*C39B10.1(ok2789) X.*	x0
RB2269	*flp-34(ok3071) V.*	x0
RB2472	*nep-26(ok3412) II.*	x0
RB2627	*srg-69(ok3686) II.*	x0
RB5001	*ZC434.9(ok5212) I.*	x0
RB5002	*srx-125(ok5810) V.*	x0
RB669	*wee-1.1(ok418) II.*	x0
UP148	*sem-5(cs15) X.*	x2
VC1309	*nlp-8(ok1799) I.*	x0
VC1795	*nrfl-1(ok2292) IV.*	x1
VC1909	*flp-1(ok2505) IV.*	x1
VC20129	*gem-1(gk298521) X.*	x0
VC20159	*F19C6.3(gk290941) X.*	x0

strain	genotype	backcrossed
VC20199	*pms-2(gk247737) V.*	x0
VC20231	*rgef-1(gk243610) V.*	x0
VC20263	*glb-23(gk205062) IV.*	x0
VC20307	*T21D12.12(gk191670) IV.*	x0
VC20312	*R08B4.2(gk326023) X.*	x0
VC20416	*nhr-55(gk947607) V.*	x0
VC20449	*K02D3.1(gk299318) X.*	x0
VC20489	*nhr-128(gk960157) V.*	x0
VC20519	*F54H5.5(gk335875) II.*	x0
VC20522	*npr-29(gk337633) III.*	x0
VC20554	*F53F4.17(gk251960) V.*	x0
VC20624	*glb-32(gk360316) V.*	x0
VC20630	*T22F3.7(gk362826) V.*	x0
VC20743	*lmd-4(gk389517) V.*	x0
VC226	*ida-1(ok409) III.*	x0
VC2565	*frpr-3(ok3302) V.*	x0
VC273	*tag-89(ok514) IV.*	x1
VC30075	*T12B3.2(gk409439) IV.*	x0
VC30104	*tpa-1(gk414216) IV.*	x0
VC30160	*ile-1(gk427192) I.*	x0
VC30245	*B0244.10(gk446359) III.*	x0
VC40013	*frpr-3(gk240031) V.*	x0
VC40057	*dmsr-6(gk161951) II.*	x0
VC40140	*B0416.3(gk481746) X.*	x0
VC40198	*lgc-4(gk509234) X.*	x0
VC40407	*F56D5.6(gk622448) IV.*	x0
VC40500	*Y57G11C.36(gk961271) IV.*	x0
VC40589	*ZK1307.7(gk708119), sri-46(gk708025) II.*	x0
VC40598	*F57B10.4(gk712994) I.*	x0
VC40613	*frpr-16(gk722062) II.*	x0
VC40626	*tkr-1(gk729500) III.*	x0
VC40630	*Y51H7C.13(gk732116) II.*	x0
VC40679	*C25G6.4(gk759467) X.*	x0
VC40734	*nhr-194(gk784872) V.*	x0
VC40893	*Y116A8B.4(gk869095) IV.*	x0
VC975	*egas-2(ok1477) V.*	x0
ZW477	*bkip-1(zw10) II.*	x4

Table 3 – All primers used throughout this thesis and the regarding band sizes

Gene	Allel/Construct	Original Strain	Forward Inner Primer	Reverse Inner Primer	Forward Outer Primer	Reverse Outer Primer	Length WT	Length Mut.	Outer Length
C50F7.6	*gk744131*	VC40650	GAGATGAAGATGATGTTGGAAGATTGTG	CAGCAGTTCAACGACGTTTAGTTCAAT	ATTTCCTCAAACTGCTTCCTTTTAATGC	TTTTTATACCCACAACCAGGTTGGTTAA	192	243	380
F32D1.3	*gk232755*	VC20420	TCAAATTCAGAAAACCAAAAATTCTTAACG	GAACGCAGATTTTGTGTATGACGCTT	AAATTGCCAAATCTCCTACACTTTTCCT	ACATTCGTGTCTACTCTCTGGACCATTC	200	261	405
gei-1	*gk170616 III.*	VC30095	CCACATTTGTTAAATAATACATTTTCAGTCCAAAAT	AGTTCGAAGCACCTTTCGACTGTCGCG	GAATAGCACGTCTTCTGCGTGGCATC	GACACACACACACAAAAAACAACGCGTT	333	235	505
ilys-4	*gk402093 IV.*	VC20784	GGACCACACGAATCTCGAACTCTTGTC	GTAGAGATCGGGGAACAATTGGATATGGA	TTCCTCCCAGATTTGAAATTTCAACATCAA	GTGACCAAAGCGTCTGTGACGTCATTAC	249	284	477
let-23	*sa62 II.*	PS1839	TACAAAAGATGTTAGAGAGTGTGAAAACTG	TACTTTTTGGACAGCTGGAACTTCGGT	AAAATGGAAATCATTGTGTGAAAGAATG	CCAAGTTTTTAAGTGTCTCGTTTGTCAG	189	220	352
ncs-6	*gk138627 II.*	VC20189	CTGTCATTCGGCCGTTTGAGCATGTT	AATCAGAATTTTATGCATAACAAGCTCCTAAATTAAG	GTCCTCGGATAGTTCCCAGAGACAAAGG	GCAGGTGAAACAGGACTGGAACATGATT	262	324	523
R02F2.4	*gk382575 III.*	VC20720	GAGAAAAATCAAATGTGTGACTATGAAGGG	ATTCCAAGTCACACTCGTCAACGGTT	GGATATTTCTCATTTGGCAGATGCTCTT	GGCACTCAAAAATATTCTCTCGTCCATT	194	151	289
srd-32	*gk468949 V.*	VC40113	GTATTCTTGGCGAACACCTCTATAAAGT	AGAGGAAACATATGCAATACCCTAGATG	TTCTTTTCATTTGGTGTATGTGTGTATG	GCAAATCTAGCATTTTAGCAAATTTTTT	247	194	385
srx-2	*gk242439 V.*	VC30095	CTGGCACCGTCAATTATGTTTGAAGT	AATATTGAAATATCATACGGTTTCATCTC	AAGAATGGTTGTTTGGACACTTAAAACA	AAAACAAATCACAATAACACGATTCACA	199	253	397

Gene	Allel/Construct	Original Strain	Forward Primer	Forward Inner Primer	Reverse Primer	Length WT	Length WT 2	Length Mut.
ckr-1	*ok2502*	RB1923	gggtcactttcttcttggcg	ACACACCTACAAGCCCTACC	gcgaatctgaggctggatac	176	1609	320
ilys-4	*syb700*	PHX700	gaagccgccgtgaatgaaaa	CGAAGCCTGGATGAACTGTG	cagtagctcgaaaatctccgt	580	1346	142
let-23	*zh131*	AH5059	ACAACCAACCAAACACTCCT	CTACATCATGGCCGACAAGC	acaagacaacgaagacccga	373	(mut2) 1368	746
R09F10.1	*ok3119*	RB2296	tctggcttggttctactgaca	AGGACCCGTCACTTTTGGTA	gattctccttctccgccgta	200	985	393
zig-2	*ok696*	RB862	tggtttggttgcgactgaaa	ACAACGTTACGACTCTGACCT	aaagggcaactagggtgtga	371	2142	489

Gene	Allel/Construct	Original Strain	Forward Primer	Reverse Primer	Length
unc47p_FLP_D5	*bqSi542*	BN544	agagcctttcggtttggaga	GGATTGGTGCTTTTGTCCGT	~613

Table 4 – All significantly differentially expressed genes of the "FACS/RNA-seq RIS vs. all" transcriptome and their logFC

gene	logFC	gene	logFC	gene	logFC	gene	logFC
C10C6.7	9,77	*ubc-3*	4,97	*unc-104*	4,09	*mab-7*	-5,40
F46C5.7	10,12	*nlp-11*	7,52	*hsp-110*	5,45	*col-43*	-4,27
F46C5.4	9,84	*egl-21*	5,21	*glb-23*	6,41	*glb-7*	6,68
flp-11	9,75	*cal-4*	5,07	*mcp-1*	5,69	*irx-1*	4,00
ZK1307.7	9,49	*nlp-8*	7,34	*pgp-1*	-6,14	*T12A7.2*	3,92
srx-2	9,72	*T27C4.1*	7,10	*T14B4.8*	4,72	*ador-1*	5,79
ser-4	8,39	*rhgf-2*	4,88	*feh-1*	4,31	*F21C10.9*	-6,09
aptf-1	8,59	*lim-6*	7,22	*M05D6.6*	5,39	*col-41*	-5,40
tkr-1	8,40	*npr-29*	5,80	*F10E7.9*	4,70	*rskn-1*	4,79
T05A8.3	7,83	*frm-8*	5,63	*egl-18*	4,94	*R04E5.8*	4,23
F36D4.4	7,24	*W02C12.2*	4,60	*F27C1.2*	4,55	*clec-42*	-6,37
R11F4.2	8,80	*scd-1*	5,67	*pdfr-1*	4,34	*C32H11.11*	-13,00
F36G3.3	7,39	*H17B01.5*	7,48	*C04E12.4*	-6,07	*C30G7.2*	4,60
ckr-1	8,69	*dop-1*	5,66	*rund-1*	6,51	*wnk-1*	3,50
K02F2.5	7,89	*unc-119*	5,82	*jmjd-2*	5,00	*T01B7.9*	6,29
T05E7.4	7,89	*hsp-16.11*	7,29	*hsp-16.1*	8,03	*abts-3*	4,56
Y57G11C.46	8,55	*hsp-16.48*	7,85	*gst-11*	6,61	*C30H6.5*	-6,63
rcan-1	8,16	*C08G5.7*	6,58	*Y44A6D.2*	3,97	*lpr-7*	-6,15
C09G1.5	8,28	*igcm-2*	6,80	*bed-2*	6,55	*nhx-1*	-7,05
arrd-26	7,07	*kin-1*	4,62	*wrk-1*	4,12	*VC5.2*	-6,53
sprr-2	7,61	*sta-1*	4,88	*ugt-60*	-6,34	*klp-4*	3,70
srg-69	9,83	*K03B4.4*	4,90	*zig-5*	5,94	*R13H4.7*	6,13
ncs-6	6,70	*ZK1073.2*	5,85	*C44H4.6*	5,63	*sprr-1*	6,43
hsp-70	9,70	*cab-1*	5,11	*unc-51*	4,00	*dpy-4*	-4,01
C47E8.3	6,19	*lgc-4*	5,76	*C32H11.8*	-6,34	*snt-3*	5,18
sto-5	5,93	*ptb-1*	4,62	*C05D12.7*	5,58	*K11C4.2*	4,33
T04A8.18	6,31	*npr-4*	5,59	*ZK652.8*	5,66	*T06D8.10*	-5,82
B0361.4	6,66	*sad-1*	4,80	*R107.5*	6,26	*snb-1*	4,59
ptr-5	5,79	*H10E21.5*	6,30	*C01C4.3*	5,26	*avr-15*	4,08
tiam-1	5,87	*bus-8*	-5,88	*gei-3*	4,29	*lmd-3*	3,45
sbt-1	5,72	*srd-32*	6,64	*C35E7.11*	4,96	*acp-1*	-8,19
egl-3	6,80	*spv-1*	5,05	*acy-2*	5,92	*odr-2*	5,39
ida-1	5,82	*nep-26*	6,18	*AH9.6*	4,32	*F20D6.8*	4,47
ace-3	7,31	*cutl-15*	5,21	*cmk-1*	4,99	*F44E5.5*	8,61
F14B6.2	5,95	*Y39A1A.24*	5,90	*T11G6.3*	-6,05	*nhr-62*	-6,79
nac-3	5,58	*arrd-17*	6,32	*C34C6.3*	4,78	*abu-12*	-5,91
unc-47	6,27	*ztf-14*	6,43	*nhx-9*	-6,18	*npr-17*	5,39
dmsr-2	6,80	*rabx-5*	5,73	*unc-77*	4,21	*wrt-1*	-5,62
T10G3.8	5,93	*F32D1.3*	5,03	*gcy-29*	7,54	*flp-27*	3,58
sue-1	7,00	*ZC581.9*	4,99	*unc-57*	4,11	*D1014.5*	-5,09
R07A4.2	6,57	*casy-1*	5,17	*E04F6.4*	-6,02	*nra-1*	5,21
frpr-7	6,31	*Y51H4A.1*	4,77	*bus-18*	-6,15	*lact-4*	5,05
T19D7.5	6,86	*lgc-39*	5,06	*ZK1025.3*	-5,47	*let-23*	4,34
C25G6.4	6,87	*Y51A2D.18*	-6,38	*frpr-6*	5,29	*sipa-1*	3,72
F56A12.2	7,82	*F21D12.3*	5,63	*mpz-1*	3,80	*acox-1.5*	-5,45
pde-3	7,07	*T10G3.2*	7,35	*ilcr-1*	4,26	*egl-9*	3,57
unc-25	6,16	*unc-46*	5,33	*T05F1.11*	-6,55	*F54G2.1*	3,65
npr-32	7,53	*tag-89*	6,83	*myo-2*	-5,13	*unc-80*	3,38
pgal-1	5,92	*aex-6*	5,81	*col-131*	-7,41	*Y54G2A.26*	4,32
nlp-13	7,47	*glb-18*	4,72	*col-65*	-4,91	*pmp-2*	-6,30
exp-2	6,56	*agmo-1*	-8,83	*ZK822.2*	5,41	*T01G1.2*	5,57
H35B03.1	5,76	*ZK512.7*	-5,52	*pkg-2*	3,58	*Y40C5A.4*	4,49
pghm-1	5,55	*ggr-2*	6,16	*unc-13*	3,67	*mlt-10*	-4,92
lgc-53	6,57	*ilys-4*	7,04	*Y40B10A.9*	5,56	*Y41E3.7*	4,38
DH11.5	5,34	*Y43F8B.2*	4,63	*W07E11.1*	3,72	*T02E9.5*	4,36
ZK742.7	6,22	*drn-1*	5,95	*R05D3.9*	-5,77	*dpy-13*	-4,12
dmsr-6	6,24	*T10B5.4*	5,48	*snt-4*	4,53	*suro-1*	-6,20

gene	logFC
R07E3.6	-6,22
M153.4	3,89
sto-6	4,92
C24B5.1	6,36
nhx-3	-6,87
B0024.4	-6,89
C01H6.4	-6,27
glb-32	5,31
B0457.2	-5,85
nfki-1	3,84
C35C5.8	-5,42
B0334.13	-5,99
sqt-3	-3,89
F38B6.6	4,81
calf-1	3,74
F55D10.4	5,28
lad-2	4,48
nhr-238	-6,87
C34F6.10	3,53
ugt-2	-6,66
mam-2	-7,84
alr-1	4,56
ZK180.5	-4,81
osm-8	-7,34
C32H11.5	-6,20
frm-7	-5,15
egl-15	-6,08
T06A4.1	-6,21
C05E7.2	-5,79
C49C3.9	-6,63
best-3	-6,86
R02D3.1	-5,08
wdfy-3	3,50
sfrp-1	-5,96
nhl-1	-6,64
Y38C1AB.1	-6,59
cnt-1	3,97
acr-19	5,03
oga-1	4,03
dos-3	7,75
Y53F4B.45	3,27
col-174	-6,11
tpa-1	3,44
wrt-3	-6,61
C38C6.3	-6,46
T04C9.1	3,30
mbk-2	3,20
F43D2.6	-6,74
kcnl-1	3,51
wts-1	-5,63
aat-5	3,85
dyn-1	3,78
cdh-10	-4,95
svh-4	4,18
zmp-2	-5,85
tag-180	3,53
pamn-1	4,74

gene	logFC
cdgs-1	3,57
col-90	-4,25
Y53F4B.27	-6,27
C50D2.2	4,12
pqn-89	3,54
rimb-1	3,74
T07F12.4	5,24
F23H12.5	-6,52
dnj-5	3,30
tyr-6	-7,16
T16G12.1	-5,45
col-14	-4,44
F32B5.7	3,84
flp-26	5,67
dop-5	4,57
col-103	-3,61
T04F3.1	-4,37
oac-1	-6,50
nlp-33	-4,43
plc-3	3,38
W05H12.1	4,11
Y56A3A.6	-5,52
F13H8.11	-7,11
col-168	-3,66
C37C3.7	-6,91
clec-225	-6,91
Y54G2A.76	-3,96
pqn-13	-7,62
sma-6	-7,37
saeg-1	3,20
F41E7.1	-7,32
daf-5	3,68
F44E7.7	-8,20
F52G3.1	3,25
grl-15	-4,04
goa-1	3,24
F44E5.4	8,70
sea-2	3,53
T05H4.7	-7,02
bah-1	-6,26
glb-12	5,65
dhp-1	-6,56
lonp-2	-6,62
npr-13	5,03
mtm-6	4,43
slc-17.8	-6,61
ced-6	3,54
R74.8	4,17
T10B10.4	4,51
sqst-2	-7,08
F56F10.2	3,48
F47G9.4	-5,92
unc-32	3,10
K10C8.4	4,43
dep-1	3,21
T03F7.7	-5,37
frpr-19	5,07

gene	logFC
sulp-4	4,31
hum-6	-4,60
col-156	-5,38
R07D5.2	5,70
ttll-12	3,98
ugt-63	-6,56
gpdh-1	-6,74
nas-25	-6,42
E01G6.1	-5,80
ZK262.2	-6,53
Y105C5B.25	4,47
unc-79	3,47
rol-8	-3,81
col-160	-3,42
col-12	-3,47
F26E4.7	-6,09
cdka-1	3,92
W03G11.4	3,43
F28E10.1	3,15
qui-1	3,75
C35E7.2	4,05
nstp-2	-5,92
acox-1.4	-5,20
lips-3	-5,79
C25F9.4	-5,75
dpy-8	-4,43
ubc-17	5,09
rpm-1	3,26
nlf-1	4,31
elt-3	-5,69
col-161	-4,06
C08B6.4	-6,60
nfm-1	-6,51
xhd-1	-4,41
grl-16	-4,86
dmsr-3	5,81
dos-1	-5,63
F53F1.4	-3,79
col-166	-3,34
wrt-2	-6,06
K08D8.5	-6,48
col-58	-5,12
nhr-176	-7,10
mec-12	3,21
E04F6.6	-5,53
F01D5.1	-5,02
C53D5.5	-4,90
glna-2	-6,83
R07E4.1	4,00
F14B8.5	-5,89
C46H11.2	-6,52
F54C1.1	-7,25
F43C9.2	3,05
cln-3.3	-6,29
phat-2	-6,32
C24A1.3	-6,61
R03G5.6	4,08

gene	logFC
unc-2	3,74
C04F1.1	-5,26
gtr-1	5,49
nas-15	-7,41
puf-9	-4,36
H43E16.1	-6,05
K07C11.4	-5,81
R11.2	5,41
F54C9.7	4,70
nurf-1	4,76
C23H4.3	-6,43
exc-7	3,36
scd-2	3,82
kcc-1	-5,42
dnj-13	3,88
C53C7.5	3,97
F07A11.5	-3,86
ZK370.4	2,91
C02B8.12	-7,00
dmsr-1	3,98
H04M03.12	5,03
F07H5.8	-7,01
F52H2.4	4,43
gldc-1	-4,61
C12D12.1	-6,08
pll-1	3,42
unc-9	3,66
npr-23	4,03
cyp-43A1	-5,55
C32D5.12	-6,14
nhr-212	-7,72
dkf-2	2,95
lgc-43	-5,24
ZC247.2	-5,13
sol-2	4,38
F57H12.6	-3,91
lpr-5	-3,99
clec-33	-7,45
C05C8.7	-3,90
F08D12.3	-6,35
C02E7.7	-4,11
doxa-1	-7,36
C32C4.1	4,43
col-169	-3,56
npr-16	4,27
Y54E10BL.3	3,90
M02G9.1	-6,23
T22B11.4	-4,27
F17C11.2	3,58
tmc-1	-7,18
ZK1055.6	-6,29
cccp-1	3,37
unc-108	3,58
K10D11.5	-6,23
elt-6	4,57
T03D8.6	-4,57
ugt-55	-5,01

gene	logFC
C35A5.10	-6,45
K09F5.6	3,58
F55A11.7	-5,17
ugt-36	-8,71
bkip-1	4,20
Y40H7A.10	-5,90
K10D3.4	-5,18
acl-5	-5,39
C02E7.6	-3,65
crn-6	-6,04
eif-2Bdelta	-5,55
col-147	-3,28
lim-8	-4,96
C15B12.4	-6,32
snt-1	3,77
C14B4.2	-5,95
rgs-6	3,66
C46F11.6	3,91
prx-6	-6,36
acs-14	-4,05
Y37A1A.4	-7,71
W10G11.19	-5,57
ZK381.2	-7,18
col-94	-3,21
nsy-1	2,87
col-159	-3,16
F11C1.7	3,14
F54D5.15	-7,18
ugt-5	-6,37
fbxl-1	3,20
vglu-3	-6,51
K02E10.4	-6,07
kin-19	3,45
chil-13	-6,25
pah-1	-4,02
nhr-132	-5,79
sqt-1	-3,69
col-46	-5,71
nhr-71	4,12
pept-1	-5,62
C32H11.6	-6,12
col-93	-3,20
F13B12.4	-5,33
sem-5	4,10
C54G4.4	-7,68
scp-1	4,95
unc-10	3,18
rgs-1	4,16
jip-1	4,13
ZK1025.4	-8,12
F37A4.3	-6,10
lips-15	-6,60
T19D12.9	-6,60
F38A6.4	-6,35
Y7A9A.1	-5,67
nhr-69	-6,11
nhr-206	-8,19

gene	logFC
unc-40	3,38
nas-32	-6,51
myo-1	-3,93
F49E10.2	-6,45
tba-7	-6,62
acr-2	4,21
T19D12.6	2,92
cls-2	3,11
Y106G6H.1	-5,25
prk-1	-5,02
C05E11.7	-6,25
C05C12.6	5,29
elo-5	-3,41
H11E01.3	3,73
F17C8.6	4,49
F49F1.5	-3,44
C27D8.3	-5,03
pho-4	-5,53
syd-9	3,37
C15B12.1	-5,71
C05D12.3	-4,48
col-10	-3,14
efl-3	-6,37
nhr-90	-5,22
Y38C1AB.5	-5,80
grd-6	-6,00
flp-34	4,61
zip-11	-6,61
clec-28	-7,03
pmp-1	-4,82
plc-2	-6,08
col-115	-6,85
F39H12.2	-8,25
F22F7.2	-5,99
ser-7	4,65
col-77	-3,91
clec-37	-5,75
lgc-21	-5,10
gpb-1	3,41
C34C12.7	-5,22
C17H12.4	-5,53
F55C12.4	4,76
F46C8.8	-6,83
skpo-2	-6,06
T19D12.10	-6,71
K10D11.3	-7,11
F49C12.6	-6,35
arrd-15	4,42
clec-230	-3,63
C11H1.7	3,25
F14D12.1	-8,09
T24C12.3	-6,17
F30H5.3	-6,11
C34B4.3	-5,90
oxa-1	-6,35
ram-2	-3,49
let-4	-5,50

gene	logFC
unc-62	-3,31
glt-3	-5,82
nhr-205	-5,70
spe-15	3,76
col-91	-4,13
drap-1	3,53
ZK6.11	-3,72
fard-1	-6,08
cutl-23	4,02
T19C3.2	-4,60
tbb-6	-5,27
W01A8.6	-5,12
R10D12.8	-6,05
cdh-7	-4,64
clec-180	-4,02
R05H10.1	-5,19
ttr-15	-3,47
F42G2.2	-6,36
B0228.6	4,25
mlt-4	-6,04
cft-1	-5,93
F48F7.3	-8,37
T14G11.1	3,61
T07H6.1	-7,01
Y18H1A.9	-3,98
mct-6	3,10
lys-2	-4,15
anat-1	3,36
Y102A11A.6	-6,20
hif-1	2,93
Y47D3B.1	-5,43
T21C9.9	-8,64
flr-1	-6,57
acox-1.2	-6,25
rab-3	3,47
ccdc-149	3,43
H14E04.3	5,35
orc-1	-6,31
ugt-65	-5,44
mltn-1	-6,80
lin-41	2,69
del-10	-7,04
best-24	-5,45
lars-2	-4,66
inos-1	2,80
F30A10.2	-6,01
dpy-21	2,78
col-133	-2,98
acs-1	-4,34
srp-1	-5,95
apl-1	2,69
Y59C2A.3	3,14
kcnl-2	3,58
ugt-61	-6,24
F16F9.4	-6,07
ZC132.3	-6,35
W02F12.2	-6,39

gene	logFC
mca-1	-3,65
ugt-40	-5,85
T13C2.2	-6,02
ric-4	3,95
math-26	-6,49
C54C8.4	-6,46
Y41D4B.17	-6,12
ZC455.1	-5,83
Y46D2A.2	-5,17
cyp-14A2	-7,46
col-3	-2,92
F10C2.3	-6,07
nhr-16	-8,54
C04F5.8	-5,95
C26B9.3	-3,29
col-180	-3,17
ceh-79	-8,48
T20F10.5	3,67
F48G7.4	4,67
Y39G8B.10	-5,36
ver-3	-5,17
M05D6.5	3,45
src-2	-7,24
lact-5	-6,10
M03E7.4	-6,39
bgnt-1.8	-8,49
akt-2	3,17
pqn-32	-5,35
F32B4.5	2,58
Y39D8A.1	-6,06
cah-6	4,71
C46C2.2	3,22
spp-13	-3,15
math-4	-6,14
F31A3.5	4,15
fbxa-38	-6,85
glb-10	5,83
col-144	-3,75
kin-16	-5,85
math-3	-5,69
F41C3.2	-6,34
hsp-16.2	7,09
egl-8	2,70
glo-3	-5,72
oac-29	-6,28
lgc-50	4,84
unc-26	2,87
C36C9.10	4,66
B0403.6	-6,36
col-92	-4,19
pmt-2	-3,00
crb-1	-6,82
C52G5.2	-3,24
miz-1	3,16
rbf-1	3,22
col-146	-3,22
acd-3	-6,27

gene	logFC
Y37F4.1	5,94
lact-8	-5,27
F59B2.3	-4,79
ZK822.5	-5,12
nep-17	-4,14
ctsa-2	-4,36
lrp-1	-3,40
F18F11.4	-6,12
ugt-11	-6,21
Y38F1A.8	-6,78
rft-1	-6,55
Y51H4A.7	-4,67
R102.4	-3,48
K05B2.4	-6,41
chil-23	-6,06
Y97E10C.1	2,68
fut-6	-8,06
nlr-1	3,46
C05D2.8	-5,98
acd-5	-8,37
pqn-67	-6,01
F40E10.6	3,33
cnc-8	-3,00
mrpl-22	3,08
lam-1	-7,69
F44G4.7	-7,18
fbxa-219	-7,65
ptr-18	-5,33
F53B3.6	-2,99
K10H10.12	-5,15
F46C8.1	-6,80
F59A7.8	-7,85
B0205.4	-6,32
nhr-23	-4,34
ttr-29	-5,93
chs-2	-4,76
F25D1.5	-6,04
spp-7	-8,05
F21D5.3	-3,91
M04C3.1	-5,42
R03E9.2	-6,63
rig-1	3,58
C53C9.2	-3,97
svop-1	3,55
che-11	-7,02
T07F10.1	-6,87
dct-6	-5,31
tyr-4	-5,86
ZK1073.1	3,80
ifp-1	-4,83
T12A2.1	-7,08
clec-86	-5,26
vps-33.2	-4,67
chd-7	2,44
F57F5.3	-8,75
AC3.5	-3,19
ncx-8	-6,06

gene	logFC
abu-14	-4,56
mom-4	-5,04
dmd-6	2,50
F17C11.12	-5,09
hpo-34	-3,34
K10C2.1	-4,88
Y16B4A.2	-5,58
let-60	2,85
C55A6.4	-2,96
F42G4.5	-6,02
F55D12.5	-5,57
hum-9	-4,65
T09B4.8	-4,69
F46G10.2	-5,65
str-176	-7,65
T07F10.6	-7,43
R12E2.15	-3,91
clec-57	-4,88
osm-5	-5,44
tyra-2	3,66
F53B3.3	-6,51
C05D11.9	-5,04
gst-13	-3,16
Y37A1A.2	-6,05
samt-1	-4,00
his-19	-6,83
his-21	-6,83
his-51	-6,83
his-53	-6,83
C26C6.9	-3,21
pcp-1	-3,82
Y106G6H.14	-7,46
T23F11.4	3,90
T10E10.4	-5,96
nep-12	-6,70
irk-1	3,93
H06H21.8	-6,60
fmo-1	-4,80
C10A4.10	-8,20
aldo-2	-2,84
klo-1	-4,48
daf-6	-7,95
Y69H2.9	-6,15
Y38A10A.2	-7,14
col-170	-3,50
T01D1.8	-8,08
C30G12.2	-7,83
ent-7	-6,25
cng-2	-8,00
T19D12.4	-5,84
gar-3	-5,74
wdr-48	-6,60
pepm-1	-6,21
F01G10.10	-6,02
lin-24	3,38
C33E10.8	-8,51
ugt-9	-6,19

gene	logFC
C17H11.1	5,29
E02H1.5	-7,97
ckr-2	4,03
orc-4	-6,20
pqn-65	2,63
cla-1	3,10
Y39A1A.14	-6,41
trpl-3	-8,41
pkc-1	2,61
C56A3.5	-4,65
tbc-19	-8,22
Y113G7B.14	-10,83
fbxa-51	-7,95
fbxa-2	-6,46
F16C3.2	-4,47
Y55F3BR.2	-4,94
col-66	-5,19
nipi-4	-5,04
lron-15	-7,78
F55G1.15	-5,74
dpf-6	-4,71
jud-4	-6,16
ZK742.3	-6,37
lin-10	2,75
T28H11.8	-4,71
chpf-2	-6,75
nspc-19	-7,97
fipr-21	-3,86
fbxa-92	-7,04
cyp-35A5	-7,72
C01B10.4	-6,57
col-39	-3,38
M176.5	2,91
C03G6.5	-6,83
R07B1.9	-7,25
pqn-8	-7,06
thoc-2	2,50
T21B6.3	-4,86
T24D3.2	-10,54
C26B2.8	-6,26
ptr-3	-7,68
otpl-7	-6,03
ZK816.1	5,90
bmy-1	4,52
col-48	-6,04
C15C8.4	-7,00
twk-14	-5,66
fbf-2	-6,47
C30G12.1	-6,42
fbxa-90	-4,81
ZK1025.5	-7,55
C49C8.5	-4,46
F53C11.1	-5,28
sec-6	2,63
T10B10.3	4,03
F36F2.7	-7,17
D1086.2	-6,58

gene	logFC
ctn-1	2,74
tbc-16	3,95
pac-1	2,45
nas-29	-6,41
afmd-2	-5,98
Y64H9A.2	-4,19
F58G6.7	-7,25
flr-4	-6,97
T07G12.2	-6,16
nrx-1	3,64
F19C7.2	-5,97
M02B1.3	3,20
axl-1	-6,75
F46G10.4	-6,78
F11F1.1	-6,66
nhx-4	3,82
kcnl-4	-6,06
col-125	-3,19
nhr-17	3,88
nep-11	3,05
F40E10.5	-4,86
unc-82	-4,12
ugt-21	-6,14
acd-2	-6,65
ZC449.7	-6,85
D1007.13	-5,61
ZC449.2	-6,00
mes-4	-5,70
ani-3	-7,06
prk-2	-5,76
catp-1	-5,93
K09C4.5	-5,85
dod-19	-3,98
F54E7.6	-6,37
B0280.13	-7,99
R06A10.4	-7,54
F23H12.3	-6,13
cln-3.1	-5,96
istr-1	2,70
try-3	-6,03
cks-1	-7,57
acdh-6	-7,55
mam-8	-4,83
par-1	2,46
nlp-35	4,43
ZK185.5	-6,10
F58F9.3	-8,18
F13B6.1	-10,72
clec-64	-7,89
C31B8.7	-7,60
K11H12.11	-6,15
octr-1	5,11
C44H9.6	-6,95
fshr-1	-5,47
B0252.1	-6,29
T04A11.1	-5,10
T04A11.4	-5,10

gene	logFC
his-35	2,83
F21D9.4	-6,91
F02A9.1	4,80
folt-2	-5,61
clec-227	-5,22
B0454.6	-10,44
C45G7.13	-7,16
igdb-2	-5,61
col-167	-2,90
nxf-2	-6,13
ZC239.15	-10,71
C50B8.5	-6,32
T24B8.4	-4,68
ugt-7	-4,53
cdh-5	-6,10
cyp-35D1	-6,75
Y50D4B.6	-6,04
cyp-13A10	-6,20
slc-17.3	-6,11
degt-1	-6,37
grl-5	-4,60
T13H5.6	-6,30
nhr-108	-6,01
M28.8	-5,66
C17B7.5	-6,82
K01B6.3	-10,45
unc-73	2,46
F28H6.6	-7,03
C52A10.1	-3,96
sur-6	2,46
rga-5	-4,36
nca-2	3,31
C25F9.5	-6,15
Y75B8A.16	-6,12
R07E5.4	-6,18
cpt-4	-5,68
nas-38	-5,33
kal-1	3,61
Y53C12B.7	-5,89
sbp-1	-4,77
best-8	-7,37
C12D5.10	-6,41
linc-7	6,33
cyp-31A2	4,94
abch-1	-5,75
C53B7.3	-3,48
tag-10	-4,66
Y57G11A.4	-4,49
T04F8.8	-2,88
clec-229	-6,12
gcy-21	-7,63
col-137	-3,03
bbs-5	-6,03
unc-36	2,76
gtl-2	-7,37
T02B11.6	-6,05
dyf-1	-5,72

gene	logFC
ZK418.6	-6,14
F26A1.9	-5,87
osta-2	2,88
T01G5.1	-5,55
Y47D3A.14	-7,47
col-117	-2,73
Y18H1A.14	-7,49
T19C9.10	-8,21
nhr-98	-10,16
sago-2	-7,08
Y73F8A.5	3,51
mlt-3	-4,23
sri-40	-8,22
K10G9.2	3,89
T14A8.2	-5,84
col-158	-4,09
nhr-7	-6,50
cpin-1	-5,22
C09G1.4	3,29
Y34B4A.5	-5,78
F13H8.3	-5,83
apt-9	3,45
C39B10.1	4,16
grl-8	3,88
ndg-4	-5,64
pck-2	-2,98
ncs-4	-6,10
C49H3.12	-7,54
Y57G11C.31	-3,45
bus-4	-6,12
C46H11.7	-7,26
rab-37	3,78
W01C9.2	-7,46
lgc-10	5,20
W01F3.2	-5,60
rgef-1	4,99
dop-3	4,00
K07E3.4	-3,56
T13H10.2	-5,62
henn-1	3,39
Y119C1B.6	5,54
Y2H9A.4	-7,29
C08B6.10	-3,14
haf-4	-3,72
C08F11.3	-10,29
D1054.9	-3,66
mxt-1	-3,87
prx-2	-6,30
fkb-5	-4,61
ksr-2	-4,69
Y57G11C.22	3,61
cyp-35A3	-6,55
fasn-1	-2,68
gcy-8	-6,36
T07G12.3	-7,44
snt-7	5,55
che-14	-6,26

gene	logFC
col-13	-2,98
R10D12.1	-7,29
C32E8.6	-7,12
polk-1	-5,28
Y119D3B.12	3,23
nsf-1	3,15
F13D11.4	-4,56
sqst-5	-7,34
C16C10.1	-6,89
Y62E10A.19	-2,92
clec-3	-6,90
F47B8.5	-5,31
col-162	-4,99
C26D10.6	3,10
cah-1	3,49
T21F4.1	-3,04
deg-3	-5,45
twk-34	-5,85
cutl-11	-9,99
pqn-62	-6,01
aat-6	-7,34
F41B4.1	-6,05
col-130	-3,27
F35C11.4	-6,36
tag-244	-6,10
pept-3	3,19
nas-30	-4,96
kin-15	2,62
swt-3	-4,99
F27C8.2	-6,51
try-10	-5,67
C04G6.2	-5,83
pat-9	-5,43
ctc-3	2,45
Y9C9A.16	-5,95
mab-9	-4,88
ceh-92	-6,48
F56D5.6	-4,47
ZC84.6	-6,43
F13H8.6	-9,89
frm-2	-4,71
lron-1	-7,56
R10E8.1	-6,45
fut-2	-6,58
nab-1	2,46
best-18	-4,60
let-805	-2,47
lgc-11	-5,98
F44G3.10	-5,65
Y102A11A.2	-10,33
wee-1.3	-7,67
M03F4.6	-2,74
acr-7	-5,75
H10E21.4	-3,79
F23F12.3	-5,84
zipt-2.1	-4,56
slc-17.1	3,20

gene	logFC
scl-6	-6,82
R193.2	-4,58
arrd-20	4,89
E01G6.2	3,68
dmd-4	-6,42
lev-10	2,66
C16D9.4	-10,24
F10C1.9	-5,36
cyp-13A6	-5,83
D1022.4	-3,06
clh-2	-4,82
W06H8.5	3,15
ogdh-2	-2,94
F36H9.5	-9,89
F13D12.6	-3,64
F42C5.4	-5,60
K08B5.2	-7,18
best-4	-6,63
Y69A2AL.2	-9,95
F56A4.10	-5,69
fbxa-166	-7,66
K04G11.3	-6,67
D2007.2	-6,72
F55G11.8	-3,54
pgp-2	-4,42
klu-1	4,07
dct-1	4,47
ech-9	-6,33
T02B5.3	-6,38
C55B6.1	-7,38
ceh-62	4,14
C15F1.1	-5,91
zag-1	3,88
ugt-6	-5,22
Y44A6C.1	3,33
lap-2	2,64
T06G6.6	-4,10
F33G12.6	2,79
F32H5.4	-5,97
peli-1	4,46
F32D8.3	-9,62
Y73B6BL.47	4,48
fzr-1	2,69
otpl-3	-4,96
T05H4.15	-7,37
F09A5.2	-6,99
H10D18.5	2,59
ctc-1	2,76
unc-18	2,64
B0403.5	-6,89
F36D1.7	-3,49
clec-36	-5,91
F36G9.3	-10,11
bus-1	4,22
dus-2	-5,93
best-16	-5,60
C26B9.5	-3,81

gene	logFC
F35A5.8	2,87
cpr-6	-3,78
daf-11	-9,71
clec-53	-5,77
C13A2.1	-6,26
gtl-1	-5,26
C49A9.2	-6,55
F45D11.14	-5,62
F28H7.3	-2,75
oac-51	-5,10
F15B10.3	-9,43
C50F4.6	2,63
T23G5.3	-8,29
M05D6.9	-7,11
T17H7.7	-5,39
C15C6.1	-6,41
cyp-35C1	-4,65
Y54E10A.6	-6,23
nhr-125	-6,03
T18D3.7	3,18
M01B2.8	-9,49
F58H7.1	-6,50
Y47G6A.14	-9,77
T07F12.1	-6,10
H03E18.2	-6,98
E04F6.15	-6,74
C46E1.3	-6,83
ugt-25	-4,96
sys-1	-7,19
R10E8.8	-7,06
math-37	-9,67
lipl-1	-5,98
C04E6.12	3,18
B0348.5	-6,22
C27B7.7	-7,18
fbxa-175	-6,71
R03H10.2	-5,51
F59B10.4	-5,94
ZK669.5	-6,29
ugt-33	-7,27
cutl-5	-6,14
hpo-6	-3,69
F11E6.8	-5,24
asd-1	3,85
T20D4.3	-10,46
egl-6	-9,22
Y39B6A.8	-6,90
igcm-4	3,74
F54D5.5	-9,10
best-9	-6,62
sams-1	-3,30
F56F10.1	-3,03
math-34	-9,55
ZK973.1	-4,91
H20E11.1	-4,13
R07G3.8	-5,79
cth-2	-2,81

gene	logFC
ptr-16	-5,41
K11D12.9	-6,66
asns-1	-5,58
xbx-9	-4,31
F26F12.5	-9,04
moe-3	-9,91
M03C11.1	3,57
xbx-6	2,50
ins-5	-9,41
par-5	3,26
Y67D2.4	-5,51
EGAP9.3	-5,92
F11E6.9	-3,02
hot-9	-9,59
T16A9.3	-6,59
F15B9.8	-4,90
Y4C6B.7	-2,49
inx-6	-5,66
nhr-110	-9,06
pals-14	-6,72
acdh-12	-3,28
Y22D7AL.9	-7,32
dgn-1	-4,74
unc-45	-6,35
algn-14	-6,54
T01D3.6	-5,11
nstp-3	-4,13
fbxa-190	-9,58
puf-8	-5,99
mth-1	-5,79
F18E9.4	-6,04
F35C11.5	-9,29
srh-30	-6,51
T25B9.1	-2,55
chil-24	-4,67
D1007.8	-9,50
R12C12.9	-4,87
asp-12	-6,61
set-15	-7,23
C31H5.6	-5,65
fbxa-182	-9,56
T05A8.5	-9,11
cyp-37B1	-4,55
his-43	-8,71
gst-27	-2,52
fah-1	-2,88
set-32	-6,63
bro-1	-9,00
his-18	-9,26
C09F9.7	-9,51
C49F5.7	-2,83
R12H7.4	-7,23
Y53G8AR.7	-6,52
brf-1	-4,20
K04C2.5	-7,04
F23F1.6	-9,08
F35H8.2	-10,21

gene	logFC
E01G4.5	-9,01
F20D6.10	-7,01
K10D11.6	-6,55
T20D4.13	-6,46
Y97E10AR.4	-9,40
zig-3	-4,75
M03F8.1	-6,97
F10D11.6	-4,25
T09A5.4	-9,13
C32H11.3	-7,27
R10E4.1	2,31
C47E12.3	-4,29
Y4C6B.3	-9,05
ptr-20	-5,81
ZK287.1	2,84
C49F5.8	-6,67
R12E2.14	-2,52
T04G9.4	-2,63
C08B6.3	-5,65
chil-22	-6,79
E02H4.7	-5,67
math-42	-6,02
F28B4.3	-3,59
C15H9.4	-9,34
ifta-1	-6,51
C17F4.2	-10,06
C28G1.5	-3,46
F55A11.6	-3,08
F57B1.9	-6,65
tbc-18	3,18
ugt-46	-4,66
aat-4	-7,59
D2089.3	-6,12
K01A6.6	4,81
W01C9.1	-6,94
C42D4.3	-3,34
Y37H2A.1	3,06
C35A5.5	-6,26
daf-16	2,21
F55G1.1	-7,48
bli-5	-7,00
gei-13	-4,66
che-7	-6,90
C05B5.5	-7,59
tol-1	2,77
ZC513.14	-6,42
his-38	-6,85
snn-1	3,13
Y105E8A.25	-3,20
cgt-2	-9,29
ztf-18	-3,86
ZC116.1	-4,49
K02E7.5	-9,35
lron-11	3,98
hpr-17	-8,86
K10G4.5	-6,57
hsp-16.41	7,23

gene	logFC
fbxa-21	-10,04
F53F1.6	-10,07
frpr-15	-8,79
C35A11.2	-6,82
tnc-2	-2,59
Y7A9C.1	-6,11
Y18D10A.23	-8,93
C13C4.6	-9,36
clec-26	-7,06
F01D5.5	-3,50
F21C10.4	-9,15
F07H5.10	-8,91
srsx-27	-7,18
Y45G12C.4	-8,98
C48E7.6	-5,23
akap-1	3,81
srw-71	-9,13
T19D2.2	2,71
tre-5	-6,47
atf-5	-2,95
daf-14	3,49
T03F6.3	-5,12
ugt-44	-5,87
mig-13	-7,01
T26C5.5	3,10
Y53F4B.25	-6,57
tmem-231	-5,62
ZK1225.1	-8,86
nhr-93	-7,70
K08H2.7	-9,40
spe-10	-5,48
D2030.2	-3,48
H23N18.4	-6,83
knl-1	-5,53
egl-4	2,13
nspc-3	-10,49
pgp-3	-4,65
cil-7	-5,65
ncr-2	-8,71
Y61A9LA.7	-5,01
nep-22	-3,79
C18G1.8	-6,72
B0205.9	-5,19
C27A2.8	-5,70
dsl-7	-7,25
egl-19	2,89
frpr-16	3,86
F55G11.2	-3,27
fbxa-101	-6,76
F13D2.1	-3,74
C37C3.10	-8,77
nep-18	-9,65
grd-7	-6,44
clec-21	-6,24
amx-1	-5,39
hda-3	2,98
clec-38	-10,52

gene	logFC
oig-8	-5,98
hlh-33	-9,29
apd-3	2,61
W03D8.11	-6,64
B0334.3	-3,26
pqn-37	-5,72
nphp-1	-5,61
C06B8.2	-5,93
taf-7.1	-5,52
R08C7.4	-6,43
ZC412.3	-3,04
his-58	-7,54
kbp-2	-6,34
snf-12	-5,26
F59D12.3	-7,57
ZC376.3	-5,82
acox-3	-3,50
zipt-22	-6,50
ghi-1	-6,27
ets-4	-4,36
F49D11.6	-6,67
Y39B6A.29	-6,61
R02D5.7	-6,04
his-59	-6,59
mls-2	-6,40
ZK1010.8	-9,04
Y38H6C.20	-6,92
C16B8.2	-7,01
nhr-210	-7,47
C35B8.3	-4,80
F54D1.1	-9,64
grk-1	2,52
set-27	-6,04
unc-105	-5,92
zim-2	-8,88
C50C3.1	-9,28
ZK6.8	-6,80
T07A5.1	-6,22
plx-2	-5,50
M02D8.5	-7,44
B0222.11	-7,23
C50B8.6	-6,75
rbr-2	2,35
mis-12	-6,74
T26C5.2	-5,24
saps-1	-4,54
F53G12.4	-6,90
K02C4.2	-5,36
R07B1.13	-9,93
lgc-36	-7,25
F09C12.6	-8,79
Y105E8A.8	-9,28
B0507.10	-9,23
W04G5.4	-6,48
C50F2.4	-5,69
col-119	-3,44
Y17G7B.17	3,53

gene	logFC
Y39H10B.2	-6,66
Y66D12A.19	-7,07
mam-3	-4,28
arrd-13	3,55
chil-19	-4,87
F54B11.4	-9,03
ani-2	-6,24
F31F4.11	-5,51
cyp-33C3	-6,64
elks-1	2,58
C03F11.2	-5,92
K12H4.7	-3,58
exos-4.2	-9,18
lec-10	-2,53
K09A9.6	-4,40
D1046.2	-4,86
C45E5.3	-9,70
hpk-1	2,17
fbxa-210	-6,67
Y51F10.7	-2,52
oac-14	-6,13
ZK402.3	-9,68
T05A7.1	-6,55
comt-2	-6,12
C17G10.1	-4,75
clec-242	-6,18
gad-2	-8,71
T22F7.5	-6,25
pals-1	-8,65
daf-37	-9,38
elf-1	-4,93
C14A4.9	-9,73
cyp-34A8	-2,99
R08B4.4	-5,68
ZC376.2	-6,26
R09H10.2	-9,00
Y42A5A.3	-8,87
acc-4	3,91
Y69H2.10	-5,67
M153.3	-8,75
daf-4	2,38
C23H4.2	-5,50
F35D2.6	-7,02
T19C3.7	-6,32
W07E6.3	-6,20
twk-10	-4,93
sre-20	-8,54
him-14	-6,65
F28G4.2	-5,50
twk-28	-5,69
R13A1.10	-8,71
C36B7.4	-8,38
T21B4.15	-9,00
R10E8.6	-6,47
reps-1	-6,40
ptr-22	-10,18
arrd-28	-6,97

gene	logFC
R06F6.12	-5,66
nhr-117	-6,08
mtcu-1	-5,42
DH11.2	2,55
clec-173	-5,65
nspc-20	-3,19
T06G6.3	-5,96
srm-4	-6,52
far-3	-2,45
cept-1	-5,40
K10C9.9	-8,45
ZK1055.4	-8,34
ift-81	-4,99
C52E2.4	-6,50
strm-1	-5,71
W02D9.10	4,17
C23H4.7	-5,05
col-89	-5,05
ZK1307.1	-3,40
pat-12	-3,17
F23D12.3	-7,28
C02G6.1	-7,68
C53B4.1	-7,42
Y47D3A.32	-6,26
hlh-13	-6,44
C39D10.7	-8,40
H06H21.11	-6,25
ugt-53	-8,99
gly-18	-8,31
nmr-1	-8,44
F25E5.5	-5,92
R09H10.5	-4,21
C27A7.5	-3,35
C55C3.1	-8,87
F43C11.6	-8,29
H41C03.2	-6,66
T22D1.18	-6,50
D2021.4	-6,79
F35F10.7	-8,33
R07B7.8	-5,52
nekl-1	-5,81
K09F6.4	-9,05
oac-58	-5,05
bbs-1	-6,53
F49H6.5	-6,41
clec-167	-6,41
T14B4.2	-5,39
nas-23	-9,73
gpa-3	-6,39
rol-3	-7,03
T20D4.5	-5,61
attf-3	-8,33
dod-17	-3,71
Y59E9AL.4	-6,10
nhr-139	-6,22
F35E12.9	-4,32
amx-2	-4,93

gene	logFC
cyp-44A1	-3,80
T23E1.1	-6,58
E04D5.4	-5,88
his-7	-9,26
spat-2	2,72
C10G8.3	-6,79
C56G2.4	-4,51
F41G3.3	-5,84
fbxc-53	-8,88
ZK1193.2	-6,07
C05A9.2	-6,80
F13C5.3	-6,30
col-139	-7,61
fbxc-51	-9,71
gst-42	-2,65
cpx-1	4,44
ptr-8	-4,08
C54E4.4	2,94
nhr-202	-6,72
mltn-3	-6,51
eel-1	2,09
lgc-54	4,41
F32H2.8	-8,71
ZK829.3	-5,88
C07B5.2	-8,89
F35F10.4	-6,06
hsd-3	-7,11
R05A10.6	-9,57
C34H4.1	-5,23
klp-6	-8,37
Y48G10A.2	-6,51
Y59H11AR.4	-5,98
egl-47	-6,03
nas-14	-8,52
Y51H4A.25	-6,95
unc-76	2,16
T14B4.9	-5,85
hum-10	-6,29
hhat-2	-6,82
lec-3	2,19
W01B6.3	-5,27
zfp-1	2,05
tag-164	-5,65
C06B8.7	-6,82
col-107	-2,76
pudl-1	-6,44
F28F8.7	-6,09
bgnt-1.1	-9,35
osta-1	-6,28
lgc-46	3,74
cnp-2	-6,03
srz-10	-6,20
F54H5.14	3,66
Y39A3B.1	-9,80
pqn-72	-6,81
eat-16	2,49
cysl-1	3,58

gene	logFC
tfbm-1	-7,08
nhr-161	-6,01
pals-26	-8,98
ZK1098.3	-5,99
set-23	-6,30
mks-1	-6,76
W03F9.9	-6,68
M01F1.9	-8,66
gcy-23	-5,63
C06C3.3	-5,42
vps-11	-6,68
dhs-24	-6,62
C28H8.5	-5,20
pezo-1	-2,61
amt-2	4,56
mus-101	-6,29
Y73F8A.35	-6,30
R13A5.9	3,33
lgc-1	-8,92
F32H2.11	-6,25
lge-1	-5,06
C05C8.2	-4,84
egl-36	-5,17
D2005.7	-6,41
C26G2.2	-8,76
cwn-2	-5,49
F19C7.1	-2,62
fbxa-108	-5,96
ogt-1	2,08
clec-41	-5,06
ZC416.6	-4,47
insc-1	-5,96
dod-24	-3,52
F35D2.2	-5,97
wht-1	-5,81
K09E4.2	-4,34
nas-36	-4,67
Y66D12A.16	-6,87
clec-35	-6,81
fbxa-32	-6,42
F35A5.4	-9,57
F09F9.4	-6,38
gska-3	-8,79
mef-2	3,79
unc-3	-4,36
trpl-4	-6,96
C46F4.3	-8,49
F20G2.6	-6,13
C32D5.6	-6,60
cyp-13A2	-4,42
K09E2.2	-6,63
ceh-23	-6,31
dhs-14	-4,68
Y32B12C.5	-7,70
acr-25	-6,30
M04C3.2	-4,27
anoh-1	-6,53

gene	logFC
srx-80	-9,41
C06H2.7	-6,75
nhr-114	-5,47
Y65B4A.6	-5,14
D1044.7	-5,73
R07C12.2	-4,79
C33G3.4	-4,96
clh-3	-6,94
dpy-20	-6,70
linc-96	-6,58
daf-7	-4,74
cyn-17	-4,48
F47E1.2	-5,34
pqn-42	-5,41
T21D12.7	-6,32
K08C9.8	-5,84
F42A8.1	-3,65
glr-8	-7,37
kin-2	2,21
F23F1.2	-6,05
npr-35	-6,06
F17B5.8	-6,02
ceeh-1	-2,83
kcnl-3	-9,69
oct-1	-9,42
tctn-1	-6,57
pud-2.2	-2,47
lev-8	-6,49
haf-9	-2,78
T14G12.12	-8,56
aexr-1	-6,90
Y32F6B.1	-3,25
acc-1	3,30
pho-6	-6,44
F17B5.1	-4,86
F53H2.1	-9,32
Y39B6A.30	-8,72
osm-12	-5,58
C42D4.13	-6,53
unc-130	-6,00
gst-44	-7,23
maea-1	2,60
F25B3.2	-7,68
K02E2.8	-5,57
F20B10.3	-7,03
DY3.8	-8,69
C27A2.12	-5,77
B0410.3	-3,25
H10E21.1	-6,56
srv-7	-8,83
ZC449.5	-2,91
nhr-147	-6,80
paqr-3	-6,89
Y66D12A.13	-5,96
T11F9.12	-3,91
nhr-116	-6,26
lurp-2	-9,04

gene	logFC
rab-11.2	-9,03
W07A12.4	-5,86
hmt-1	-4,21
Y47G6A.5	-5,58
D1005.2	-2,48
T04F3.5	-8,97
F09C8.1	-2,87
tor-1	-5,45
Y57A10C.9	-6,28
R10E8.7	-6,83
catp-3	-4,61
lron-10	3,03
ubc-23	-6,08
nhr-207	-8,63
ztf-26	-6,23
Y57G11C.41	-6,99
F54E2.5	-6,32
ttr-22	-6,43
Y105C5A.15	2,86
fbxa-99	-6,56
sfxn-5	-4,13
C16C8.16	-6,44
F37A8.5	4,23
clec-83	-4,79
F01G10.6	-4,56
clec-186	-4,78
fbxc-50	-8,92
Y7A9A.79	-6,98
F09B12.3	-4,15
frm-1	1,98
ZK1010.2	-4,48
nspc-13	-7,05
set-11	4,17
C12D8.15	-5,98
poml-3	-2,32
Y45G12C.1	-5,91
W03B1.3	-5,79
T12D8.5	3,18
nstp-8	-9,56
lir-3	-6,24
col-98	-2,23
F16H6.10	-6,34
col-80	-2,29
T26H5.8	-7,83
F59B2.9	-5,43
C54F6.3	-6,63
aagr-2	-3,04
ssl-1	2,40
F54E2.1	-4,17
dat-1	-5,20
Y41C4A.17	3,84
C05D12.4	-5,05
clec-85	-2,88
mgl-2	5,21
K08F9.3	-7,33
srh-48	-8,88
Y87G2A.19	-3,12

gene	logFC
trxr-2	2,99
T08G5.15	-6,22
hlh-1	-6,58
myo-5	-2,51
pitr-4	-9,03
Y48G8AL.12	-4,29
fil-1	-4,14
sto-4	2,60
mam-5	-5,08
F21H7.12	-9,47
grd-12	-6,33
Y57G11C.42	-6,57
unc-29	-5,39
tax-6	2,34
ZK973.8	-6,34
gst-41	-3,23
col-56	-6,36
cwp-5	-9,63
W09C3.1	-9,31
C17H12.8	-3,94
W03G11.3	-5,50
F35B12.3	-3,68
Y73B6BL.36	-6,46
H40L08.3	-6,25
C06E7.88	-6,60
R12C12.8	-5,74
C54D10.5	3,78
H20E11.2	-6,06
C36E8.4	-6,54
trp-1	3,15
cex-1	-8,93
W05B2.2	-6,97
nhr-273	-6,52
xbx-3	-5,86
B0198.2	4,11
nhr-208	-6,93
ZC434.3	-4,43
arrd-10	-6,59
adm-4	-4,76
nhr-140	-6,34
C01B10.10	-4,86
nhr-286	-5,99
E01A2.5	-4,70
cut-6	-6,38
irld-15	-9,20
T13G4.4	-6,06
rab-14	3,21
W02B12.4	-5,67
evl-18	-5,94
F36D1.8	-6,88
Y73E7A.8	-5,23
icl-1	-2,88
ifd-2	-4,85
H03E18.1	-3,98
F37A4.6	-9,70
C03H5.5	-6,52
mvk-1	2,25

gene	logFC
Y43E12A.2	2,88
eol-1	-6,44
T28C12.1	-6,72
pud-1.2	-2,29
F08F3.4	-3,26
adt-2	-4,17
T24D5.2	-6,03
F28C6.9	-6,74
C05D12.1	-5,71
mca-3	1,94
egg-5	-6,15
Y102A11A.1	-5,40
ZC373.5	-5,50
lgc-55	3,74
B0218.5	-9,01
R02D5.6	-6,10
lrr-1	-6,37
ZK328.6	-6,30
clh-4	-6,10
R07B7.10	-5,38
sdz-27	-6,86
gst-26	-2,53
cyp-36A1	-4,35
F38B6.3	-7,18
galt-1	-5,96
gab-1	-4,91
T04D3.5	2,64
grl-7	-3,82
oac-24	-5,06
Y37A1B.7	-5,57
fbxa-187	-6,64
myo-6	-3,33
F23C8.13	4,06
B0554.7	-5,77
C33D3.3	-6,06
oac-31	-7,13
T20D4.9	-10,23
tag-38	-6,17
D1014.7	-9,16
B0212.3	-5,45
cutl-12	-6,77
T28C12.2	-6,82
R10H10.3	-2,85
ZK180.6	-4,22
nep-16	-6,16
old-1	-5,93
ttr-23	-4,12
ZK1037.6	-7,71
B0280.7	-4,80
F56F11.2	-9,13
mlt-7	-3,59
nhr-258	-6,55
ZC513.5	-4,49
scav-2	-6,49
wrt-4	-8,06
aex-3	2,86
vbh-1	2,25

gene	logFC
acs-5	-3,02
K01D12.9	-3,38
T02E1.8	5,38
linc-83	-8,75
F45B8.3	-5,98
T07E3.3	3,03
T23G5.2	2,19
F40A3.7	5,18
spin-2	-6,76
F53F10.2	1,97
aqp-5	-6,73
F01D4.8	-9,60
F19C7.4	-6,07
VF13D12L.3	-2,83
clec-9	-7,95
lgc-12	-4,56
ugt-51	-5,11
C49G7.3	-3,26
Y70C5A.3	-5,31
dhs-21	-3,13
F13E6.2	-5,62
B0393.5	-6,39
nhr-145	-6,05
F49B2.6	-4,75
C43H6.6	-5,86
math-35	-6,42
F42C5.6	-5,69
K07G5.5	-4,40
unc-34	3,74
ztf-30	-5,90
K09H9.8	-2,93
hlh-6	-5,59
lon-3	-3,27
T12E12.6	-5,80
F25B3.5	-9,85
C09G9.5	-6,20
C09D4.1	-3,81
F07H5.3	1,90
paf-2	2,88
mdt-17	-5,80
Y41G9A.10	-5,96
math-14	-6,99
lyst-1	-6,59
rnt-1	-5,19
F45E1.4	-8,35
C26B9.2	-7,01
tyr-1	-3,14
C06H5.6	-4,63
F41E6.11	-5,06
Y105C5B.9	-5,41
F15A4.6	-3,13
sex-1	-6,32
trk-1	3,74
sox-3	-9,17
F07G11.4	-6,69
che-3	-4,68
sulp-5	-7,15

gene	logFC
H35N09.1	-4,96
W02F12.8	-3,39
lips-16	-6,57
C06G1.2	-6,47
hmit-1.1	-4,97
qdpr-1	-2,70
mlt-11	-2,97
T03G6.3	-4,26
C50D2.6	-5,80
csa-1	-5,18
spe-47	3,95
F31F4.1	-9,79
F58E6.13	3,64
asp-3	-2,79
dct-15	-6,65
nekl-4	-6,52
Y102A11A.9	-5,31
nhr-36	-6,42
nhr-251	-10,08
spc-1	1,91
col-149	-3,40
rap-3	-8,98
F20A1.4	-7,35
grsp-3	-8,43
F40F9.10	-5,35
nas-33	-6,78
R07E3.1	-2,59
W05F2.4	-2,87
W03D2.6	-7,09
R02E4.2	-5,35
F09G2.1	-5,17
pitp-1	2,28
pals-34	-6,29
lact-2	-3,45
T22B7.7	-6,51
hmr-1	2,07
fkb-4	-3,03
fbxc-40	-6,60
abts-1	2,35
lnp-1	-4,66
K07G5.4	-6,92
lron-2	-5,88
lgc-20	-5,62
Y41G9A.2	-5,20
F10D7.10	-4,53
K04H4.2	-4,22
F53F4.4	-5,62
pqn-31	-4,74
T03F1.11	-2,09
pqn-57	-5,58
daf-38	4,00
rom-3	-6,55
snt-5	2,68
R10H10.6	-6,32
inx-1	3,27
R08E5.3	-2,30
C34H4.2	-4,44

gene	logFC
ZC13.2	-6,14
abu-13	-4,46
F47E1.3	-5,80
gba-4	-3,46
twk-11	-6,19
F14D7.12	-6,49
nhr-179	-5,64
ceh-33	-6,91
clec-34	-5,69
C24A3.1	-5,60
chil-3	-5,94
Y97E10AR.2	-5,63
Y81G3A.4	-6,08
T09F5.12	-5,00
otpl-5	-6,57
hgo-1	-2,85
pqn-87	1,88
tor-2	-6,19
ptp-4	-5,31
F54B11.11	-6,95
chd-3	2,00
spat-1	-6,72
M04F3.3	-6,45
clec-258	-4,17
pmk-2	2,86
ncx-7	-5,35
ctsa-1	-3,49
T27D12.1	-3,35
str-154	4,41
F54D10.5	-4,65
R07G3.7	-4,55
ZK218.4	-7,08
nhr-67	5,30
frpr-11	-5,19
ets-5	-6,86
R06C7.6	-4,88
C24A8.6	2,82
pkn-1	-4,50
pho-1	-3,28
math-45	-4,97
mut-2	-5,44
K01A2.3	-5,80
Y37D8A.2	-3,59
svh-5	2,68
T24C4.5	4,27
ctl-1	-2,48
F55G11.7	-6,89
exc-4	-5,70
F21H7.2	-6,03
C26B9.7	-10,08
F54E4.3	2,89
cpz-2	-2,88
Y69A2AR.31	2,72
R09H10.1	-6,22
mth-2	-6,15
dhs-20	-3,68
kvs-4	3,21

gene	logFC
ZK262.3	-5,73
Y40H7A.4	-7,59
Y73B6BL.31	-4,20
C34F6.9	2,64
ugt-13	-4,25
npr-6	4,07
mml-1	2,82
T06E4.7	-5,25
dct-17	-4,87
srx-45	-5,32
cfz-2	3,09
C03G6.6	-7,19
nfya-1	-5,36
mltn-12	-5,94
R09F10.1	-3,11
spin-1	-4,85
F07C3.2	3,72
mks-6	-5,16
Y39G8B.7	-4,72
C28H8.2	-5,72
C24A3.4	-5,62
pacs-1	-2,68
ser-6	4,15
T09E11.11	-10,33
nhr-220	-5,41
F30A10.3	2,46
pqn-44	4,02
ncx-4	3,09
D1046.4	-5,95
lpr-4	-2,96
clec-165	-7,60
aex-1	-5,68
C17E4.10	3,18
cyp-35A4	-6,96
Y106G6D.6	-3,24
nspc-16	-5,23
W09H1.1	-4,85
gbh-1	-4,95
F08G12.11	-4,34
prx-5	-4,49
hid-1	2,72
cyp-32A1	-5,10
sup-18	-5,54
dmd-7	2,53
dyc-1	-3,18
sek-6	-6,41
ZC374.2	-5,42
pptr-1	2,08
odr-1	-7,09
poml-4	-2,32
flp-13	-4,72
acs-6	-5,47
ZK673.11	-5,32
E02H1.2	-4,21
C44B7.11	-3,68
ctbp-1	2,82
nhr-188	4,61

gene	logFC
F56C9.6	-9,57
nhr-112	-6,92
F15D4.5	-7,49
igdb-3	-7,96
rsef-1	-5,14
ZK328.7	-6,81
C11H1.5	-4,99
C29F3.7	-4,31
gei-18	-5,42
npa-1	-2,39
grsp-2	-9,38
ost-1	-2,04
pole-2	-6,28
E02C12.8	-5,09
F01D5.3	-3,00
ceh-57	-6,45
ZK470.2	3,05
nhr-245	-2,60
T21D12.12	3,12
col-20	-8,78
F13B9.2	-5,24
tep-1	-2,34
glr-1	3,02
F48E3.9	-6,26
sma-3	-4,68
Y22D7AL.11	-6,14
C18H7.11	-7,87
R09B5.11	-4,64
T13C5.7	-5,31
C05E7.1	-6,48
K10G6.4	-6,26
osr-1	-5,27
des-2	-5,08
F28F5.6	-5,10
Y47H9C.1	-3,62
nphp-4	-5,10
F20G2.5	-6,15
Y75B12B.11	-5,32
pals-39	-4,06
C34E7.4	-3,71
C36B1.9	-4,51
ugt-32	-6,54
mnp-1	-5,08
cyp-13A12	-7,11
ftn-2	-2,30
calu-2	3,01
clec-209	-3,30
ceh-2	-6,01
C50B6.3	-5,21
irld-34	-5,41
T18D3.6	-4,89
cdf-2	-3,45
aip-1	3,12
T01C8.3	-5,67
C04E12.5	-4,73
nhr-263	-9,90
alh-9	-3,01

gene	logFC
pan-1	2,08
odc-1	-4,50
lin-3	-4,73
F22F4.1	-3,57
C36A4.11	-5,98
gnrr-5	-5,34
M142.8	-4,27
W09D6.1	-5,74
clec-67	-3,08
C46F2.1	-6,07
nhr-151	-5,90
C25G6.1	-5,94
C02G6.3	-5,51
gst-15	-4,92
lpr-3	-3,65
srf-3	-8,71
B0244.4	-9,46
cblc-1	3,05
his-17	-8,80
K02E10.7	3,58
Y69A2AR.16	2,49
Y102A11A.5	-2,57
F31A3.3	-8,92
chil-25	-6,84
F57C7.4	-6,18
itr-1	-2,75
clec-265	-2,95
F33E2.10	-6,22
T24B8.3	2,54
Y54G2A.37	-7,56
C49F8.1	-5,11
R09D1.9	-9,49
cdh-8	-6,90
K09C4.4	-5,78
F16C3.1	-4,66
C38C3.4	-4,65
K03D3.2	-4,40
F46H5.7	-2,05
msi-1	2,22
Y43F8B.3	-4,37
gck-4	-4,46
sul-1	-5,38
F47B10.9	-5,44
cyp-34A10	-9,38
brd-1	-6,35
ZK856.14	-9,42
fbxa-93	-5,61
R09D1.12	-6,17
B0244.6	-7,06
C29E4.11	-5,97
Y6E2A.4	-5,59
frpr-3	4,34
pqn-22	-3,59
lys-8	-2,19
cdh-4	2,46
nstp-6	-5,50
C48B6.3	-5,34

gene	logFC
F39B2.8	2,37
T27A10.6	-4,54
cpz-1	-3,25
ceh-83	-7,38
ZK896.4	-4,81
Y119C1B.3	-6,32
C44H9.5	-6,79
F37H8.5	-2,82
olrn-1	4,24
acdh-11	-3,12
fbxb-101	-5,19
F40G9.5	-4,63
nas-7	-5,78
ZC443.4	2,59
T19D7.6	-6,26
B0464.9	2,90
F47B10.5	-4,30
gcst-1	-2,48
ppk-1	2,27
F44E2.3	2,87
F17C8.8	-5,36
C14H10.2	-4,24
npr-18	-5,00
C15C8.8	-9,85
F38A1.9	-6,65
crf-1	2,73
col-182	-4,99
ugt-12	-2,97
Y56A3A.33	-5,55
arrd-23	-5,82
gsa-1	2,76
comt-1	-6,12
sec-3	-4,44
ugt-14	-6,13
mab-23	-6,00
pyk-2	-3,76
Y34B4A.6	-2,32
nhr-203	-5,27
Y54G2A.41	4,83
F15B9.6	-4,76
F35G2.5	-5,49
fbxa-66	-7,37
sre-1	-5,65
F56D3.1	-3,59
ZC449.1	-4,87
C18E3.3	-4,65
W03G1.5	-3,90
ZK512.2	-3,41
srx-58	-9,94
D2023.1	-3,79
Y50D7A.13	-5,25
K08D8.4	-4,46
K10G6.5	-5,15
bar-1	-3,88
Y48E1B.8	-3,10
tcl-2	-7,45
Y67H2A.9	-4,51

gene	logFC
cul-6	-6,31
K03A11.6	-5,63
tdo-2	-2,58
C41G7.8	-7,03
D2096.10	3,63
C33A12.19	-2,91
unc-15	-2,99
dpy-9	-3,16
T02C5.1	-3,58
vps-25	1,90
F33E2.4	-5,96
F09B12.5	-6,25
lgc-23	-5,05
gei-8	2,01
efn-2	2,77
F33A8.7	-3,27
pals-37	-7,38
akt-1	2,16
F13B12.3	-7,23
nlg-1	-4,20
K08D8.3	-5,05
unc-58	2,44
srp-8	-5,71
ZK1248.15	-5,97
C10B5.3	-5,93
F58B4.5	-2,80
ttr-26	-3,71
ppat-1	-3,89
C17F4.12	-9,36
fbxa-39	-4,69
mrp-6	3,87
Y71H2AM.9	-4,42
fbxa-189	-6,11
F53A2.1	3,47
C05C12.4	-2,75
bath-37	4,59
F23H11.6	-5,83
apa-2	2,04
spon-1	-3,59
gbb-2	2,69
ZC196.1	-6,42
col-34	-2,11
R11G10.3	3,52
F22E5.8	-5,74
arl-5	-5,12
Y32F6A.5	-2,98
C14C6.2	-2,76
faah-1	-2,26
T09B9.1	-4,24
ZC239.14	-7,31
clec-50	-3,12
B0491.7	-4,42
M03F8.5	-5,29
pals-6	-7,45
gba-2	-5,81
gst-5	-2,20
hprt-1	-3,28

gene	logFC
sto-3	3,48
slo-1	3,01
W04B5.3	-4,44
memb-1	-5,55
hot-7	-5,56
srtx-1	-6,56
srx-68	-6,00
Y71H2AM.14	-5,95
T01B7.8	-5,82
Y43F8B.14	-6,65
F14H12.3	-4,00
Y105C5A.24	-4,52
cey-1	2,33
oac-34	-6,86
scl-14	-5,76
Y37F4.8	-5,18
nhr-180	-6,07
Y6B3B.7	3,19
C14C11.2	-5,78
htp-1	-5,73
C40H1.9	-6,48
vha-6	-2,05
Y105E8A.3	-2,45
dnj-9	-4,64
R03H10.7	-4,27
acr-11	-5,22
acd-4	-6,65
ccep-290	-4,26
slcf-1	-5,03
rgs-2	2,90
R102.11	-4,13
F13H10.5	-5,28
F48G7.8	-4,69
nhr-138	2,29
E01G6.3	-4,10
F53B1.8	2,72
gpb-2	2,50
K02E7.6	-4,67
F22D6.9	-5,77
F01F1.15	-3,57
glna-1	-4,13
clec-210	-5,58
irld-6	-7,24
F55H12.3	-4,69
T12D8.9	-3,48
Y57E12AR.1	3,60
ceh-30	-5,92
str-31	-4,51
sqt-2	-2,71
zer-1	1,84
acr-12	3,25
aak-2	2,21
mec-18	-3,43
madd-2	2,95
sma-2	-2,77
nhr-40	2,55
fbp-1	3,50

gene	logFC
Y73C8B.3	-3,66
lron-5	-3,76
R04B3.2	-4,12
acs-12	-3,96
frpr-9	-7,29
C03B1.7	3,21
Y11D7A.3	-2,93
F55F3.4	-7,43
mua-3	-2,59
clec-4	-4,54
T13F2.4	-5,64
fbxa-87	-5,99
srr-2	-6,28
F40F11.3	4,36
pvf-1	-4,31
chst-1	-6,02
irg-7	-2,85
C46A5.6	-6,10
sro-1	-4,74
ncl-1	1,86
C18H7.6	-5,55
lron-3	2,54
cld-9	-4,71
R03G8.3	-6,10
F48A11.4	-4,37
nas-3	-3,46
Y77E11A.12	-5,40
sre-13	-5,18
hlh-30	1,84
F29G6.1	-4,15
vacl-14	-4,99
ttx-1	-6,21
ctns-1	-3,92
maph-9	-6,63
sel-12	3,07
syd-1	2,60
gcy-18	-5,87
dyf-18	-6,06
daf-1	2,35
F56C4.1	-6,29
F29B9.5	4,22
C17G10.13	-5,63
T08G5.3	-4,30
tap-1	-3,57
ncx-10	-6,19
unc-1	2,72
C18A11.1	-2,78
C04F6.7	-9,77
oac-30	-4,44
Y54E10A.12	-5,18
sup-1	2,18
F15A4.5	-4,66
F33D4.6	-3,20
K07E1.1	-2,22
T19B10.8	-5,01
zip-12	-3,82
F20D6.5	-3,98

gene	logFC
sax-3	2,07
pha-4	3,02
Y54G2A.32	-4,09
Y69H2.15	-5,66
mig-21	-7,13
pals-24	-3,67
F40E3.5	-6,14
mocs-1	-7,36
fkh-7	2,30
R09A1.2	3,94
ZK993.5	-5,64
syg-1	-4,85
cutl-18	-5,85
W02H5.2	-5,80
Y23H5B.8	-5,19
C01G6.5	1,78
F49C12.15	-5,77
nhr-100	2,22
cyp-33D3	-5,88
srt-28	-5,42
ced-11	-5,90
F28C1.3	2,07
C31C9.7	-2,09
clec-66	-2,87
T05C12.11	-7,13
eat-2	-6,16
C02H6.3	-7,74
C06E8.5	-5,83
F09B9.5	3,41
dct-5	-3,35
F31C3.6	-4,11
ttr-33	-2,84
C44H9.4	-7,03
F13B6.2	-3,97
sym-3	-5,39
Y41E3.22	-5,00
F07A5.4	3,32
clec-169	-4,35
C02B10.5	2,27
apm-1	-4,49
C29F3.3	-4,69
elo-3	-4,95
dhrs-4	-4,01
glc-1	-3,55
Y119D3B.13	-4,03
acl-12	2,47
F58G6.9	-4,59
vglu-2	-3,11
F20D1.1	2,76
figl-1	3,11
myo-3	-2,81
mks-3	-6,11
cat-2	-5,60
ttr-2	-3,04
fbxa-74	-6,38
bgnt-1.3	-6,64
C44C10.3	-5,47

gene	logFC
clec-17	-3,48
abf-6	-2,59
dpy-23	2,57
C55A6.12	-5,78
F26G1.9	-7,64
C06C3.10	-5,08
Y45F3A.9	-4,55
cosa-1	-6,36
W03D8.8	-5,81
dlk-1	2,07
C15C7.7	-4,30
F13H6.3	-2,95
F38B6.2	-4,66
Y41D4B.14	-4,52
T28F2.2	2,48
acr-17	4,14
Y48G1A.1	-5,68
ocr-2	-5,71
fbxa-27	-4,52
acox-1.3	-6,12
cgr-1	-2,72
F27B10.1	2,75
C27F2.1	-4,72
eps-8	-2,09
lgc-27	-2,68
F01D5.2	-5,27
dnj-28	-6,00
F17C11.13	-7,78
epi-1	-2,51
ZC434.9	2,35
F57C2.5	-1,96
fat-1	1,96
abu-7	-5,35
T04F3.4	-2,52
ugt-22	-3,79
F35B3.4	-4,26
his-41	1,89
B0507.1	-4,35
trcs-2	2,33
nhr-213	-7,37
ent-2	2,29
fbxa-158	-4,88
vab-3	-3,94
tab-1	-5,27
R07C3.16	-6,95
ugt-1	-4,03
jmjc-1	-3,14
B0563.6	3,00
odr-10	-5,92
R11A5.3	4,52
gba-3	-2,33
ugt-41	-4,59
T22D1.11	-5,95
lgc-35	-5,69
T28A11.17	-5,96
F58B6.1	-3,90
T05B11.7	3,32

gene	logFC
nas-9	-3,89
T20F5.4	-5,51
F40F12.9	-4,83
myrf-1	1,71
E01B7.2	-5,75
chil-21	-5,09
frpr-14	-3,85
F45D11.2	-2,91
F45D11.3	-2,91
F45D11.4	-2,91
cua-1	2,55
pck-1	3,18
glc-4	3,08
nhr-198	-5,54
hda-4	4,07
acr-9	3,08
ZK1290.10	-5,77
B0563.7	-4,69
C40H1.8	-4,21
col-62	-5,41
F52D10.2	-7,20
acy-3	-4,77
lip-1	2,74
C17F4.3	-5,98
F07H5.4	2,34
dyf-6	-4,19
dhod-1	-3,03
cky-1	-5,84
nhr-148	-5,18
Y11D7A.10	3,31
R13H4.8	-4,39
cpr-3	-2,82
C18A11.4	-3,92
C27A7.3	-7,31
eff-1	-5,27
klf-3	-5,43
F13H10.9	-4,98
mul-1	-3,27
aqp-11	-3,18
K04F1.9	-2,80
klp-20	2,99
M03E7.1	-6,85
C24H10.1	-7,10
F59G1.4	2,73
clec-24	-6,01
cyp-31A1	2,35
F26E4.3	-2,53
cka-2	2,18
M01B2.13	-4,55
K08F9.1	-5,79
snf-3	2,39
fbxa-84	-5,55
syx-7	1,91
ZC250.4	-3,14
ceh-22	-5,56
mlst-8	-4,98
scc-1	-4,18

gene	logFC
sulp-1	3,90
unc-22	-2,74
Y51B9A.6	-7,10
T07G12.5	-4,22
rib-2	-5,69
oig-2	-5,84
C18A11.3	-3,77
lst-1	-3,43
nspc-18	-5,24
C15H9.11	-4,64
T01B7.13	-3,65
ugt-23	-3,24
tpxl-1	-3,87
clec-31	-6,22
srd-27	-5,50
F41E6.12	-4,42
fbxa-176	-7,44
ZK596.1	-5,04
itsn-1	2,65
F32D8.10	-5,16
clec-80	-4,13
col-142	-2,06
K10H10.10	-6,08
F17B5.6	-5,61
cil-1	-5,42
F46F2.3	-2,09
T08D2.2	-5,41
F21F8.6	-6,72
aph-2	2,15
W04E12.7	-2,61
npr-21	-3,94
clec-187	-3,12
C44F1.1	-4,76
T21C9.6	-4,95
B0310.3	-6,91
trx-2	-4,51
F56A4.2	-4,26
F32H5.1	-3,47
T13C2.7	-4,73
kin-9	-5,57
cyp-35B2	-4,95
nlp-26	-4,32
ZK250.13	-4,25
Y119D3B.21	-3,61
T22F3.8	-6,23
acd-1	-4,05
F57F4.4	-2,17
W03F8.3	-4,36
vit-1	-5,01
F52B10.3	2,58
C50F2.2	2,98
ZK809.8	-2,20
lim-7	-3,37
clec-185	-4,01
cyp-33C1	-9,68
F48E8.4	-3,60
F30F8.1	-3,67

gene	logFC
C14C6.5	-2,54
ent-4	-5,51
K08E7.5	-4,07
mtm-3	1,71
Y87G2A.16	-5,69
F41G3.2	-5,53
F36H9.2	-5,28
D1007.10	-6,10
ins-24	2,18
nphp-2	-4,62
iars-2	-5,81
lbp-1	-2,34
ads-1	-2,72
T06A1.5	-3,18
C33G8.13	-6,63
rfip-1	-2,58
nspe-7	-6,11
Y39B6A.27	-6,86
maco-1	2,45
H05C05.1	-5,10
F10A3.4	-5,07
F39H12.3	3,04
ZK1307.2	-3,15
gsnl-1	-2,36
tag-290	-4,18
Y43F8C.13	-4,43
F40A3.3	-2,03
tmem-135	-3,60
cyp-13A1	-6,06
Y18D10A.11	-5,13
clec-166	-4,57
fipr-23	-10,03
K01D12.5	-5,43
nth-1	-6,20
W05E10.5	3,02
gsk-3	2,78
C05E7.3	-4,88
magu-3	2,55
M60.7	-6,75
F45D3.4	-3,26
cls-3	2,28
pals-32	-6,63
dsl-5	-6,73
kcc-2	2,21
oac-53	-7,10
F08F1.3	-5,01
C23G10.11	-6,97
nhr-1	1,86
H40L08.2	-2,17
K09H9.5	-4,06
nmgp-1	-2,86
F11E6.11	-4,52
gst-38	-3,44
duxl-1	-3,61
smk-1	1,97
sodh-2	-6,02
F55G11.3	-5,94

gene	logFC
tag-273	-2,46
vpat-1	-5,32
srb-16	-6,33
H40L08.1	-2,80
clec-10	-3,90
T10E9.8	-6,43
T10G3.3	-4,32
hphd-1	-2,91
R07B1.5	-4,77
hasp-1	-5,26
gst-6	-2,03
pqe-1	2,03
R02E12.4	-5,45
eyg-1	-5,62
fbxc-23	-5,96
srt-7	-5,78
abhd-3.1	2,39
F28B12.1	3,71
rad-54	-6,51
ppk-2	3,03
pgp-13	-6,15
aqp-1	-4,17
K11H12.4	-6,34
VM106R.1	2,60
ZC155.4	-6,60
mps-2	2,06
C35A11.4	-3,09
F26F12.4	-6,70
fbxa-209	-5,85
pdl-1	2,95
otpl-1	-6,84
skr-1	1,69
W02D7.5	-4,38
dao-2	-2,28
Y36E3A.2	-5,85
F16F9.1	3,17
bli-2	-6,62
aptf-2	-4,49
fbxb-88	-7,20
Y97E10AL.1	-7,38
mec-1	-3,37
F31D5.2	-6,58
pyr-1	-1,94
T06F4.1	2,49
rab-19	2,26
clec-56	-3,07
pho-12	-6,45
ndnf-1	-3,73
nhr-216	-6,92
F57B9.3	-6,37
abhd-14	2,96
cyp-13B1	-3,96
drag-1	-6,51
cpr-8	-4,73
T16G1.5	-6,42
drd-1	-2,97
efk-1	1,96

gene	logFC
F47B10.3	-7,24
nhr-236	-6,72
sql-1	2,13
F32B4.4	2,72
T10B5.10	3,41
ldp-1	-3,29
gba-1	-3,81
C50B6.9	-6,60
F56D5.4	2,63
twk-17	2,41
rpb-5	-3,96
bath-43	2,14
K07H8.11	-5,71
F35A5.1	-2,15
K12H6.12	-4,23
T28D9.3	-3,42
set-16	1,74
Y54E10BR.2	-5,08
rpn-11	2,29
ZC21.3	-3,22
abu-10	-2,99
ptr-12	-4,42
R03A10.5	-4,35
D1086.12	-1,91
col-127	-2,60
eipr-1	2,53
Y71H2B.5	2,33
stn-1	2,45
tag-147	2,33
nhr-129	3,03
svh-2	-2,64
ZK512.1	-5,15
lpr-2	-5,13
Y41D4B.15	-6,68
C34F6.7	-4,53
F55D12.2	-2,76
pgrn-1	-3,68
unc-31	3,26
K11D12.8	-6,85
ugt-30	-5,65
gcy-9	-5,15
ttr-24	-2,07
fipr-10	-6,23
taf-3	2,46
cfim-2	2,13
acds-10	-2,81
F14B8.6	-2,68
gfi-1	-3,85
Y25C1A.2	-4,58
daf-21	1,69
inx-3	-6,20
F48G7.13	-6,30
Y73F4A.3	-2,93
lipl-6	-5,60
prx-10	-4,29
lmp-2	-2,48
cyp-25A2	-2,73

gene	logFC
C08F1.8	4,39
Y53F4B.18	-5,14
fbxa-89	-5,41
C29F5.1	-2,32
pdhk-2	2,01
T27F6.7	2,94
lips-7	-5,47
F08D12.7	-4,91
daf-10	-4,88
bbs-2	-5,88
lat-2	-5,06
hmg-1.1	1,99
trhr-1	-5,20
ptr-13	-6,82
R07H5.8	-2,51
F49E8.6	2,03
tmc-2	-3,33
ZK228.4	-6,13
clec-78	-4,59
F46A8.1	-5,31
F46C5.10	-4,66
dlc-5	-6,28
W04D2.6	1,80
C32D5.3	1,94
glb-6	-4,26
zmp-3	-3,73
Y95B8A.12	3,36
W02B12.13	-5,82
F16C3.3	-4,50
abu-15	-3,38
F44A2.5	-2,33
hpo-19	-2,09
F14F3.4	-5,02
lst-5	3,08
gfrp-1	-2,93
pup-2	-5,54
T05G5.1	-3,46
B0365.9	-3,71
C02F4.4	-2,15
T15B7.1	-2,43
sptl-2	-3,69
C28A5.2	-6,27
oac-59	-3,92
mrp-8	-3,78
C16B8.3	-2,40
str-131	-6,09
T27C5.12	-6,26
ced-9	3,26
lact-7	-4,60
cyp-14A5	-6,09
W03F9.4	-3,80
grd-14	-2,82
scl-5	-6,13
pqn-92	-3,37
F13H10.8	-2,47
stg-1	-5,02
haly-1	-3,49

gene	logFC
Y38E10A.28	-6,57
clec-1	-3,18
Y41D4B.18	-5,38
atf-2	-4,31
let-526	1,64
grd-13	-1,86
4R79.2	-4,64
F20C5.5	-5,02
nduo-1	1,67
T05E12.6	-4,38
Y110A7A.21	-3,97
ZK54.3	3,87
clec-62	-4,17
alg-5	-5,20
lbp-2	-1,75
T24H10.4	2,69
ZC443.1	-2,45
clec-63	-1,73
unc-41	1,97
pitr-3	-6,76
C17F4.7	-1,87
hrpf-2	2,16
F47B8.8	-2,34
pks-1	-4,32
zak-1	-3,63
T05E11.9	-1,81
B0286.1	2,77
ptc-1	2,17
Y53G8AL.1	-3,52
B0546.4	2,90
T28H10.3	-3,96
H05C05.2	2,87
C49F8.3	-3,70
clec-150	-1,89
F32D8.7	-3,42
tiar-3	-5,26
T17H7.1	-3,86
F48G7.5	-2,60
R04A9.6	4,03
H20E11.3	-3,73
sli-1	2,27
apb-1	2,17
acox-1.6	-2,87
cyp-34A6	2,34
dmsr-8	-6,09
dnpp-1	-2,25
fbxa-91	-4,82
R05H11.1	-3,85
alh-10	-2,19
T28A8.4	-6,69
npr-7	3,25
Y65B4A.8	-2,57
unc-69	1,83
H18N23.2	1,72
pqn-41	2,17
F53A10.2	1,83
pat-2	-2,15

gene	logFC
F57G8.7	-6,22
K08E7.6	3,71
K04A8.1	-4,60
ZK1025.8	-6,63
glt-7	-4,50
sym-1	-3,18
bgal-2	-3,88
inx-19	-5,00
mrp-4	-3,80
F54D5.7	-1,90
pqn-15	-5,75
phat-4	-3,28
F17C8.9	-2,79
ugt-47	-3,44
F11A5.15	-5,11
tom-1	2,21
jac-1	1,95
C50F4.8	-2,72
lys-3	-8,20
T02G5.7	-2,85
srg-49	-6,24
tsen-54	-6,10
cpr-5	-2,88
top-2	2,28
C34D10.1	3,62
H12D21.9	-2,88
F35E12.6	-2,78
F59B10.3	-3,22
C24G6.2	-3,59
C14A11.5	2,65
glh-3	-5,39
irg-4	-3,78
Y106G6H.6	-3,88
hst-3.2	3,56
ceh-24	-4,63
unc-7	-5,06
col-83	3,03
dhc-4	-3,53
nhr-41	-4,52
T24E12.5	-4,72
B0252.5	-6,97
T05F1.9	-4,91
cyp-33A1	-3,23
his-37	1,77
C42D4.2	-7,61
gdi-1	2,01
T25C12.3	-3,80
acl-3	-3,91
pqn-26	-5,40
cyp-29A3	-3,77
eef-2	-2,64
F35C11.6	-4,07
Y23H5B.3	-6,05
dod-6	-3,14
nhr-158	-4,63
R05D11.9	-2,71
irld-11	-6,18

gene	logFC
ZK669.2	-4,47
nhr-88	2,49
K09F6.6	-4,72
osm-11	-2,23
T07D10.3	-5,49
nnt-1	-1,99
gei-14	-5,00
trp-2	2,98
Y37H2C.1	-6,53
F28G4.4	-6,82
C29G2.6	-4,57
C18B2.5	-2,07
Y51H7BR.7	-6,41
F48E3.2	2,70
lin-40	2,06
tnt-3	-2,26
T13C5.9	-5,30
ZK742.4	-6,71
ZK470.14	-4,01
Y50D4B.1	2,28
grl-21	-2,42
F46C5.2	3,14
mct-3	-3,59
F22F1.3	3,65
npr-24	3,65
hrp-2	2,23
T19D12.5	-4,41
tnt-4	-3,34
dsc-4	-4,00
bbs-4	-4,56
F53C3.4	4,81
C25F9.14	-2,30
spg-7	-5,48
Y11D7A.5	-4,04
dhs-4	-2,10
R11G1.6	1,99
dhs-27	-4,67
irld-40	-5,97
hxk-1	1,96
col-157	-2,62
C45B2.2	-1,99
ins-27	3,33
secs-1	-5,05
C33E10.1	-5,21
nhr-167	-6,55
F46F11.10	-4,73
C18E9.5	-2,99
F23D12.11	-2,47
clec-76	-3,32
cyp-33C7	-4,83
asp-14	-2,48
R04E5.9	2,41
chil-28	-5,11
F36H2.3	-3,16
ensa-1	2,22
lin-59	1,72
pitr-5	-6,45

gene	logFC
ska-3	-3,72
acsd-1	-3,66
tsp-14	1,85
ral-1	-2,02
acr-14	-3,75
F42G2.5	-5,04
acl-7	-3,53
chil-18	-5,96
atic-1	1,84
mpk-2	-3,32
ain-1	1,63
mltn-10	-5,06
Y55B1BL.1	-2,79
saeg-2	2,44
Y71H2AM.10	2,13
F46G10.1	-2,46
T20F7.5	-4,84
bpl-1	-2,61
ipgm-1	1,62
R08D7.1	-3,46
lec-8	-1,76
fbxa-137	-4,54
F46A8.13	3,16
hrdl-1	1,82
M01H9.3	2,27
glb-5	-4,77
C48B4.3	3,79
C15A7.2	3,36
sav-1	-3,51
C53B4.3	-3,78
vhl-1	-6,04
T04A11.2	-5,14
T04A11.5	-5,14
C29F7.1	-4,00
linc-25	3,27
vha-5	-1,89
T25B9.3	3,91
scrm-1	2,85
lips-17	-4,15
F18A11.2	-1,93
col-145	-2,34
Y105C5B.5	-1,88
T08H10.1	-2,06
T12G3.4	-2,56
gar-2	2,23
F11D5.7	-6,64
pes-5	-6,09
nlp-30	-4,03
F26C11.1	-6,18
C07D10.1	-6,36
F18E9.3	-3,10
egas-4	-5,49
rpn-2	1,94
W01C8.5	-1,82
ubc-16	-3,39
C23G10.5	-3,77
ensh-1	-5,28

gene	logFC
Y54F10BM.1	3,35
C03H5.6	2,95
F16B4.2	-4,00
C47B2.9	-4,04
W03F8.6	-2,26
lin-9	2,14
Y54G11A.4	-3,37
nhr-56	2,59
mtrr-1	-3,46
F52E1.14	-2,54
pak-2	2,45
ifc-2	-2,59
ugt-59	-4,16
F09F9.2	-3,12
inx-16	-5,96
cbl-1	-3,01
math-22	-4,38
F21A3.11	-4,14
T20B6.3	-4,95
inx-12	-1,63
pdi-2	-1,93
attf-4	1,77
ras-2	-4,79
maph-1.1	1,92
B0244.5	-4,68
cgef-1	2,04
PDB1.1	-2,45
marg-1	-4,95
clec-65	-2,39
Y59C2A.1	-5,54
pud-2.1	-1,91
twk-25	-5,55
ceh-44	1,68
F58H1.2	-4,37
btb-17	-2,48
T24C12.4	-3,85
F49E12.12	-5,15
gpa-15	-6,57
trr-1	1,80
K08E3.5	-1,71
fbxa-136	-7,87
F23B12.4	-2,04
fbxa-164	-7,26
C45E5.1	-4,93
let-268	-3,92
mup-4	-3,62
grdn-1	3,55
W02B12.1	-2,52
fbxa-80	-3,45
M117.1	2,23
his-62	-5,26
LLC1.2	-2,04
nduo-5	1,48
lpr-6	-2,39
pals-19	-3,51
cyp-14A4	-5,57
F57A8.1	1,82

gene	logFC
F13H8.5	-4,42
pqn-39	2,16
fre-1	2,21
sodh-1	-1,69
R12A1.3	-2,22
cyp-35A1	-6,42
ncs-2	1,69
T20F5.6	1,82
dhs-7	-4,53
Y32H12A.6	2,68
C26C6.8	-5,66
F45D11.15	-1,98
F45D11.16	-1,98
W04G5.10	-6,73
C06A8.3	-1,91
cyp-29A4	-5,92
exc-6	-4,65
str-162	-6,00
ubc-25	1,74
gpx-6	-1,80
sdn-1	1,89
F59E11.7	-2,75
fkb-3	-3,44
clec-54	-2,71
gpa-17	-2,80
srh-276	-5,64
unc-5	-2,39
snx-14	2,11
F13H6.5	2,82
nhr-178	-4,55
C27H5.2	-2,31
Y50D7A.8	2,44
C52A10.2	-5,62
C15A11.7	-2,93
Y57G11C.38	-5,35
cest-1	-4,88
C25F9.10	-2,20
pes-4	2,85
F55G11.4	-4,11
mnr-1	-3,86
ced-8	-5,81
K08D9.2	-6,24
sta-2	-4,35
col-128	-2,84
flp-2	-2,56
T24G10.2	2,23
ceh-88	2,37
imb-2	1,89
dhs-28	-2,22
fbxc-52	-3,40
gad-3	-2,86
R02F2.1	2,08
phg-1	-3,08
F39D8.3	-3,60
C27A2.5	-5,87
C35D10.13	-5,97
cyp-33C12	-5,94

gene	logFC
T06D8.2	-5,35
vps-32.1	1,99
nhr-193	-6,88
upp-1	2,38
F48C1.6	-2,59
F35H12.1	3,07
jph-1	2,05
ain-2	1,55
cyp-33C2	-5,42
bag-1	2,82
M05B5.4	-2,48
F55H2.7	-3,03
ZC15.10	3,94
Y47H10A.5	-7,57
aex-4	-4,99
ttr-32	-3,82
cpi-1	-1,58
ZK896.3	-5,76
ndx-1	2,62
fkb-7	-2,30
denn-4	2,55
fkh-9	1,72
K03H6.5	-3,61
H06I04.1	2,55
Y92H12A.2	1,90
igeg-2	-7,22
C16H3.3	2,02
cal-5	-1,57
btb-5	4,89
col-176	-1,94
T24B8.5	-2,73
prp-6	1,60
sulp-3	-3,55
ceeh-2	-3,26
K01D12.1	-6,50
hsp-17	-2,82
H13N06.2	-5,20
plk-3	-4,48
fbxa-52	-5,73
Y43C5A.3	-2,50
F28C6.5	-2,87
ptl-1	2,37
M04G7.3	3,71
gtbp-1	1,94
F20G2.3	-1,74
B0393.7	-4,56
ZC123.1	-4,50
clec-74	-7,33
del-2	-5,16
nhr-155	-6,97
C34E11.2	-6,78
haf-6	-1,95
flp-18	3,26
C18B12.6	-3,78
cec-1	2,30
M28.10	-4,15
psd-1	-1,76

gene	logFC
pitr-1	1,72
ntl-2	2,06
col-140	-5,14
act-2	2,45
ptr-6	-4,82
F36F12.1	-6,66
M02E1.1	2,15
dcp-66	1,92
K06H6.1	-5,67
F54D5.4	-2,40
lgc-30	-4,56
tut-1	-2,84
phat-1	-5,03
osm-1	-3,74
ncs-1	3,77
unc-70	1,55
H02F09.3	-7,41
cam-1	1,82
ctps-1	-5,63
F53F4.15	-5,77
C31E10.5	-5,27
tni-4	-2,00
che-2	-4,93
B0454.9	3,09
pho-7	-5,23
C25F6.8	-4,17
suds-3	-3,61
oac-7	-5,91
hecd-1	1,47
lgx-1	2,69
C50B6.7	-5,32
Y75B8A.24	1,71
col-108	-4,86
T04C12.8	-4,58
nrf-6	-4,47
Y45F10B.13	-1,84
cdo-1	-2,00
T07D4.5	-3,45
T19B10.2	-2,20
fpn-1.2	-3,74
hpd-1	-2,35
lpd-3	1,73
F49C12.14	-3,92
mrp-3	-3,45
M01B12.4	2,12
srap-1	-2,04
clec-7	-3,61
thn-2	-5,60
C15B12.8	-4,79
cdr-7	-2,73
imp-2	1,57
mccc-1	-2,56
ugt-17	-3,81
rskn-2	1,53
smp-1	-2,62
F19C6.4	-4,67
unc-64	2,14

gene	logFC
Y37D8A.4	2,57
F57F5.1	-2,18
hizr-1	-4,58
ttr-21	-2,39
pho-13	-3,60
pqn-36	-3,81
R13D11.4	2,90
gsp-1	1,95
Y48G8AR.2	-4,15
C49G9.2	-4,59
lsm-6	3,92
T16G1.4	-3,79
Y54G2A.45	-2,16
Y54F10AM.6	-4,07
spt-16	1,79
T10E9.3	-2,36
F59C6.16	-3,62
pals-17	-5,90
F59E12.15	2,07
C30F12.5	-2,00
srr-6	-6,15
pisy-1	2,46
C52B11.5	-2,45
oac-57	-4,14
F21C10.7	-1,87
dyb-1	3,45
fip-5	-2,10
ugt-8	-2,59
T24F1.4	3,32
mig-18	-2,74
hmg-11	2,56
F10F2.2	-1,96
maf-1	2,44
gst-31	3,86
Y42H9AR.5	-3,49
cpr-1	-1,97
clec-61	-3,16
M03B6.4	-4,06
let-99	-3,42
npr-15	2,86
D2092.4	-2,28
ugt-4	-5,84
cyp-34A1	-6,82
sop-3	2,22
pin-2	-3,77
R05G6.9	-3,73
H36L18.2	2,71
T22F7.3	-4,86
C30E1.9	3,08
K09B3.1	-3,43
clec-13	-3,40
T22C8.3	2,73
sre-4	-3,69
zfp-3	2,45
cul-3	2,64
ddx-15	1,63
bas-1	-2,92

gene	logFC	gene	logFC	gene	logFC	gene	logFC
Y37E3.1	1,79	*C24H10.3*	-4,26	*R02D5.1*	2,28	*ocr-4*	-5,27
Y61A9LA.3	2,14	*fbxa-114*	-3,68	*H01G02.3*	2,37	*cdr-1*	-2,85
bcc-1	-4,58	*F59C6.14*	-2,41	*mpst-1*	-3,83	*ZC328.3*	-3,54
T25G3.3	-2,12	*spp-10*	-2,40	*gly-6*	-1,70	*C10C5.2*	-5,83
ham-3	2,24	*dpy-28*	2,03	*B0310.1*	-2,11	*wago-2*	3,15
C18A3.1	-3,62	*elo-4*	-6,26	*F49C12.12*	2,02	*ZK131.11*	-2,08
Y57G11C.9	1,47	*lgc-34*	-1,72	*hot-3*	-3,52	*gly-2*	-3,41
gcp-2.1	-2,17	*cpr-4*	-1,79	*R05F9.9*	2,13	*zig-9*	-4,96
nhr-15	2,53	*ptr-2*	-3,41	*mrp-5*	-1,90	*F45D3.3*	-1,76
mec-6	2,39	*R07E3.2*	-3,90	*phat-5*	-4,65	*vhp-1*	1,91
spr-5	2,14	*inx-18*	-2,50	*nhr-115*	-3,67	*ugt-57*	-4,02
C54D10.3	-2,67	*pmt-1*	-2,08	*haf-1*	-5,89	*F53E4.1*	-2,71
pole-1	-3,26	*F19C6.3*	3,04	*far-4*	-5,92	*C18H9.5*	-4,14
pgp-11	-4,95	*C26E6.12*	-2,20	*D1054.5*	-5,91	*T19A6.4*	-4,91
K04F10.2	-4,06	*M03E7.2*	-2,27	*Y41C4A.29*	2,45	*abf-5*	-1,71
F53B3.5	-3,36	*nid-1*	-1,84	*csb-1*	-6,50	*trpp-11*	1,79
F58H1.6	-4,18	*col-155*	-1,85	*ZK185.3*	-3,58	*C16D9.5*	-4,94
neto-1	2,81	*pola-1*	-3,40	*ptd-2*	-3,07	*F25H8.2*	-3,48
ftt-2	2,25	*C05D2.10*	1,91	*lfi-1*	1,69	*irk-3*	3,01
fbxa-4	-5,16	*hsp-1*	2,50	*ccb-2*	2,67	*aagr-1*	-3,32
cutl-21	-4,26	*zipt-3*	-3,35	*ins-29*	2,32	*ZK721.3*	3,14
C39E9.7	-6,49	*ctb-1*	2,05	*F09E5.12*	3,32	*T19H12.6*	-3,43
pqn-60	-2,26	*gst-4*	-2,60	*H23N18.5*	-3,96	*ceh-48*	2,71
rrc-1	-2,77	*C01H6.8*	-1,69	*dhs-25*	-1,84	*lbp-3*	-2,44
F21C10.13	-4,33	*rad-26*	2,01	*math-18*	-4,14	*F41F3.3*	-2,40
emb-4	1,78	*C25H3.11*	-3,52	*xpa-1*	-3,67	*T13F3.7*	-3,56
pcm-1	1,53	*K10B3.1*	-3,92	*rpa-2*	2,05	*snx-27*	1,87
D2045.8	-2,84	*F22G12.5*	2,05	*C11G6.2*	6,33	*dve-1*	-3,87
cdc-14	-2,93	*tyra-3*	2,54	*C06G1.1*	-3,76	*aars-1*	-2,14
scm-1	2,65	*ZC434.10*	-4,15	*acs-3*	-4,84	*F58D5.5*	1,94
B0334.6	-4,16	*nspc-14*	-3,23	*pyc-1*	-1,90	*F53C11.4*	1,78
asp-2	-1,71	*unc-4*	-4,55	*xpo-1*	1,48	*endu-2*	-1,70
C28C12.4	-1,93	*Y105C5B.15*	-3,62	*W08G11.3*	2,73	*rsf-1*	-1,88
cit-1.2	2,11	*mlc-3*	-1,55	*W03F9.1*	3,09	*agt-1*	-3,34
pdi-6	-1,92	*F25E5.2*	-3,45	*gsr-1*	-1,80	*F45G2.9*	-3,81
unc-98	-2,09	*pmp-5*	-1,97	*M162.5*	-6,13	*dpy-31*	-2,44
F25E5.8	-1,94	*glb-25*	2,95	*ech-1.2*	-2,03	*tre-2*	1,82
lmn-1	1,48	*nas-11*	-3,59	*aho-3*	2,27	*T22B2.6*	-2,47
F58F9.1	2,42	*attf-2*	1,78	*cca-1*	-2,27	*Y106G6G.6*	3,01
abu-8	-2,73	*asic-2*	-4,05	*cogc-6*	-3,46	*col-126*	-2,18
fbxa-29	-5,36	*let-756*	-3,25	*mtm-9*	2,57	*F41G3.10*	-4,47
vars-1	-2,65	*klp-7*	1,89	*elt-2*	-2,68	*unc-112*	-1,70
H34I24.2	-2,82	*pqn-71*	-2,60	*ech-8*	-4,09	*Y51H4A.8*	-2,42
best-7	-4,69	*F59B10.5*	-2,13	*Y40B10B.1*	-6,30	*col-104*	-2,63
F15H10.8	-4,29	*cdk-11.1*	-2,34	*F48D6.4*	-2,00	*pct-1*	1,64
ZC395.5	-1,94	*mai-1*	1,94	*lips-1*	-3,62	*T28H10.2*	-3,47
ZK662.2	-2,01	*nmy-1*	-1,62	*fmo-4*	-3,15	*Y47D3B.6*	-3,30
supr-1	2,75	*sek-3*	-2,39	*mdt-29*	2,01	*nck-1*	1,55
lgg-2	2,23	*ZK1307.9*	2,69	*snrp-40.2*	-3,84	*F34D10.6*	-2,99
ugt-20	-4,60	*aldo-1*	1,80	*lst-6*	1,72	*unc-83*	-1,53
ugt-49	-3,69	*scl-3*	-4,23	*his-32*	-3,66	*C14B1.3*	2,15
ZK863.8	-1,74	*F52E1.9*	-4,09	*ttr-8*	-3,73	*ifb-2*	-2,00
ncam-1	-2,53	*ubq-1*	1,71	*C54D10.10*	-3,49	*R01E6.2*	-2,92
kqt-3	-4,20	*F22E5.21*	-6,27	*acs-4*	1,61	*col-17*	-2,51
T12B3.2	-1,92	*sulp-8*	-3,42	*cpna-2*	-2,80	*ZK1320.13*	2,87
nlp-31	-3,76	*trcs-1*	3,10	*asp-4*	-1,83	*C32H11.4*	-2,77
W05H7.1	3,76	*W03D8.2*	-4,07	*cht-1*	-6,23	*rhr-1*	-1,85

gene	logFC
F09F7.5	-3,27
mltn-9	-3,11
ugt-62	-3,32
ddr-1	-3,98
fitm-2	-2,26
wah-1	-2,98
ZK858.5	2,16
Y39A3CL.7	-3,03
wrn-1	-3,11
cyp-35B1	-3,97
Y66H1A.5	-1,56
trm-1	-2,27
Y49E10.18	-2,53
icmt-1	3,43
K06H6.2	-5,98
nhr-106	-3,82
pgam-5	-2,74
C44C10.4	-4,57
fipr-2	-1,88
F08D12.2	-1,80
T05H10.1	1,41
tag-234	-2,99
nhr-68	-3,31
ahr-1	-4,46
F13B12.2	-3,94
twk-29	2,09
abcf-1	-2,65
uaf-1	1,85
math-39	-4,50
pqn-25	-3,29
M03D4.4	-4,14
tat-4	-1,74
col-141	-2,46
C03B1.14	-4,50
R12C12.6	1,63
zig-7	-1,91
tre-3	-1,80
Y37H9A.3	1,74
C18H9.6	-3,09
trp-4	-3,88
che-12	-2,75
fox-1	2,08
Y22D7AL.7	2,68
T19D12.1	-3,57
lron-6	-3,51
C52D10.3	-3,56
twk-12	2,18
fipr-1	-2,51
T06D8.3	-3,93
M106.8	2,58
ZC376.6	-4,06
R08F11.4	-3,45
emb-27	-4,13
taf-1	1,66
hpo-15	-2,92
coh-4	3,16
D1022.3	-4,25

gene	logFC
tba-8	-1,39
T01D1.4	-3,26
C14H10.3	1,57
ape-1	1,47
pdr-1	-2,74
ZK1010.10	2,26
mkk-4	2,51
Y26E6A.2	3,19
C25D7.5	-5,40
F14F9.3	-5,39
Y47D9A.1	-1,53
alh-8	-1,88
mecr-1	-1,51
hoe-1	-3,99
kynu-1	-2,94
mig-10	-3,23
pqn-18	1,77
F47B8.10	-6,02
math-20	-4,04
fbxa-79	-5,18
cyp-34A9	-3,91
eat-5	-3,23
paa-1	1,72
ceh-20	-3,03
M88.4	-5,53
hum-8	-3,68
jnk-1	2,46
F35D11.4	-4,98
Y41C4A.8	-4,90
plst-1	-4,26
F59E11.2	-4,08
bet-1	1,88
vamp-8	-2,14
grl-14	2,63
ZK652.6	1,85
Y32B12B.4	2,46
lipl-5	-1,90
C01G10.15	-3,89
C13C4.4	2,51
pbo-5	-3,63
idhg-1	1,68
bus-19	-2,16
sop-2	2,00
ZK822.4	-2,51
lact-3	-2,48
ZK287.7	-4,51
Y71F9B.9	-3,40
tram-1	1,63
F13C5.5	-2,74
vamp-7	2,13
dpy-22	1,38
C55A6.7	-3,14
gbf-1	1,42
dcap-1	2,11
acs-20	-3,37
cyp-33E3	-3,30
gcy-32	-3,15

gene	logFC
cnt-2	1,67
F10D11.2	-2,71
F59C6.11	-3,12
nuc-1	-2,12
R11D1.1	1,99
C48B4.13	-5,69
T18D3.9	2,46
nhr-49	1,74
C01B4.7	-2,66
Y19D10A.4	-2,66
clec-204	-3,56
dpy-6	-1,94
dph-2	-3,08
fipr-22	-6,00
swsn-4	1,36
T09F5.1	-2,21
arr-1	2,18
C56C10.4	-4,10
nlp-27	-2,30
Y119C1B.10	2,56
zmp-6	1,90
ubr-5	1,57
cyp-23A1	-4,27
scav-4	-2,48
Y105E8A.14	2,71
marc-5	2,48
F46B6.2	-3,43
qua-1	-1,69
C17E4.6	1,87
C23H3.9	-2,00
C18G1.6	-4,53
max-1	1,68
vps-22	1,60
ZK105.6	-2,98
fahd-1	-1,86
F33H2.2	-2,40
alh-4	-1,61
clec-12	-4,27
sre-14	3,11
C33F10.4	-5,40
mab-5	-3,50
F11D5.1	1,83
Y34D9A.8	3,43
Y106G6D.7	1,73
unc-16	1,44
dhs-18	-2,43
daf-9	-4,12
Y73F8A.26	-3,75
R08E3.1	-3,44
Y51H7C.5	1,80
C54E10.6	2,49
lips-8	-5,48
act-5	-1,79
gadr-6	-3,82
flp-4	-3,55
grd-5	-2,21
E02H9.3	-2,53

gene	logFC
prmt-6	-4,87
Y62F5A.9	-2,38
slc-25A10	1,62
C27D9.2	-4,13
T01H3.2	1,82
mrg-1	1,96
W04A8.1	-4,24
M60.4	-1,86
sms-1	1,54
phy-2	-2,46
F32H5.3	-2,03
ekl-6	-2,37
K10D6.2	-2,45
F29B9.8	-3,59
cdk-9	2,52
ndx-3	-3,49
clec-25	-4,68
R166.6	2,37
C18H7.1	-5,99
col-111	-2,22
aph-1	2,18
srt-42	4,25
F56C11.6	-3,63
ntp-1	-1,59
M01G12.9	-4,59
K11G9.2	-4,00
fbxa-180	-6,23
ZK1320.7	-2,93
his-65	-6,15
ttr-27	-1,55
cmd-1	2,16
K10D3.6	-2,73
C49G7.7	-5,34
hpo-28	-2,06
Y105C5B.3	-5,74
T01D1.3	-3,35
F31F7.2	-4,75
Y54E5A.8	-1,97
scav-3	1,85
ZK813.5	-3,61
dpyd-1	-2,68
C30F2.2	-4,61
fbxa-55	-3,88
ZK909.6	-4,20
asd-2	-2,16
F35D2.1	-5,28
bra-1	3,66
F44F1.4	3,04
Y39G8B.9	-1,35
ttr-59	-2,50
Y71G12B.25	-4,90
F08F3.10	-2,77
Y62H9A.15	-2,52
oac-40	-5,63
T03F1.6	-3,75
lpin-1	-1,72
M116.2	2,33

gene	logFC
pcp-2	-3,71
F56C9.8	-2,19
kmo-2	-4,49
H24G06.1	1,30
dpy-10	-1,90
F21A3.3	-3,11
W06H8.6	3,26
Y102A11A.3	-2,81
T07D3.6	-5,21
T28D9.1	2,42
C46F11.4	1,83
cst-2	2,41
F08G2.4	3,18
C49A9.3	-3,67
txdc-9	2,35
skpo-3	-3,46
srp-2	-2,87
C25E10.8	-2,41
C05G5.5	-3,94
irg-6	-6,29
irg-3	-1,89
npr-3	2,48
ergo-1	2,04
hhat-1	-2,40
let-92	1,49
gly-15	-5,22
srr-4	-4,37
ing-3	1,83
ZC239.6	1,96
zipt-20	4,15
mdl-1	2,30
gsp-2	1,66
F32D8.15	2,81
emc-2	1,67
D1086.8	-1,82
M03F8.3	1,67
Y73F4A.1	1,76
col-73	-2,94
nono-1	2,09
idhg-2	-2,03
ttr-28	-1,83
Y55F3BR.10	4,39
apr-1	-2,80
ric-7	1,37
sptf-2	-4,10
gcy-12	2,25
ntl-3	2,29
ras-1	-1,85
F59D12.1	3,22
Y76A2B.4	-3,31
K02E11.4	-2,82
M01H9.4	-2,38
daf-19	1,49
F07B7.12	6,11
wrt-10	-2,62
mksr-1	-5,80
F49F1.7	-2,12

gene	logFC
C39D10.8	-1,63
C14C11.4	-3,72
gly-10	-2,06
Y53C10A.5	1,81
hum-4	-3,29
acs-19	2,10
flh-1	2,59
pgp-10	-3,42
R08D7.5	2,27
paqr-2	2,04
glb-27	2,41
B0303.14	2,46
F41G3.21	-2,82
cyp-32B1	-2,41
ZC8.6	1,87
ceh-89	2,82
Y95B8A.2	-1,88
wrt-9	-3,10
T16G1.7	-2,68
prx-12	-4,70
Y54G2A.7	-3,51
T13H5.1	-2,71
rfc-1	-2,01
Y69H2.1	-2,89
klo-2	-3,84
gbh-2	1,89
F58F9.4	-5,29
tbc-8	2,77
pdk-1	2,28
pqn-85	1,55
F22E5.13	3,01
oac-32	-7,21
Y65B4A.2	1,71
C27H5.4	-2,98
gei-4	1,70
lev-11	-1,43
rsy-1	2,03
C06E7.2	2,10
xbp-1	2,27
C14A4.12	1,88
cth-1	-3,53
mab-3	-5,52
nspb-11	-3,43
cnx-1	1,39
Y38H6C.16	-4,18
F40A3.2	-2,27
Y17G7B.8	-3,59
mdt-26	2,31
C45G9.5	-2,63
F53F4.12	-4,52
F45E1.1	2,29
Y37E11B.7	-3,63
K12B6.9	-1,79
cima-1	-1,73
spr-3	-4,41
tag-131	-2,47
elpc-1	-2,40

gene	logFC
Y73B6BL.35	1,97
nrde-4	-2,72
Y37A1B.5	-3,78
ZK1055.2	-5,56
F36H9.7	3,59
nspc-17	-2,58
C01B9.1	-4,21
eat-20	1,69
efl-2	2,93
lem-3	-2,93
arrd-6	-3,60
F27E5.7	-3,26
snb-2	-3,34
xrn-1	1,81
fmi-1	-2,92
grl-9	2,58
dhs-5	-2,83
T26F2.2	-5,18
Y17D7C.3	1,83
clec-15	-3,45
C36A4.4	-2,22
Y43F8B.24	-5,05
sqv-3	-2,65
ugt-39	-4,15
clc-3	-3,16
nspc-7	-3,36
sdpn-1	-3,76
W09G12.7	-3,85
F56E10.1	1,83
alh-3	-1,42
nkb-1	1,91
F58E6.4	-2,15
T13F3.6	-3,57
ZK430.7	-3,45
cyp-29A2	-3,40
gln-6	2,48
C48E7.1	-3,53
Y55B1BR.2	2,12
nas-37	-2,04
clik-1	-1,42
usp-39	2,41
fbxa-88	-5,84
fipr-24	-2,17
R166.2	1,68
ketn-1	-1,50
ubh-1	2,05
F21F3.6	1,46
vab-23	-2,84
F39H12.1	-3,12
cdkl-1	2,19
frm-4	1,37
nipa-1	1,95
K08D9.6	-6,02
avr-14	2,27
Y69A2AR.1	2,12
ric-3	1,85
K08B12.1	-3,24

gene	logFC
K11G12.6	1,81
heh-1	-2,54
C05B5.8	-2,22
B0379.1	-1,73
del-6	-1,50
lin-8	2,57
aagr-4	-1,96
ifa-1	-2,87
dct-18	-2,11
vab-7	-5,10
T11B7.2	2,73
R13H4.2	-1,47
T07D3.4	-2,35
pyk-1	1,57
bca-1	-3,01
efl-1	2,55
egg-6	-3,57
srx-56	-6,48
col-105	-5,43
Y37H2A.14	-2,32
C43F9.11	-4,80
fbxc-55	-5,56
athp-2	1,55
T28D6.5	1,71
C07G3.10	2,45
tlk-1	1,32
pqn-24	-3,48
K08C7.4	3,23
R151.2	-2,27
del-5	-3,78
R01H10.4	-3,88
mboa-3	-3,31
cut-2	-2,19
ttx-7	1,65
ech-6	-2,78
unc-122	2,63
F41D9.2	-1,73
his-20	-4,98
his-22	-4,98
his-52	-4,98
gex-3	-2,26
hrpk-1	1,34
F55F3.2	-2,61
ttn-1	-1,61
bet-2	1,75
eat-6	1,29
mog-1	1,38
F19H8.2	-1,79
sqv-4	-2,57
lin-25	-1,89
clh-6	-4,12
tpra-1	1,61
rom-2	-3,19
Y39G10AR.32	2,27
F53A3.1	-1,87
C25H3.3	-3,84
H04M03.3	-1,43

gene	logFC
ctg-1	-1,78
ZK1320.2	-1,51
F02D8.4	-1,72
Y46D2A.1	-4,20
akir-1	1,65
hlh-11	1,23
fhod-1	-2,59
arid-1	2,85
B0001.8	1,90
R119.5	2,20
Y57A10A.24	2,77
Y9C12A.1	2,57
ntl-4	1,47
C54D10.13	-2,34
F18A11.5	1,85
lec-9	-1,59
wdr-5.3	3,01
F18A11.3	1,60
mec-4	-2,79
F42A6.6	-2,86
got-1.2	2,20
F17C11.11	-3,20
C30G4.4	-2,38
K10B2.4	1,18
fbxa-18	-5,28
tars-1	-1,83
F25H2.12	-3,10
F59B8.1	1,93
gpap-1	1,94
bed-1	2,31
C25H3.10	-1,88
H24K24.4	-3,95
ugt-52	-5,34
unc-52	-1,61
ric-19	1,81
spd-2	-3,62
F35H10.10	-3,38
F23F1.4	-1,54
aqp-4	-3,07
B0035.1	1,59
srx-111	-6,05
grld-1	1,56
C24B9.3	-2,59
nduo-4	1,86
hot-6	2,25
mpst-3	-2,91
W07G4.5	1,66
cpl-1	-1,50
R166.3	2,21
nhr-103	2,23
R07A4.3	-1,80
T10B10.8	-3,11
maph-1.3	2,64
daf-36	-3,31
pals-23	-3,49
C14A4.6	-2,58
C30F12.2	-4,29

gene	logFC
let-2	-1,99
Y54E2A.10	2,82
fbxa-128	-3,96
kle-2	1,82
D2096.6	-2,76
lec-2	-1,40
F53F1.2	-3,27
C07A12.7	1,43
ZC443.3	1,62
ltd-1	-2,97
srg-25	-2,89
M195.2	-3,80
tag-304	1,87
C29F5.3	-4,40
C09F5.1	-2,25
C05G5.1	1,68
snap-1	2,06
pfd-6	-1,25
ZC190.4	-1,60
cat-1	-4,11
sng-1	2,47
hsp-25	-1,38
jmjd-5	-4,43
lid-1	-2,40
F52G2.3	-3,55
grl-4	-3,06
glf-1	-2,35
rdy-2	-3,68
ZK185.2	2,07
ZK524.4	1,66
ccg-1	-1,54
zbp-1	1,61
fbxa-11	-4,20
F44A2.3	-2,21
F23B12.7	-1,66
C01F1.5	-4,67
let-70	1,54
ZK643.5	2,40
F53B2.8	-2,57
svh-1	-3,78
tag-179	-3,43
gcy-36	-2,87
F47G4.4	2,13
baz-2	1,81
Y73F4A.2	-1,37
D2096.12	-2,75
hmbx-1	-3,09
lam-2	-3,66
clec-43	-3,45
dhs-13	-3,14
cnb-1	1,50
kel-8	1,58
tbc-17	2,24
ppk-3	-3,51
rde-1	1,51
Y75B8A.13	1,70
dgk-4	1,77

gene	logFC
D1054.8	-1,62
dhhc-3	1,79
srab-4	-4,76
T28C6.8	-1,55
F25A2.1	-4,00
fars-3	-1,63
C36B1.11	-2,74
C09E9.1	2,33
sulp-2	-4,05
oxy-4	-2,27
T27E4.1	1,78
deb-1	-1,60
Y38H6C.8	2,51
abhd-5.1	-3,00
R06F6.14	-2,53
chp-1	1,29
ifo-1	-1,63
asns-2	-2,81
nhr-54	-3,58
pqn-73	-4,71
btb-16	-2,31
gna-1	-2,47
his-3	-3,26
gpa-7	3,73
F22F7.7	2,13
F45G2.10	-2,37
nep-1	1,62
cfp-1	1,66
F31C3.3	1,62
spp-16	-1,41
T07D1.2	-2,07
Y54E10A.10	-2,34
sqv-8	1,99
ugt-31	-5,66
C39E9.8	-1,66
T16H12.9	-3,24
gln-3	-1,37
F09B9.4	-2,94
B0310.6	-2,56
catp-8	1,32
D1086.1	-1,85
nep-2	2,31
orc-5	1,88
sec-31	-1,82
taf-6.1	2,61
tbx-2	-1,75
T10E9.14	-2,85
pgp-6	-5,06
T01D3.3	-3,33
sgk-1	-1,76
R09F10.5	2,28
ZK858.6	1,35
F52H2.3	-2,85
Y48G1BM.6	2,92
F23F12.12	-2,12
K07A1.3	1,69
sym-2	-1,29

gene	logFC
B0361.9	-1,83
T25D10.1	-2,11
gck-1	-2,12
apc-11	2,28
C34D1.4	-1,90
gpc-2	2,08
ran-2	-1,59
gta-1	-1,78
F44D12.2	-3,72
F35G12.12	1,57
aakg-3	2,73
H14A12.3	1,31
C14F11.6	-1,52
dyf-13	-3,96
R10H1.1	-1,64
mec-17	-1,23
F43H9.4	-3,19
his-9	-2,89
his-13	-2,89
D2092.8	-1,42
egl-13	1,87
enu-3.1	2,11
EGAP4.1	-1,43
fbxa-146	2,42
glb-24	1,83
F11E6.6	2,49
nas-13	-5,11
F40H3.2	-1,65
F46F3.3	-4,05
sac-1	1,63
strl-1	-1,54
Y47D7A.13	-2,02
nfyb-1	1,91
Y105C5A.1	1,95
F13G3.3	-3,42
dpy-5	-2,18
sup-12	1,77
dct-11	-2,32
flcn-1	1,62
D2005.1	1,79
zig-10	2,42
ifb-1	-1,65
Y39F10B.1	1,55
W08E12.2	-2,23
C17H11.6	1,27
inx-13	-1,25
C01G10.6	-2,20
Y73B3B.5	2,66
sdc-2	-1,78
M04D8.7	-3,62
Y11D7A.9	-4,66
D2024.5	1,91
R12E2.7	-1,40
clp-1	1,35
ddx-17	1,16
K06A9.1	-3,82
C50F4.1	-2,01

gene	logFC
F44F4.3	-4,37
nhx-6	-5,52
fbn-1	-2,13
K09G1.1	-1,41
drr-1	-1,68
T03G6.1	-2,76
F12A10.1	-2,17
pud-1.1	-1,65
F33H12.7	-4,34
cutl-16	-4,63
C48B6.2	-2,29
aly-3	1,67
C36B1.6	-2,50
ZC443.2	2,41
ttr-16	-1,23
ZK792.5	1,32
F32D8.1	2,48
arrd-18	2,11
M03B6.5	-2,28
clec-5	-3,47
xbx-1	-3,87
Y94H6A.10	-1,63
cdc-42	1,33
srh-28	-3,81
F19F10.12	-1,95
ttm-5	-2,27
fbxa-61	-3,72
F52C12.1	2,95
lon-2	1,99
ajm-1	-2,57
tbc-6	-1,79
C53A3.2	-3,03
D2024.4	-1,96
T26A8.1	-1,59
W10C8.5	-2,29
ubc-14	1,55
pgp-9	-2,59
K06G5.1	-2,02
nape-2	-1,78

Table 5 – All significantly differentially expressed genes of the "sci-RNA-seq RIS vs. all" transcriptome and their logFC

gene	logFC	gene	logFC	gene	logFC	gene	logFC
flp-11	9,24	*rpl-3*	-1,60	*myo-3*	-4,23	*dmsr-6*	2,25
akap-1	3,63	*eef-1A.1*	-1,33	*nduo-5*	-2,09	*tos-1*	1,54
srx-2	3,77	*dmd-7*	2,45	*gem-1*	2,84	*T12D8.9*	-3,06
srg-69	3,44	*unc-108*	2,15	*Y105C5A.15*	2,18	*F32D1.3*	3,28
T05A8.3	4,66	*F46C5.4*	2,30	*aptf-1*	1,32	*pck-2*	-2,77
F53F4.17	3,35	*mpz-1*	2,27	*unc-13*	2,05	*rpl-33*	-2,38
rabx-5	3,98	*F52G3.1*	2,21	*epi-1*	-3,88	*Y11D7A.10*	2,25
ZK1307.7	4,44	*unc-54*	-6,01	*mup-2*	-4,11	*unc-27*	-3,16
srsx-18	2,71	*daf-16*	2,14	*F56A12.2*	2,19	*gdh-1*	-2,23
Y57G11C.46	3,61	*rps-9*	-1,86	*unc-44*	1,72	*K07H8.10*	-2,73
ser-4	4,64	*tpa-1*	2,81	*gei-3*	2,47	*rpl-5*	-1,04
R11F4.2	3,77	*avr-15*	3,44	*sto-4*	1,93	*F52H2.4*	2,68
nep-26	3,40	*eef-2*	-1,64	*H17B01.5*	2,58	*F41C3.5*	-3,78
cab-1	4,09	*pghm-1*	3,71	*npr-13*	1,91	*ubc-3*	1,76
kcc-2	2,99	*ins-24*	1,82	*unc-22*	-4,13	*dim-1*	-3,20
ckr-1	4,44	*Y43C5A.7*	1,98	*rskn-1*	2,47	*rps-5*	-1,21
egl-9	2,73	*dmsr-3*	3,46	*mlc-3*	-3,64	*nbid-1*	2,02
gap-1	3,92	*ZK742.7*	2,36	*tnt-2*	-3,92	*fbxa-3*	1,61
Y39A1A.24	2,99	*sem-5*	2,49	*W05F2.4*	-3,43	*mct-6*	2,28
arrd-26	3,07	*ptr-5*	2,75	*C10C6.7*	2,38	*lam-2*	-3,09
C01C4.3	3,09	*unc-57*	2,13	*dys-1*	-3,47	*pat-2*	-2,84
nlp-8	5,06	*nhr-71*	2,30	*fib-1*	-3,09	*rpl-19*	-1,19
K03B4.4	3,32	*dig-1*	-4,93	*rps-2*	-1,41	*acer-1*	-2,79
T12A7.2	3,44	*lgc-4*	3,18	*F19C6.3*	2,79	*his-37*	1,74
wee-1.1	3,18	*unc-15*	-5,08	*arrd-17*	2,36	*his-37*	1,74
ncs-6	3,11	*tkr-1*	2,41	*F01G4.6*	-2,71	*his-37*	1,74
egl-3	4,20	*hif-1*	2,10	*Y41E3.7*	2,02	*ZC449.8*	1,68
scd-1	3,23	*K02F2.5*	4,28	*C02B8.3*	1,97	*frpr-3*	1,32
abts-3	2,60	*maf-1*	3,10	*T21D12.12*	1,93	*lam-1*	-2,89
pck-1	2,63	*F35H12.6*	2,24	*B0286.1*	2,11	*snb-1*	2,38
pgal-1	4,03	*gsk-3*	2,08	*ser-7*	2,13	*DH11.5*	2,79
mbk-2	2,33	*ost-1*	-4,30	*let-2*	-3,98	*C25G6.4*	2,20
T27C4.1	3,98	*cpna-2*	-4,86	*tiam-1*	2,95	*rbf-1*	3,19
wnk-1	2,10	*H10E21.5*	3,48	*ketn-1*	-3,41	*rpl-7A*	-1,58
pamn-1	3,16	*rcn-1*	2,76	*clik-1*	-3,81	*alh-8*	-2,68
ttn-1	-7,25	*T07E3.3*	1,99	*tag-89*	1,83	*CD4.1*	1,69
frpr-16	3,47	*sprr-2*	2,22	*pat-10*	-3,54	*gcy-12*	2,13
egl-21	4,05	*unc-89*	-4,60	*catp-7*	2,10	*rpl-15*	-1,27
kin-1	2,36	*F44E5.5*	2,10	*nog-1*	-2,67	*mlc-1*	-2,98
nlp-11	4,84	*F44E5.5*	2,10	*F35A5.1*	-3,21	*rps-18*	-1,32
sbt-1	4,08	*mig-6*	-4,08	*csq-1*	-3,20	*F44E5.4*	1,88
rps-0	-1,98	*zig-5*	3,50	*syd-9*	1,94	*F44E5.4*	1,88
cmk-1	2,71	*F54D1.6*	3,15	*npr-29*	2,45	*T05E7.4*	2,28
nlp-13	4,21	*fln-1*	-3,29	*mvk-1*	1,68	*dpy-21*	1,77
sca-1	-4,14	*ida-1*	3,23	*sue-1*	3,88	*F46C5.7*	1,15
ilys-4	3,37	*mtm-6*	2,05	*far-2*	-3,78	*Y39G10AR.11*	1,83
flp-34	2,88	*R02F2.1*	1,88	*mlc-2*	-3,31	*icl-1*	-2,95
far-1	-5,85	*rpl-4*	-1,12	*ace-4*	1,59	*H06I04.3*	-2,48

gene	logFC
pkg-2	1,81
C39B10.1	1,50
glb-23	2,23
dop-3	2,52
F21C10.7	-2,86
ckr-2	2,25
ant-1.1	-1,25
Y64G10A.6	1,74
T01H8.2	2,64
rpl-6	-1,16
him-4	-3,36
hda-4	1,80
F20D6.8	3,00
F13H10.1	0,59
F40A3.7	2,14
spv-1	2,27
klu-1	1,86
lev-11	-3,01
atp-2	-1,36
F46H5.3	-2,62
kin-29	2,24
hpk-1	1,81
npr-32	1,56
ptb-1	2,44
glb-32	1,71
ins-27	1,59
nhr-67	1,63
pde-3	1,96
ttr-16	-2,92
pkc-1	1,85
act-4	-2,03
C34F6.9	2,28
icd-1	-2,13
C34F6.10	2,87
unc-73	1,58
F57A8.4	1,78
dur-1	-2,80
pqn-89	1,83
F42H10.3	1,57
W07E11.1	1,72
goa-1	1,51
ccg-1	-2,74
mgl-2	3,11
hum-9	-2,55
unc-32	1,49
unc-52	-2,73
cpn-3	-2,48
K05F1.6	1,74

gene	logFC
rpl-25.2	-2,34
calu-1	-2,52
exp-2	2,51
C35E7.11	2,31
act-3	-2,63
act-3	-2,63
W02D9.10	2,50
nucb-1	1,69
plc-3	1,91
F36D4.4	1,90
gcy-28	1,36
F38B6.6	2,76
hsp-6	-2,33
rps-19	-1,36
tps-2	-2,59
F55C12.4	2,77
rpl-16	-1,11
dmsr-1	1,57
flp-1	4,01
snap-1	1,60
B0361.4	1,58
aqp-2	-2,62
sma-9	1,49
nlp-37	2,05
T05G5.1	-2,47
nap-1	-2,27
nduo-4	-1,13
osta-2	1,83
tnt-3	-2,63
lgc-53	1,89
unc-46	1,76
ile-1	1,69
rpl-11.1	-2,90
col-175	0,88
rpl-13	-1,04
unc-47	1,73
ZK792.5	1,69
pac-1	1,32
H05L03.3	3,67
gon-1	-2,53
lec-5	-2,66
T23F11.4	2,32
rpl-12	-1,21
lit-1	1,36
C36E8.1	-2,20
rpl-28	-1,70
npr-16	1,57
F27C1.2	1,58

gene	logFC
sul-2	2,34
jph-1	1,56
K09A9.6	-2,21
C10E2.5	1,01
Y71G10AR.4	1,51
igcm-2	1,58
C27F2.8	-2,33
icd-2	-1,80
lars-1	-2,16
W06H8.6	1,65
glb-7	1,30
unc-77	3,06
apl-1	1,84
bkip-1	1,50
Y45F10B.13	-2,31
phf-5	2,40
lea-1	-2,07
rps-6	-1,07
inf-1	-1,98
cpl-1	-2,44
T10G3.8	1,42
atn-1	-2,16
K02D3.1	1,34
rps-7	-1,03
cyc-1	-2,10
ZC15.10	0,97
rps-3	-0,88
ZK822.2	2,52
unc-82	-2,12
spp-10	-2,12
egl-45	-2,10
mrck-1	-2,20
rack-1	-0,92
rps-4	-0,92
lgc-54	1,13
K07C5.4	-2,11
C05G5.1	1,40
dlk-1	1,98
pqn-22	-2,28
Y73B6BL.14	0,83
nhr-40	1,42
unc-40	1,67
dkf-2	1,72
T24H7.2	-1,98
atp-6	-1,02
F58D5.5	1,28
mel-28	-2,11
F40E10.6	1,76

gene	logFC
let-607	1,26
zig-2	1,90
eat-16	1,43
snt-4	2,37
lec-6	1,94
imp-2	1,53
ztf-27	1,49
zig-10	1,55
ctb-1	-0,94
M176.5	2,84
mak-1	-1,99
atic-1	2,28
C50D2.2	1,33
pdi-3	-1,72
unc-112	-2,07
ser-1	1,49
sos-1	-2,06
ZK652.8	1,73
asp-4	-2,17
catp-6	-2,02
vhp-1	1,38
kcnl-1	1,84
qars-1	-1,95
egl-4	1,18
cah-1	1,84
F28C1.3	1,50
T01B7.9	1,92
sta-1	1,49
F28B12.1	1,39
col-107	-4,36
ist-1	2,27
rps-11	-0,98
Y82E9BR.3	-1,32
puf-12	-1,84
dmsr-2	1,92
adss-1	-1,95
acs-17	-2,08
F26F12.8	1,40
abcf-2	-1,70
T18D3.7	1,55
rig-4	-2,31
unc-83	-1,85

Table 6 – All significantly differentially expressed genes of the "sci-RNA-seq RIS vs. neurons" transcriptome and their logFC

gene	logFC
flp-11	7,26
srg-69	1,88
srx-2	2,08
ZK1307.7	2,62
F53F4.17	1,78
F54D1.6	1,67
srsx-18	1,35
gap-1	2,23
cab-1	1,84
egl-3	1,82
wee-1.1	1,69
rabx-5	2,22
T21D12.12	0,87
pgal-1	1,65
pqn-89	0,92
nlp-8	3,01
egl-21	1,67
T27C4.1	1,65
C10C6.7	1,09
R11F4.2	2,06
akap-1	1,66
sbt-1	1,76
ser-4	2,80
nlp-13	2,24
K02F2.5	2,13
nlp-11	2,69
Y57G11C.46	1,97
T05A8.3	3,15
nep-26	2,63
K03B4.4	1,69
wnk-1	1,48
pghm-1	1,33
arrd-26	1,49
sma-1	2,07
ckr-1	2,54
plc-3	1,03
T07E3.3	0,88
frpr-16	1,91
aptf-1	0,54
chdp-1	-1,77
Y39A1A.24	1,37
pamn-1	1,42
ced-6	0,54
let-23	1,47
lfi-1	-1,51
egl-9	1,29
T05E7.4	1,20
tiam-1	1,33

gene	logFC
cle-1	-2,19
madd-4	-2,30
plc-1	-1,79
abts-3	1,38
F46C5.4	0,98
H10E21.5	1,57
tpa-1	1,35
sprr-2	0,95
ins-27	0,65
sue-1	1,66
rcn-1	1,53
ncs-6	1,54
T12A7.2	1,70
ida-1	0,86
fmi-1	-1,64
pkg-2	1,26
C01C4.3	1,46
ZK822.2	1,46

Table 7 – All significantly differentially expressed genes of the "sci-RNA-seq ALA vs. neurons" transcriptome and their logFC

gene	logFC
flp-24	5,92
let-23	3,41
flp-7	3,71
pgal-1	2,26
mnr-1	3,02
nlp-8	3,89
nhr-93	1,52
R11.2	1,98
ptr-24	2,18
F43D9.1	1,31
T10E10.3	1,49
pbo-5	1,50
F41B4.2	3,69
gnrr-7	1,60
ver-3	1,58
plc-3	1,63
Y42A5A.1	2,75
pde-3	2,10
flp-13	4,61
vab-8	2,06
C04A11.1	1,19
Y71A12B.12	1,68

Table 8 – Genes enriched in all three RIS transcriptomes

gene	mean logFC	FACS/RNA-seq (RIS vs all) logFC	sci-RNA-seq (RIS vs all) logFC	sci-RNA-seq (RIS vs neurons) logFC
flp-11	8,75	9,75	9,24	7,26
ZK1307.7	5,51	9,49	4,44	2,62
ser-4	5,28	8,39	4,64	2,80
ckr-1	5,22	8,69	4,44	2,54
T05A8.3	5,22	7,83	4,66	3,15
srx-2	5,19	9,72	3,77	2,08
nlp-8	5,14	7,34	5,06	3,01
srg-69	5,05	9,83	3,44	1,88
nlp-11	5,02	7,52	4,84	2,69
R11F4.2	4,88	8,80	3,77	2,06
K02F2.5	4,77	7,89	4,28	2,13
Y57G11C.46	4,71	8,55	3,61	1,97
nlp-13	4,64	7,47	4,21	2,24
C10C6.7	4,41	9,77	2,38	1,09
F46C5.4	4,37	9,84	2,30	0,98
egl-3	4,27	6,80	4,20	1,82
T27C4.1	4,24	7,10	3,98	1,65
sue-1	4,18	7,00	3,88	1,66
nep-26	4,07	6,18	3,40	2,63
rabx-5	3,98	5,73	3,98	2,22
arrd-26	3,88	7,07	3,07	1,49
pgal-1	3,87	5,92	4,03	1,65
sbt-1	3,85	5,72	4,08	1,76
T05E7.4	3,79	7,89	2,28	1,20
ncs-6	3,78	6,70	3,11	1,54
H10E21.5	3,78	6,30	3,48	1,57
cab-1	3,68	5,11	4,09	1,84
egl-21	3,64	5,21	4,05	1,67
sprr-2	3,59	7,61	2,22	0,95
pghm-1	3,53	5,55	3,71	1,33
aptf-1	3,48	8,59	1,32	0,54
Y39A1A.24	3,42	5,90	2,99	1,37
tiam-1	3,38	5,87	2,95	1,33
ida-1	3,31	5,82	3,23	0,86
K03B4.4	3,30	4,90	3,32	1,69
C01C4.3	3,27	5,26	3,09	1,46
ZK822.2	3,13	5,41	2,52	1,46
pamn-1	3,11	4,74	3,16	1,42
frpr-16	3,08	3,86	3,47	1,91
akap-1	3,03	3,81	3,63	1,66
T12A7.2	3,02	3,92	3,44	1,70
abts-3	2,85	4,56	2,60	1,38
egl-9	2,53	3,57	2,73	1,29
tpa-1	2,53	3,44	2,81	1,35
wnk-1	2,36	3,50	2,10	1,48
pkg-2	2,22	3,58	1,81	1,26
plc-3	2,11	3,38	1,91	1,03
pqn-89	2,10	3,54	1,83	0,92
T21D12.12	1,98	3,12	1,93	0,87
T07E3.3	1,96	3,03	1,99	0,88
ins-27	1,86	3,33	1,59	0,65

Appendix

11. Acknowledgements

First, I want to thank my supervisor Dr. Henrik Bringmann for giving me the opportunity to do my PhD in his lab and to work with those fascinating little worms. I highly appreciate the constant support I got, the trust he had in my project and the insights about the life of a scientist.

Furthermore, I also want to thank Prof. Ralf Heinrich and Dr. Oliver Valerius, for being members of my thesis committee, for the support they gave me during the meetings, but also besides it.

The MPI BPC, with all of its scientists and non-scientists, is an honorable institute, for which I am proud that I had been a part of it. Also the GGNB with its great support for its students and my beautiful city Göttingen, have to be mentioned at this place.

I also thank my collaboration partners, which were mentioned throughout the thesis, for working with me on this exciting story.

One name has to be emphasized here: Maximilian Fritz
Science was his passion. And, although he passed away way too early, he will leave a footprint in science, for being a key part of the story of this thesis and the paper we plan to publish about it. I guess, he would have been proud of it.

I want to thank all my colleagues, with whom I was able to work with, in the last four years. Thanks for Silvia Gremmler for keeping the lab running in the background! And the group we have right now provides such an enjoyable atmosphere during working hours and outside of it. For this, I want to thank: Inka Busack, Yang Hu, Anastasios Koutsoumparis, Elisabeth Maluck, Marina Sinner, and Yin Wu. For those who will join, I am looking forward to our time in Marburg and Royal Worm Force, season two.

One old colleague and now friend, I want to mention here separately, is Michał Turek. Thank you for explaining me the lab and all the methods in the beginning, and now for proof reading my thesis. I hope we will meet soon again so I can pay my beer dept.

Also, thanks to the student assists I had over time, for keeping my worms growing and happy, while I was busy with experiments. By name: Yelena Sargsyan, Konstantina Kolotourou, and Natalia M. Parra.

Coming close to the end of my thesis, I want to thank all my friends in- and outside the world of science who supported me and had an open ear, whenever I felt overwhelmed by scientific reality.

This is also true for my lovely girlfriend Nadine Storjohann, who is there for me on so many levels. Thanks for that, and I am also looking forward to our next step and the time together in Marburg.

Finally, I want to thank my family. My sister and her boyfriend, for providing a warm place, which always feels like home when I visit. And my parents, for what I can hardly describe with words. I am grateful for all the support you gave to me in various ways over all the years. Without you two, I could not have been the scientist I am today, and I know that. Thank you.